UNIVERSIDADE DE LISBOA

Faculdade de Medicina Veterinária

FIBROPAPILLOMATOSIS AND THE ASSOCIATED CHELONID HERPESVIRUS 5 IN GREEN TURTLES FROM WEST AFRICA

JESSICA CORREIA MONTEIRO

CONSTITUIÇÃO DO JÚRI
Doutor Luís Manuel Morgado Tavares
Doutora Ana Isabel Simões Pereira Duarte
Doutor José Alexandre da Costa Perdigão e Cameira Leitão

ORIENTADORA
Doutora Ana Isabel Simões Pereira Duarte

CO-ORIENTADORA
Doutora Ana Rita Caldas Patrício

2019

LISBOA

This thesis was financed by Centro de Investigação Interdisciplinar em Sanidade Animal (CIISA) of the Faculty of Veterinary Medicine, University of Lisbon. The fieldwork was funded by a grant from the MAVA foundation attributed to the Institute of Biodiversity and Protected Areas from Guinea-Bissau. The investigation was carried out at the Virology Laboratory of Instituto Nacional de Investigação Agrária e Veterinária (INIAV) under the supervision of Doctor Margarida Duarte and Doctor Ana Duarte.

CIISA
FMV - ULisboa

iniav

UNIVERSIDADE DE LISBOA

Faculdade de Medicina Veterinária

FIBROPAPILLOMATOSIS AND THE ASSOCIATED CHELONID HERPESVIRUS 5 IN GREEN TURTLES FROM WEST AFRICA

JESSICA CORREIA MONTEIRO

DISSERTAÇÃO DE MESTRADO INTEGRADO EM MEDICINA VETERINÁRIA

CONSTITUIÇÃO DO JÚRI

Doutor Luís Manuel Morgado Tavares

Doutora Ana Isabel Simões Pereira Duarte

Doutor José Alexandre da Costa Perdigão e Cameira Leitão

ORIENTADORA

Doutora Ana Isabel Simões Pereira Duarte

CO-ORIENTADORA

Doutora Ana Rita Caldas Patrício

2019

LISBOA

To my mother and grandfather, for giving me everything

ACKNOWLEDGEMENTS

First of all I'd like to thank my mother, not only for taking care of me all these years, but also for pushing me in the right direction. If it wasn't for you I wouldn't have been able to fulfil my life long dream. Little by little I will get there and it's all thanks to you.

Thanks to my grandpa for also supporting me all these years and my family for being my life line. I am so lucky to be part of the Correia gang and to have all these wonderful people by my side. Hopefully, I'll make you all proud.

To Professor Ana Duarte for always been there even when it is wasn't easy.
To Doutor Margarida Duarte for stepping in and helping me, especially when I was lost.
To Doutor Rita Patrício for your patience and kindness in guiding me through all of this process.
To all three of you, my eternal gratitude. Not only do I have my Masters thanks to all of you, but also life long tools that will guide me in the future and make me a better professional.

I'd also like to thank the INIAV Virology team for taking me in and making me feel welcome.

Thanks to the IBAP team for letting me be part of this amazing work and all the help along the way.

Thanks to Fernando, not only for your help but your amazing company the whole way.

A big thanks to the HVL team. It was a short time but it felt like being with family. Thanks for the guidance and care you all gave to me.

And to all my friends, thanks. Through all the complaining and hardship you guys helped me come out of the other side, hopefully wiser and better for it. Omar number 1 fan club!

RESUMO

FIBROPAPILOMATOSE E O CHELONIA HERPESVÍRUS 5 EM TARTARUGAS-VERDES DE ÁFRICA OCIDENTAL.

A avaliação da sanidade de animais selvagens é uma preocupação crescente, à medida que mais evidências apontam para a ligação intrínseca entre o meio ambiente e a saúde animal.
A fibropapilomatose (FP) é uma doença neoplásica panzoótica que afeta tartarugas marinhas, principalmente tartarugas-verdes. Embora os tumores sejam benignos, quando atingem dimensões maiores podem impedir funções vitais e levar à morte das tartarugas. A FP está relacionada com a presença de uma infeção pelo Chelonid herpesvirus 5 (ChHV5) e em paralelo com a degradação dos habitats de alimentação das tartarugas.
A Guiné-Bissau e a Mauritânia são hotspots para as tartarugas-verdes, sustentando a maior população desta espécie em África, no entanto, até à data, não existia informação científica sobre a prevalência de FP nestas áreas.
Este estudo analisou 108 tartarugas-verdes capturadas entre 2018 e 2019 quanto à presença de FP e utilizou a PCR em tempo real (qPCR), após implementação e validação deste método, para detetar a presença do Chelonid Herpesvirus 5 (ChHV5) em 76 desses indivíduos. Fragmentos da glicoproteína B, UL18, UL34 e ADN polimerase também foram amplificados a partir das amostras da Guiné-Bissau e da Mauritânia, por PCR convencional, e sequenciados, para inferência filogenética.
Os resultados mostraram uma prevalência de FP de 27% (n=32): 36% em Guiné-Bissau e 28% na Mauritânia. A probabilidade de contrair FP decresce com o aumento do tamanho das tartarugas e a maioria dos animais com FP estavam apenas ligeiramente afetados pela doença. Analisaram-se 28 biópsias de tumores, das quais 24 (86%) foram positivas para o ADN de ChHV5, tal como 32 (42%) das 76 amostras de pele saudável examinadas. A análise filogenética revelou que as sequências virais se separaram em quatro grupos filogeográficos: Pacífico Este, Atlântico Ocidental / Este das Caraíbas, Centro-Oeste do Pacífico, e Atlântico. As sequências da Guiné-Bissau e da Mauritânia agruparam com exemplares do Atlântico.
A prevalência de FP foi moderada comparativamente com áreas de maior atividade antropogénica, o que era esperado, dado que os locais de estudo têm baixo impacto humano. As tartarugas mais jovens parecem mais suscetíveis à FP, possivelmente por serem naïves à doença e a adquirem no local de alimentação costeira. A deteção de ChHV5 na maioria das amostras de tumores é consistente com o seu papel como agente etiológico de FP. No entanto, em algumas das tartarugas assintomáticas também se detectou ADN do ChHV5, sugerindo a implicação de outros fatores na expressão da doença. A análise filogeográfica sugere um fluxo genético de ChHV5 ao longo da costa oeste de África, possivelmente mediado pela migração de tartarugas infetadas.
Este estudo estabeleceu linhas de base sobre a prevalência de FP e de infeção por ChHV5 para tartarugas-verdes da África Ocidental. Estes dados podem ser usadas para avaliar os impactos da atividade antropogénica e alterações climáticas. É aconselhado a monitorização sistemática desta doença para avaliar a sua evolução nestes locais-chave.

Palavras-chave: Fibropapilomatose, tartaruga-verde, *Chelonia mydas*, Chelonid Herpesvírus 5, ChHV5, Guiné-Bissau, Mauritânia, Análise filogenética

ABSTRACT

FIBROPAPILLOMATOSIS AND THE ASSOCIATED CHELONID HERPESVIRUS 5 IN GREEN TURTLES FROM WEST AFRICA

The health assessment of free-ranging animals is an increasing concern as more evidence points to the intrinsic link between the environment and animal health. Fibropapillomatosis (FP) is a tumorigenic widespread disease affecting sea turtles, with more incidence among green turtles, *Chelonia mydas.* Although benign, large FP tumours can impede vital functions, such as feeding, vision and swimming, and impede organ function, leading to death. FP is a multifactorial disease, putatively linked to an infection by the Chelonid herpesvirus 5 (ChHV5) and to degraded habitats.

Guinea-Bissau and Mauritania are hotspots for the green turtle in the Eastern Atlantic. Guinea-Bissau hosts the largest rookery for this species in Africa, with strong connectivity with foraging grounds in Mauritania. However, until this date no information was available concerning the prevalence of FP and of ChHV5 in these sites.

This study analysed 108 green turtles, captured between 2018 and 2019, for the presence of FP, and used real-time PCR (qPCR) for the detection of ChHV5 DNA in 76 of those individuals. Partial sequences of the ChHV5 UL34 gene were amplified by conventional PCR and sequenced for phylogenetic analysis, including published sequences of ChHV5. The results showed an FP prevalence of 27% (n=32): 36% in Guinea-Bissau and 28% in Mauritania. FP probability decreased with increasing body size and most turtles were only mildly affected. From 28 tumour biopsies analysed, 24 (86%) were positive for ChHV5 DNA, as were 32 (42%) of 76 samples of the normal skin from both FP-afflicted and asymptomatic turtles. The phylogenetic analysis segregated viral variants into four groups: Eastern Pacific, Western Atlantic/Eastern Caribbean, Mid-west Pacific and Atlantic, and sequences from Guinea-Bissau and Mauritania clustered with the Atlantic group. FP prevalence cannot be compared to nearby geographical sites due to lack of information however, when compared with human-disturbed areas it was moderate, which was expected as our study sites have low human impact. Smaller turtles were more susceptible to FP, potentially because larger individuals acquire resistance over time. Detection of ChHV5 in most tumour samples is consistent with its role as aetiological agent of FP, however some asymptomatic turtles were also infected, supporting that other factors are involved in disease expression. We found evidence for recent ChHV5 gene flow along the West coast of Africa, potentially mediated by the migration of infected turtles. This study has established baselines on FP and ChHV5 prevalence for West Africa green turtles, which can be used to assess impacts of anthropogenic activities or climate change in the near future. Systematic monitoring is advisable to assess evolution of disease at these key sites.

Keywords: Fibropapillomatosis, Green turtles, *Chelonia mydas*, Chelonid Herpesvirus 5, ChHV5, Guinea-Bissau, Mauritania, Phylogenetic analysis

TABLE OF CONTENTS

FIGURE LIST

TABLE LIST

TRAINING PERIOD ACTIVITIES

The curricular internship is inserted within the Study Plans for a Master's degree in Veterinary Medicine at the Faculty of Veterinary Medicine (Faculdade de Medicina Veterinária- FMV). The official period in which the internship occurred was from October 2018 until June 2019, and consisted of two parts: field and laboratorial work.

Field work

This part of the internship was conducted in the Bijagós Islands, situated northeast of the country Guinea-Bissau in West Africa, where two fieldtrips were conducted. A total of 4 weeks were spent there, from the 20th of October until the 10th of November and then from the 23rd to the 29th of March 2019. The first part of the field work was based on the island of Unhocomozinho and Unhocomo Grande. Here, the work consisted in capturing juvenile sea turtles from in the water for processing and sample collection. The second part of the field work was conducted at Poilão Island, a nesting site for the green sea turtle (*Chelonia mydas*). The work was carried out under the guidance of Doctor Ana Rita Caldas Patrício, Post-Doctoral researcher at MARE – Marine and Environmental Sciences Centre, ISPA, Portugal & University of Exeter, UK.

Laboratorial work

The investigation was done at the Instituto Nacional de Investigação Agrária e Veterinária (INIAV) under the supervision and guidance of Doctor Margarida Duarte, of the Virology Laboratory of INIAV and Professor Ana Isabel Simões Pereira Duarte, of the Virology and Molecular Biology Laboratory (CIISA), Faculty of Veterinary Medicine (FMV) of the University of Lisbon (ULisboa).

To develop my study I used several techniques such as:

- DNA extraction and quantification
- PCR
    - Real-time PCR
    - Conventional PCR
    - Nested PCR
- Producing and transforming competent cells
- DNA purification from agarose gels
- Enzyme hydrolyse
- DNA sequencing

Additionally, I also learned computer methodologies for obtaining, analysing and manipulating genetic data. For this I used Clustal Omega, Mega X, DNA Baser, BEAST and R. For the statistical analyses I used RStudio.

Figure 1- A work-flow diagram of the structure of Section 1- State of the Art.

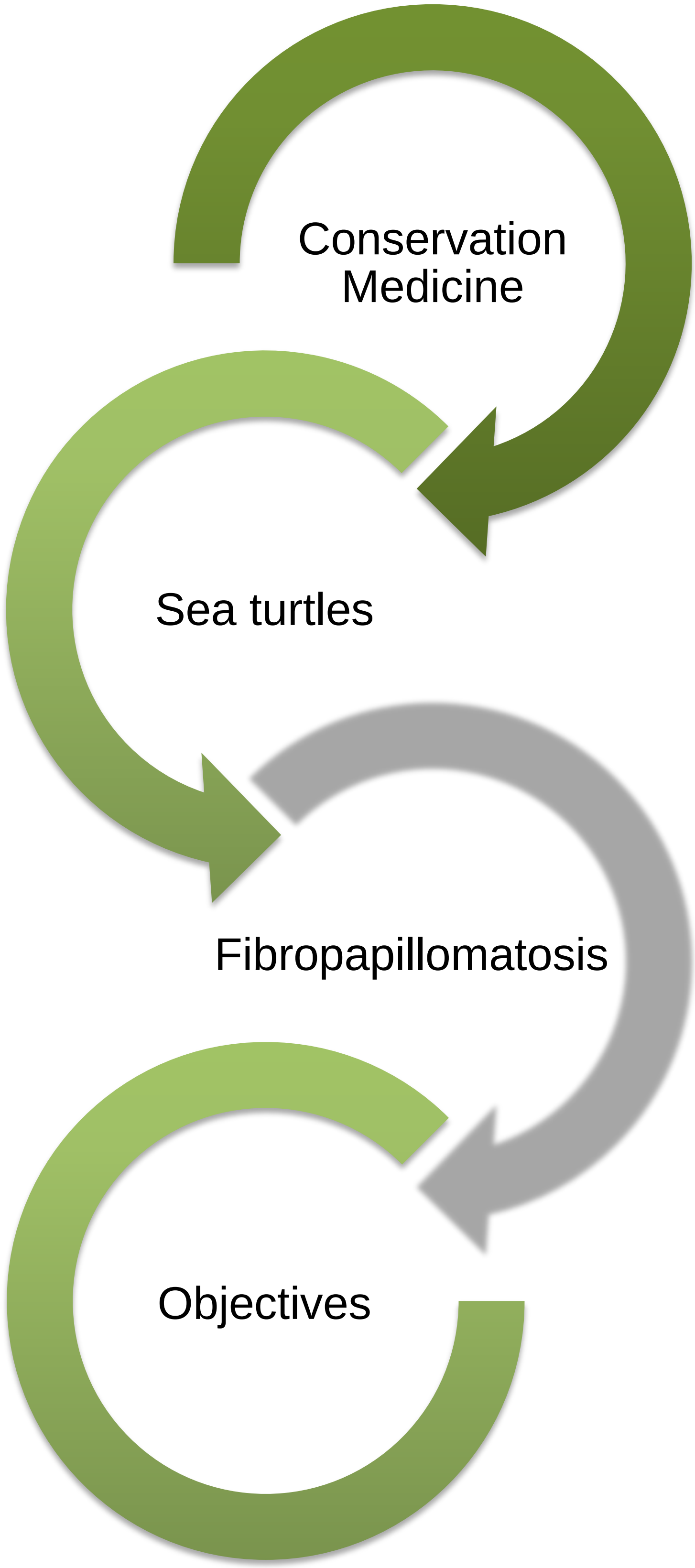

1. STATE OF THE ART (Figure 1)

1.1. Conservation Medicine

1.1.1. Definition of Conservation Medicine

Conservation medicine, a concept that first appeared in the literature in the 1990s, describes the vast ecological framework of health. It represents an arising interdisciplinary field that studies the two-way interactions between certain pathogens and diseases as well as between species and ecosystems (Aguirre, Ostfeld, Tabor, House, & Pearl, 2002). It examines the world and ecological health problems through the conjugation of the studies of the environment, animals and humans. All three are intimately related and, in order to better understand and remedy ecological health problems, multiple disciplines are needed (Deem, 2015b).

The ultimate goal of Conservation Medicine is to create healthier ecosystems, to conserve biodiversity, and to recognise and treat diseases that affect rare or endangered species. It also studies both the impacts of changes in the global biodiversity and how that affects the preservation and transmission of diseases (Aguirre et al., 2002). Biodiversity is a broad term for biological variety, that englobes the wide variety of genes, species and ecosystems that constitute life on Earth. It provides a number of essential services, social and economic contributions from natural ecosystems (Rands et al., 2010).

Within the past two decades, the human population has grown exponentially, surpassing seven billion individuals in the year 2012. This has led to an increased anthropogenic pressure on the environment and has put the long-term survival of several wildlife species at risk. Climate change, habitat degradation, introduction of invasive species, illegal trade of wildlife and exposure to emerging pathogens are major threats to biodiversity. More importantly these threats can have synergistic effects, i.e. one can potentiate the other. For example, global warming can lead to altered host-pathogen interactions and increase disease prevalence or virulence (Patrício et al. 2016). Hence the need to create a multi-disciplinary approach where both the cause and effect should be addressed (Deem, 2015b).

There are various areas that benefit from having a veterinarian, namely in wildlife capture and immobilization, in addressing wildlife health issues and in using them as sentinels to identify new diseases or epidemics of old diseases (Reading, Kenny, & Fitzgerald, 2013). Veterinary medicine uses the three role players (human, animal and environment) to assess health as a whole (one health concept). Veterinarians are able to realise that wildlife health, and subsequently, their conservation, is only able to flourish in healthy environments, and are able to help create them (Deem, 2015a). Additionally, if there is a disease that affects the health of endangered species, veterinarians are able to study its epidemiology, pathology and clinical implication. Furthermore, they must be educators and help spread the message with regards to health continuum that exists within ecosystems that support biodiversity (Deem, 2015b).

Through the combination of biomedical, ecological and veterinary sciences, we are able to explore the connections between ecological causes of changes in both animal and human health, to discover the environmental sources of pathogens and pollutants, and assess the consequences of diseases to wildlife populations (Aguirre et al., 2002).

1.1.2. Conservation importance of sea turtles

Our planet is currently contended to be in a new epoch, "Anthropocene", which in other words signifies that humans are the drivers of the planets' health. Humans have transformed over a third of the planet's surface. We consume 35% of the products from the oceanic shelf and use 60% of the available freshwater each year. Furthermore, animal-based protein consumption is estimated to rise 50% yearly by 2020 (Pauly & Christensen, 1995; Postel, Daily, & Ehrlich, 1996; Rojstaczer, Sterling, & Moore, 2001; Vitousek, Ehrlich, Ehrlich, & Matson, 1986). This increased anthropogenic pressure has also impacted cross-species microbial mixing and exposure to new pathogens that further threatens species survival, including humans. The new "Anthropocene" era has led to a steady escalation of species extinction rates and to the reduction of the animal taxa (Deem, 2015a).

There are seven living species of sea (or marine) turtles that are divided into two taxonomic families, the Dermochelyidae that contains the leatherback turtle, and the Cheloniidae that englobes the other six species (Poloczanska, Limpus, & Hays, 2009). According to the Red List of the International Union for the Conservation of Nature (IUCN Red List), the leatherback (*Dermochelys coriacea*), the loggerhead (*Caretta caretta*) and the olive ridley turtle (*Lepidochelys olivacea*) are classified as vulnerable, the green turtle (*Chelonia mydas*) is classified as endangered, and the hawksbill (*Eretmochelys imbricata*) and the kemp ridley turtles (*Lepidochelys kempii*) are critically endangered worldwide (Romero Zarco et al., 2018), while the flatback turtle (*Natator depressus*) is classified as 'data deficient'.

The seven sea turtle species have roamed the Earth for at least 110 million years, when they became a distinct group from the other aquatic turtles (Paladino & Morreale, 2001). They are slow maturing animals built to last for many decades. Their unique body armour, which equips them with protection from their natural enemies, has not changed much since the time they swum the seas alongside the dinosaurs (Poloczanska et al., 2009).

The conservation of sea turtles is fundamental due to their crucial link with the marine ecosystems. They have the capacity of transporting food from a productive system to a less fertile one. For example, they provide nutrients taken from the marine ecosystem to the coastal area through decomposing organic material (Reis & Goldberg, 2017). This process also occurs on the nesting beaches. Each reproductive female deposits hundreds of eggs (approximately 500) during the nesting period containing high concentrations of energy. Some of these are consumed by predators and detritivores that breakdown the organic material into simpler forms of energy (Bjorndal & Jackson, 2003; Bouchard & Bjorndal, 2008; Reis & Goldberg, 2017).

Moreover, sea turtles also act as consumers, prey, competitors, predators and hosts to a diverse number of parasites and pathogens (Bjorndal & Jackson, 2003; Reis & Goldberg, 2017). They are in symbiosis with a large number of other species, such as, shrimp, remoras, the epibionts on their carapace and filament algae (Reis & Goldberg, 2017).

Besides help maintaining the health of the seagrass beds and coral reefs and other ecological functions, they have major cultural and tourist significance. Sea turtles have become the face of many conservation efforts worldwide. Whether they are used as a symbol for conservation or as a "marketing" strategy, they are able to draw attention from society and motivate people in favour of worldwide conservation (Frazier, 2005; Reis & Goldberg, 2017).

1.1.3. Factors that affect the conservation of sea turtles

Sea turtles were abundant animals in the tropical and temperate oceans until the 19th century, however, currently they suffer countless environmental pressures, mostly man-made. The IUCN-Species Survival Commission Marine Turtle Specialist Group have recently classified the five major threats to sea turtles worldwide. They include fisheries bycatch, coastal development, pollution and pathogens, direct take and climate change (The State of the World's Sea Turtles (SWOT), 2019).

The fishing industry is estimated to kill thousands of sea turtles each year. Large commercial fisheries, such as long-liners and shrimp trawlers, catch numerous turtles as by-catch. Even though most are incidentally caught and thrown back to the sea, many suffer injuries or die as a result of swallowing hooks or becoming entangled in nets. This mass fishing also causes disruption to their food supply and habitat (Paladino & Morreale, 2001; SWOT, 2019).

The sea turtle habitat is also being highly attacked. With shrinking coastlines, a rise in vehicles and ships traffic, artificial lighting and coastal pollution, the marine environment has suffered a huge degradation. This has direct impacts on the sea turtle nesting and foraging areas, causing a decline in population numbers (Reis & Goldberg, 2017; SWOT, 2019).

Recent research also shows that climate change has affected sea turtles to an extent not known before. The rise in sea levels and high frequency of extreme weather events has destroyed some of the nesting beaches. Furthermore, temperature alterations have impacted the natural sex ratios of the hatchlings favouring female-biased ratios. Even the migratory patterns seem to have been altered (Reis & Goldberg, 2017; SWOT, 2019).

Historically, sea turtles are also victims of direct taking by humans. They are traded and killed all over the world. In the global market they may be used for their oil, leather, carapace to make jewellery and other luxury items, and for their meat and eggs (SWOT, 2019).
Lastly, the marine pollution is harming the sea turtles in many ways. Their nesting behaviour and hatchling orientation can be disrupted by light pollution (SWOT, 2019). In the sea, plastic pollution and discarded fishing gear, which turtles may ingest or get entangled in, petroleum by-products and other debris can affect their health and weaken their immune system, potentially leading to the rise of emerging infectious diseases (EIDs) and other health issues (SWOT, 2019) .
Human-mediated climate change may also increase disease prevalence in the marine environment or cause deviations in host−pathogen relations and disease virulence (Patrício et al. 2016). Climate change causes stress to the marine life causing disruption in the normal ecosystem functions and exacerbating diseases (Cavicchioli et al., 2019). Many pathogens of marine taxa are sensible to temperature changes, and most host-pathogen systems are expected to experience more frequent or severe disease impacts with warming (Harvell et al., 2002). Rise in sea levels and temperature affect the spread and transport of pathogens as well as their replication. Additionally, selective harvesting of healthy individuals can increase FP prevalence in a sea turtle population (Stringell et al., 2015).

1.1.4. Sea turtle conservation in Guinea-Bissau and Mauritania

Sea turtles are large-scale migratory reptiles. They are able to travel hundreds or even thousands of kilometres between their nesting and feeding areas (Putman, 2018). In the shores of Africa, there are various sea turtle habitats with resident populations, as well as seasonal visitors or transients. Sea turtles that hatch in distant shores, such as South America, the Caribbean, and the Central Atlantic, may spend time in African waters (Monzón-Argüello et al., 2010), while hatchlings from coastal Africa may also cross the ocean to forage in the Americas (Patrício et al. 2017). This demonstrates the challenges that exist in understanding Africa’s sea turtles, due to the enormous scale and complexity of the task; they are among the least studied in the world.
Guinea-Bissau, a small West African country, is known for its protected areas as part of the country’s efforts to maintain its biodiversity and conservation of protected species (Airaud, Regalla, Barbosa, & Betunde, 2016). In 2004, the Guinean government created the Institute of Biodiversity and Protected Areas (IBAP), an autonomous entity with the capacity of developing policies and regulations which aim to protect the environment and biodiversity. The IBAP implemented a National Action Plan for the Conservation of Sea Turtles, with admirable success, especially in the Bijagós Archipelago, just off the Guinea-Bissau coast. It is estimated that the green turtle nesting population at the Bijagós Archipelago is the third

largest in the Atlantic ocean and the sixth worldwide, with an average of 25,436 nests from 2013 and 2014 (Patrício et al., 2017). Additionally, important foraging grounds have been identified in the archipelago, such as Unhocomo. The IBAP monitors and protects both nesting and foraging areas.

Another major area in West Africa for green turtles is the Banc D'Arguin National Park (PNBA), in Mauritania. Established in 1976, its cold, nutrient-rich environment supports high levels of marine productivity and the main foraging area for the reproductive green turtles from the Bijagós Archipelago, they travel approximately a thousand kilometres from Guinea-Bissau to Mauritania in order to eat (Godley et al., 2010). Many immature turtles also use the waters of the PNBA, their origin is still unknown, but most likely a great proportion origin at the large rookery in the Bijagós. The PNBA also harbours small numbers of nesting turtles, including green sea turtles and sporadically loggerheads (Hama et al., 2018). On the 29th of May, 1999 the Islamic Republic of Mauritania signed the "Memorandum of understanding concerning conservation measures for marine turtles of the Atlantic coast of Africa" by CMS/UNEP, giving the sea turtle national protected status (Mint Hama, Fretey, & Aksissou, 2013).

Reports show that in recent decades, the green turtle population has declined in many islands of the Bijagós Archipelago (Catry et al., 2009). The island of Poilão is currently the only site where numerous turtles still nest. This may be due to the fact that the island is considered sacred, combined with its remoteness and the fact that it is uninhabited. Very few men are allowed to enter the land, and even then, only during religious and social ceremonies, giving the island traditional protection. Thus, the sea turtles are not disturbed during the nesting season and their only threats on this particular island is climate change (Patrício et al. 2018), and the illegal fishing in the surrounding waters, even though it violates local prohibitions and national laws (Catry et al., 2002)**.** At the coastal foraging grounds, both at the PNBA and in the Bijagós, there is not enough information to completely understand threats, but conflict with fisheries is known to occur, as well as intentional illegal harvesting. The presence of FP disease had not been assessed before the present study.

1.2. Sea turtles

1.2.1. *Chelonia mydas* (Green sea turtle)

The green sea turtle is the most abundant marine turtle in the West African coastal waters. Its carapace is green or dark greyish-green with four pairs of lateral plates. The adults can range in straight-line carapace length (SCL) from 80 to 120 cm, with marked geographical variation, and they can weight up to 200kg (Paladino & Morreale, 2001). Its head is small with a single pair of pre-frontal scales, four pairs of post-orbital scales and a serrated lower jaw, and the front appendages have a single claw as opposed to the hawksbill that has two (Figure 2) (Knöbl, Reiche, & Menão, 2011).

Figure 2- Photo identification of a juvenile green sea turtle (original).

Like other sea turtle species, the green sea turtle has a complex life-cycle with ontogenic habitat shifts. After emerging from their nest in the sand, the hatchlings disperse in the ocean and have an epipelagic life-style. This stage is referred to as the “lost years” for little is known of their life during this period. During this oceanic stage they are omnivores, with more carnivorous tendencies. As they reach a certain size and become juveniles they recruit to coastal habitats, where they can remain for decades, and start feeding from the bottom (Patrício, Diez, & van Dam, 2014). They may graze on seagrass meadows, feed on macroalgae and even on small invertebrates (Reis & Goldberg, 2017). Due to the low nutritional value of this diet they have a slow growth rate (Baptistotte, 2007). As juvenile and adults they inhabit neritic shallow waters, typically up to 20 meters in depth, between the latitudes of 40ºN and 40ºS, where there is rich vegetation, and they are rarely seen in the open sea. The adult green turtles make cyclic migrations between the foraging areas and the nesting/reproductive area (Baptistotte, 2007).

1.2.2. Viruses that affect sea turtles

The global climate change that has arisen is documented to have increased the interactions among wildlife, domestic animals and humans. All this has resulted in the rise of EIDs. A number of diseases in wildlife species have been documented with direct links to species survival rates and in some cases, have led to their extinction. Some examples of infectious diseases with major impacts on wildlife populations are chytridiomycosis in amphibians, canine distemper in carnivores and fibropapillomatosis in sea turtles (Deem, 2015b). The latter of which shall be discussed further ahead.

A number of pathogens and parasites have been documented to infect sea turtles. Two families of viruses (potentially six), 56 different species of bacteria, 15 species of fungi, six species of protozoa, 87 Platyhelminthes, six nematodes, four annelids and 17 arthropods (Alfaro, Koie, & Buchmann, 2006).

There are two families of well documented viruses that infect marine chelonians, namely *Herpesviridae* and *Papillomaviridae*. However, there are another four families, which members are suspected to also infect sea turtles (*Iridoviridae, Reoviridae, Retroviridae* and *Togaviridae*). The lack of information regarding sea turtles in their natural habitat and the impossibility of experimental research due to their protected status conditions the advance in the knowledge on sea turtle diseases (Alfaro et al., 2006).

All reptile herpesviruses are part of the subfamily *Alphaherpesvirinae* (McGeoch & Gatherer, 2005). Currently, there are six herpesviruses that have been documented in chelonids, herpesvirus 1 to 6 (ChHV1 to ChHV6). ChHV1, ChHV5 and ChHV6 are described in marine turtles, whereas the rest are known to affect freshwater turtles. However, ChHV1 to ChHV4 still have not been sequenced fully therefore are not recognised by the International Committee on Taxonomy of Viruses (ICTV) (Rodríguez, Duque, Steinberg, & Woodburn, 2018).

These viruses infect both captive and free-ranging chelonians. In most of the research previously published it has been possible to isolate and sequence the virus, however due to the various diagnostic methodologies used and the inconsistency in the molecular follow-up it is difficult to proceed to the nomenclature of all the chelonian herpesvirus. Currently these are named Chelonid Herpesviruses, nevertheless, it is likely to change as more information becomes available, namely phylogenetic information (Rodríguez et al., 2018).
Grey-patch disease is an infection that affects mostly captive sea turtles between the ages of 56 days and 1 year old. A herpesvirus (Chelonid herpesvirus 1, ChHV1) has been identified as the causative agent of these epizootic skin lesions. These lesions begin as small circular papular lesions that eventually coalesce and form the characteristic patches. The more severe outbreaks of this epizootic disease appear in the summer where the high temperatures and over-crowding become a trigger for the reactivation of this herpesvirus (Jacobson, 2007).
Another disease that mainly affects captive green sea turtles is lung, eye and trachea (LET) disease. The main characteristics of this disease are pneumonia and development of caseous material that cover the globes, cranial oral cavity, the glottis and the trachea. Clinical signs include an opened mouth of the individual and harsh respiratory sounds. Through transmission electron microscopy (TEM) a herpesvirus (Chelonid herpesvirus 6, ChHV6) was identified within the affected cells and later on confirmed by subsequent analyses to belong the subfamily *Alphaherpesvirinae* (Jacobson, 2007).
The most studied infectious disease to afflict green sea turtles is fibropapillomatosis (FP) which has been linked to Chelonid herpesvirus 5 (ChHV5).

1.3. Fibropapillomatosis

1.3.1. History

In 1938, Smith and Coates first described cutaneous papillomas, fibromas and fibropapillomas in a captive green turtle from the New York Aquarium, originally from Key West, Florida (Smith & Coates, 1938). Even though FP has been identified numerous times after, only in the 1980s did the disease reach epizootic proportions and now has been reported in every ocean (Herbst, 1994; Jones, Ariel, Burgess, & Read, 2016).
After the first report of FP by Smith and Coates the estimated prevalence in the Florida Keys region was 1.5%, which rose to 20-60% in reports made in the 1980s. Subsequently, in the 1990s the disease emerged in the Eastern Pacific, Hawaiian Archipelago, Indonesia and Australia, making the disease panzootic (Herbst & Klein, 1995; Herbst, 1994; Jones et al., 2016).

1.3.2. Epidemiology

Among free-ranging sea turtles, FP is mostly found in juveniles, following their migration and recruitment to shallow inshore waters, typically in tropical and sub-tropical areas (Jones et al., 2016). Sea turtles that inhabit inshore waters where there is a large anthropological concentration have higher prevalence than individuals that live in deeper open waters (Knöbl, Reiche, & Menão, 2011).

Sub-adults and adults are also affected by FP, however in a lesser number (Herbst, 1994; Knöbl et al., 2011). Among juveniles, the disease is mostly observed in turtles with a carapace length of 40 to 60cm and between 10 and 30kg (Knöbl et al., 2011; Work & Balazs, 1999).

The possible explanation for this age differentiation may be that juveniles affected with FP either succumb to the disease or gain acquired immunity which, later on, gives them protection (Van Houtan, Hargrove, & Balazs, 2010). The facts that survival probabilities of juvenile aggregations do not seem to be affected by FP prevalence and that tumour regression has been observed in many sites, support the latter hypothesis (Patrício, Diez, Van Dam, & Godley, 2016).

Herd immunity could also be a factor in FP prevalence in certain populations. Patrício et al. (2016) showed that in Puerto Manglar, after a large outbreak of FP epidemic, there was a high disease recovery rate. The fadeout of the disease could be due to the turtles becoming resistant to FP and therefore less individuals are susceptible to the disease (Lloyd-Smith et al., 2005). Epidemic cycles appear to depend on the recruitment of new individuals, naïve to FP, since affected turtle populations are able to recover over time (Patrício et al., 2016).

Furthermore, there has not been any reports of FP in pelagic post hatchling (Herbst, 1994). There also is no significant difference in prevalence between male and female green turtles (Work, Balazs, Rameyer, & Morris, 2004).

Even though the disease is more frequent in green turtles, it has been observed in most sea turtle species; *C. caretta* (Herbst, 1994), *L. olivacea* (Aguirre, Limpus, Spraker, & Balazs, 1999), *L. kempii* (Harshbarger, 1991), *E. imbricata* (D'Amatto & Moraes-Neto, 2000) and *D. coriacea* (Huerta et al., 2002).

Various studies conducted in Australia (Flint, Patterson-Kane, Limpus, & Mills, 2010), Puerto Rico (Patricio, Velez-Zuazo, Diez, Van Dam, & Sabat, 2011) and Florida (Hirama & Ehrhart, 2007) suggest that FP does not affect the sea turtle population recovery or survival rates. The concern with FP is at an individual stand point. The tumours that form, although benign, may become fatal depending on their location, growth rate and degree of invasiveness. Therefore, understanding and monitoring this disease is a priority research area for sea turtle conservation for it is a threat to the survival of these threatened species (Jones et al., 2016).

1.3.2.1. Aetiology

Recently, molecular techniques, such as polymerase chain reaction (PCR) and *in situ* hybridization, have shown a strong statistical association between the Chelonid herpesvirus 5 (ChHV5) and FP tumours, and this is now the main research area (Page-Karjian, 2019).

The epizootic nature of FP led researchers to speculate that the disease was caused by an infectious agent. Herbst et al. (1995) were the first to successfully infect healthy animals with FP. In order to perform this, Herbst transferred cell-free lesion extracts, which were previously filtered through a 0.45µm syringe filter, from turtles that had tumours and inoculating it in a young captive turtle that was theoretically naïve to the disease. In three of the four experimental groups, all the turtles developed FP lesions, while the control animals that were housed in the facility under the same conditions did not develop the disease during the same study period. This information supports the speculation of an infectious agent that causes FP, namely a viral agent (Jones et al., 2016).

There are a variety of viruses that are capable of inducing neoplasms such as the ones observed in FP. In consequence, some of them were investigated as potential aetiological agents, such as Papillomavirus (Herbst, 1994), papova-like virus (Lu et al., 2000), retrovirus (Casey et al., 1997) and herpesviruses (Jacobson et al., 1991; Quackenbush et al., 1998; Herbst et al., 1994, 2004).

The biggest limitation to understanding the pathogenesis and aetiology of FP was the inability to grow ChHV5 *in vitro* (Herbst & Klein, 1995; Herbst, 1994; Work et al., 2009). Some studies attempted to grow the virus in fibroblasts or keratinocytes and were unsuccessful (Work, Dagenais, Balazs, Schettle, & Ackermann, 2015). This impasse is common to diseases in which the agent cannot be cultured *in vitro*, but are still known to be the causative agent, such as the herpes simplex and polio viruses (Alfaro-Núñez et al., 2016; Lipkin, 2009).

However, a recent study (Work, Dagenais, Weatherby, Balazs, & Ackermann, 2017) was able to grow the virus in three-dimensional structures made from turtle skin, namely in skin biopsy specimens (plugs) and in organotypic cultures (rafts). This was the first instance this method was employed to grow a non-mammalian organism and of *in vitro* culture of ChHV5. These findings are crucial for the advancement of the confirmation of ChHV5 as the etiological agent of FP and help elucidate the epidemiology and transmission of the virus.

Early molecular studies had concluded that while ChHV5 could be detected in lesions from skin biopsies, it was rarely detected in normal skin biopsies (Lackovich et al., 1999; Quackenbush et al., 1998). These results supported a strong correlation between the virus ChHV5 and the presence of FP (Jones et al., 2016). Quackenbush et al. (2001) successfully amplified ChHV5 from normal skin samples from turtle with FP lesions, implying furthermore the virus with the disease. These results could reflect an early or latent stage of the infection and also proved that ChHV5 is more common than previously thought. Latency is a feature typical of herpesvirus, so such results were expected (Jones et al., 2016). Resembling other vertebrate herpesvirus, ChHV5 infections are estimated to be life-long and with high host specificity (Herbst et al., 2004; Page-Karjian et al., 2017).

There are three lines of evidence that associate ChHV5 with being the primary etiological agent to cause FP. The first is that in every tumour analysed by PCR ChHV5 DNA has been yielded (Alfaro-Nuñez & Thomas, 2014; Herbst, Ene, Su, Desalle, & Lenz, 2004). The second line of evidence is that herpesvirus particles in FP infections have been observed using electron microscopy based on location, size and morphology (Jacobson, Buergelt, Williams, & Harris, 1991). Third, the successful experimental transmission of the disease to naïve FP green sea turtle by Herbst et al. (1995).

More recently the presence of ChHV5 has been detected in turtles macroscopically FP-free, suggesting that the development of disease is not due to virus infection alone. Other factors should be considered, such as interaction host-pathogen-environment, host immunity, viral load and the severity of each variant. It is still to be determined whether FP lesions are the result of a single causal agent or if it is the result of multiple factors. However, it is clear that it is an infectious disease with strong links to ChHV5 (Jones et al., 2016).

1.3.2.2. Environmental factors

The surrounding environment is particularly important to marine turtles. They are animals that have a long-life span and a complex life history. During their lifetime, they travel thousands of kilometres and access a whole range of different habitats. However, once recruited into a near-shore foraging area, they tend to exhibit a high degree of site fidelity. This site fidelity means that the turtles persist in certain locations to feed even if the environment has suffered unfavourable changes. Any damage or destruction of the foraging areas may result in detrimental effects on the sea turtle population that inhabits them (Jones et al., 2016).

Environmental factors may play a fundamental role in the multifactorial problem that leads to the development of FP. The chemical contaminants that are often disposed in the oceans degrading the quality of the water may act as immunotoxins or even cause cellular/genetic damage in turtles. They may also provoke disruption of the neuroendocrine function by indirectly disturbing the turtles' immune system. Herbst (1994) showed that there was a positive correlation between the prevalence of FP in green sea turtles and near shore waters associated with agriculture, industry and urban development.

Eutrophication of the oceans and invasive macroalgae may also be linked to high prevalence of FP (Van Houtan, Smith, Dailer, & Kawachi, 2014). The increase in nutrients in the environment, leads to an increment in the amount ingested by the green turtles. Arginine is of particular significance as it is involved in cell inflammation, immune dysfunction, promoting viral tumours and is also known as biomarker for herpesvirus (Van Houtan et al., 2010). Van Houtan et al. (2010) demonstrated how an increased intake of arginine could promote the herpesvirus and contribute to tumour formation. Later, Van Houtan et al. (2014) demonstrated that FP prevails in eutrophic waters where turtle may consume large quantities of arginine. In this study it was estimated that the sea turtles increased they intake of arginine by 5 to 14 times (Van Houtan et al., 2014).

Even though the mentioned studies show a strong correlation between the prevalence of FP in green sea turtles and areas where the quality of the water is degraded (Van Houtan et al. 2010), it is difficult to identify one specific contaminate. The studies developed in the past focused on chemicals that persist in the environment or can bio-accumulate. However, the genetic damage may be a result of long-term exposure or from transient exposure. This means that future studies should be expanded to include all types of contaminants and the effects they may have on sea turtles. Nonetheless, the practicality of such investigations is daunting due to vastness of the marine environments and the unknown possible causes of FP (Jones et al., 2016).

The marine turtles can be sentinel indicators of marine ecosystem health (Aguirre et al, 2004), due to their longevity and close proximity to inshore habitats. Since FP has been found to be associated with turtles exposed to poor water quality, disease monitoring may be a vital tool to assess the health of inshore marine habitats. Researching the epidemiology of this disease is mutually beneficial for marine turtles, other species in the ecosystem and humans alike (Jones et al., 2016).

1.3.3. Phylogeographical analysis

The ChHV5 is a linear double stranded DNA virus, enveloped with icosahedral capsid, T=16 symmetry and a diameter about 150-200nm. Phylogenetic analysis of the ChHV5 genes revealed that the virus aligns closely with other members of the *Alphaherpesvirinae* subfamily, but in a separate category. Davison and McGeoch (2010) amplified and sequenced the single-stranded DNA-binding protein (UL29), glycoprotein B (UL27), DNA polymerase (UL30) and two subunits of the DNA packaging terminase (UL28 and UL31). Following the sequencing, the results were aligned and analysed using the Bayesian phylogenetic program. The resulting phylogenetic tree showed that ChHV5 exists as an out-group which is clearly separate from the current genera (Jones et al., 2016). This led to the proposal of the virus being placed in its own genus, and in 2012, ChHV5 was placed in a newly erected genus, *Scutavirus*, of the subfamily *Alphaherpesvirinae* of the *Herpesviridae* family (Adams & Carstens, 2012). To this date, approximately 132kbp of the virus has been sequenced (Ackermann et al., 2012; Cárdenas et al., 2019).

The ChHV5 has been identified in various locations around the world and geographic variations have been identified, through alignment of partial genes. Patrício et al. (2012) identified four phylogeographical groups of ChHV5: eastern Pacific, western Atlantic/eastern Caribbean, mid-west Pacific and Atlantic. The study revealed that between nearby foraging ground the viral variant is similar, whereas the variants are considerably divergent between distant foraging regions.

Studies about the co-evolution of virus and the host (Herbst et al., 2004) demonstrated that the virus diverged prior to the separation of avian and mammalian alphaherpesvirus. ChHV5 became specific to marine turtles approximately 300 million years ago (mya) and the two most divergent phylogeographical groups separated approximately 1.6-4.0 mya. Patrício et al. (2012) estimated that the most recent common ancestor of the currently known variants existed 193-430 years ago. Both studies show that the ChHV5 has evolved with the marine turtles and that it has undergone region specific co-evolution with its host. Although more research is needed on the matter to resolve the time of divergence, these studies conclude that the virus is not new nor is it a recent mutation of an old virus. The recent panzootic outbreaks are most likely due to environment factors and modern day anthropological activities (Jones et al., 2016).

1.3.4. Transmission

The transmission route of the FP disease is still uncertain. It has not been observed in pelagic juveniles, which has led to the suspicion of horizontal transmission when the turtles recruit to the neritic zone. The sea turtles potentially experience various stressors with the change of habitats, including long migrations, adaption to a new environment, changes in population density, changes in diet, and pathogen exposure. These may contribute to a depression in the individuals' immune system and make them more susceptible to infection with ChHV5 and to the development of FP lesions. There is also the possibility that these stressors reactivate a latent ChHV5 infection and of direct transmission of the virus between co-habiting turtle during mating and aggression (Jones et al., 2016).

The virus is mostly likely shed in the skin of the sea turtles. Work et al. (2015) linked, for the first time, a capsid protein (F-VP26) to epidermal intranuclear inclusions (EIIs) that contained herpesvirus-like particles (Figure 3).

Figure 3- Epidermal skin cell from a fibropapilloma of a green turtle with intranuclear inclusions (arrow). Image by (Work, Dagenais, Balazs, Schettle, & Ackermann, 2015).

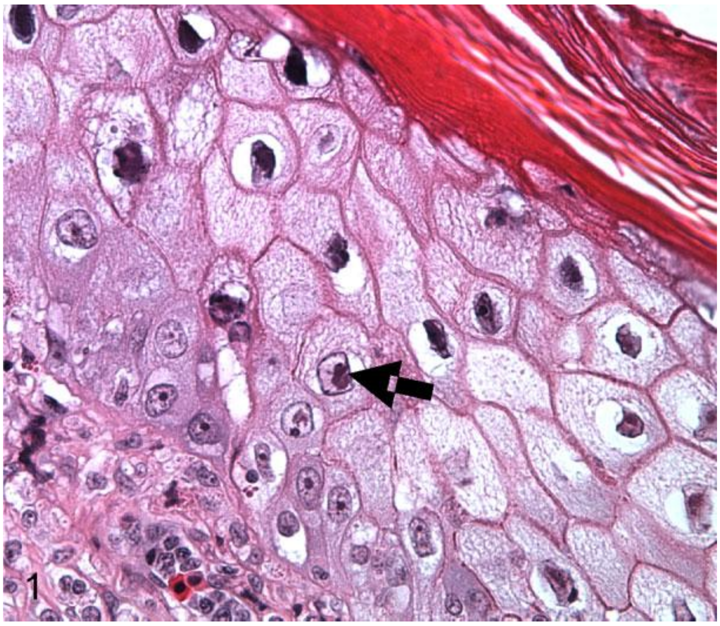

This reveals a possible location of active replication of the ChHV5 and a viable route of viral transmission. However, the study showed that viral shedding via epithelia was sporadic yet followed an exponential distribution. This means that there may be a few individuals that are responsible for intense viral shedding, called superspreaders (Work et al. 2015).

The fact that virus variants are similar within regions may be reflecting the fidelity behaviour that sea turtles tend to demonstrate to their foraging site. Such behaviour could be a key factor limiting the spread of FP among foraging grounds, if highly infectious individuals responsible for disease transmission stay resident (Patrício et al. 2016).

Other means of transmission of FP have also been studied. Some of the proposed mechanisms include transmission via virus-laden seawater, through cleaner fishes that bite the tumours (Yuanan Lu, Yu, Zamzow, & Al., 2000), and transmission via vectors , namely, the marine leech (*Ozobranchus* spp.). The leech when analysed contained significantly high viral loads, becoming the most likely candidate for a mechanical vector of ChHV5 (Greenblatt et al., 2004). However, their role has not been confirmed as for other details of the virus still have not been explained, such as the possible latent state of the virus and the involvement of other co-factors in disease expression of FP (Jones et al., 2016).

1.3.5. Clinical signs, diagnostic and treatment

FP tumours are normally easy to visualize. They can occur on any soft part of the body and have a wide number of appearances, thus any sign of a proliferative mass should be suspected of being FP. They appear as flat plaques, pedunculated, sessile, verrucous, smooth, polypoid nodules or a combination of multiples types (Page-Karjian, 2019).

Histologically, the tumours display papillary epidermal hyperplasia supported by broad fibrovascular projections with a varying ratio of epidermal to dermal proliferation (Figure 4) (Page-Karjian, 2019).

Figure 4- Histological image of the epidermal layer of a fibropapilloma. Image from (Duarte et al., 2012).

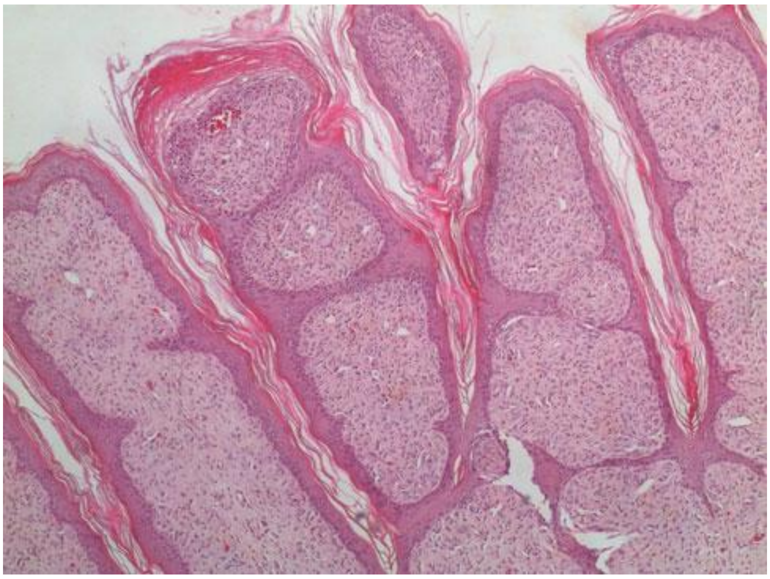

The tumours can be associated with myxofibromas, fibrosarcomas, papillomas, fibromas and fibropapillomas, where the latter is the intermediate phase of the lesion development and the other lesions are linked with other stages. In the early stage of development papilloma lesions are found whereas in the chronic phase the predominant lesion are fibromas, with proliferation of the dermal layer, whilst the epidermal layer remains normal (Herbst, 1994; Kang et al, 2008; Jones, Ariel, Burgess, & Read, 2016).

Occasionally, around the margins of the tumours, lymphocytes and macrophages may be found in moderate to large number. In some cases there is histologic evidence of tumour regression (Page-Karjian, 2019).

When an individual is infected the initial stage may either result in clinical disease or remain subclinical. It is likely that following this period there is an established latent infection in certain tissues, similar to other herpesviruses (Herbst et al., 1995; Work, Dagenais, Balazs, Schettle, & Ackermann, 2015). Herbst et al. (2008) demonstrated that there was a high prevalence (70-80%) of ChHV5 specific antibody reactivity in green sea turtle populations known to have had FP (prevalence’s from 0% to 50%), showing that infection with ChHV5 does not necessarily overt to disease (Page-Karjian et al., 2017).

Animals with severe cases of FP are often found stranded on the beach in debilitated form and cachectic. These animals often are anaemic, with leukopenia, lymphopenia, eosinopenia, heterophilia, hypoproteinaemia, hypocalcaemia, hypoalbuminemia and hyperglobulinemia. These clinical pathology findings are compatible to animals with chronic diseases and repeated antigenic stimulation (Page-Karjian, 2019).

FP is of pressing concern especially since animals affected with severe FP have poor prognosis. Their feeble general health makes them prone to secondary or opportunistic infections. Fibropapillomas are often found on the skin, the ocular and oral region, the flippers and in extreme cases the internal organs. This may bring difficulties in sight, feeding, swimming and cause internal pressure which may culminate in organ dysfunction and/or physiologic imbalances (Page-Karjian, 2019).

Cutaneous FP lesions are relatively easy to identify, however definitive diagnosis require laboratorial techniques for confirmation. Histopathology findings compatible with FP lesions and a follow-up diagnosis using molecular techniques, such as PCR, in situ hybridization or immunohistochemistry, are recommended to reach a definitive diagnosis of FP. If possible, imaging such as radiography, ultrasonography, computed tomography (CT) or magnetic resonance imaging (MRI) should be used to rule out visceral tumours, although in most case this is not possible (Page-Karjian, 2019).

For identification of viral DNA most biological swabs (oral, cloacal and ocular swabs) may be used, however they are not as sensitive as tumour and skin biopsies for ChHV5 DNA detection (Monezi et al., 2016).

When treating FP afflicted animals, supportive care is essential. The animals' overall health strongly affects the outcome of the treatment. Even though there is lack of evidence that immunosuppression is needed for FP to develop, there is evidence that the disease does lead to immunosuppression (Work, Rameyer, Balazs, Cray, & Chang, 2001), meaning boosting the immune system and avoiding stressful situations are important to try impede viral reactivation. Supportive care of the turtles includes adequate water, fluid therapy, pain management and treating secondary infections (Page-Karjian, 2019).

To treat the cutaneous tumours these should be surgically removed. Some evidence suggests that less severe FP lesion may spontaneously regress, however this should not be expected in most cases. Local or general anaesthesia should be administered with the adequate monitoring. Carbon dioxide (CO_2) laser-mediated tumour removal is the most common technique used. This method allows for minimal haemorrhage around the removal site as it also cauterizes and seal the wound while it cuts the tissue. Laser power, pulse rate and hand piece size may vary according to the surface area and depth of the tumour. In most cases sutures are not necessarily, the excision may be left open to heal by secondary intention.

Recently, electrochemotherapy has been presented as an alternative to the traditional techniques. This procedure is effective and safe, presenting complete remission in the turtles used for the study. The use of bleomycin (genotoxic drug) together with the surgery is advantageous as it permits longer intervals between treatments, which means less

manipulation and stress for the turtle (Brunner, Dutra, Silva, Silveira, & Monteiro Martins, 2014).
Pre-operative care should include analgesics and antibiotics. In the postoperative monitoring the individual should be dry-docked for up to 24 hours and there should be a careful vigilance of its recovery. The cutaneous wounds can take as little as 12 weeks to heal. However, regrowth of removed tumours may occur. One study found that 38.5% of green sea turtles experienced tumour regrowth an average of 36 days post-surgery. To prevent regrown tumours a wide margin of skin should be excised during the surgery whenever possible as the normal skin cells may be a source of ChHV5. Lowering the water temperatures in the tank by 2-5ºC may also help prevent viral reactivation (Page-Karjian, 2019).
Lastly, this disease should be considered zoonotic, so the appropriate biosecurity measures should be taken when handling the marine turtles in both field and captive situations.

1.4. Conclusions

There are many lacunas to be filled in the knowledge of FP disease, mainly as the aetiological agent of FP is still unconfirmed. It is fundamental to understand how ChHV5 is transmitted between turtles and between different regions. A useful tool for this research is molecular epidemiology, which infers the genetic differences in the virus between geographic areas. It also helps to uncover possible relationships between host lineage and viral strains, as well as the genes likely responsible for pathogenesis and viral replication. The molecular investigations on the virus will help improve the studies on epidemiology and pathogenesis (Jones et al., 2016).
Geographically, there are major information gaps, which is particularly true for West Africa sea turtles. To date there are limited reports of FP in the region (Duarte et al., 2012; Formia et al., 2007). Baseline information on FP and ChHV5 presence and prevalence are virtually inexistent and there is no knowledge on which life-stages are more afflicted or if infection is ubiquitous. Also, there is no monitoring program in place to assess disease prevalence in the long-term. Assessing key foraging grounds for the green sea turtle in West Africa will contribute to fill-in this knowledge gap and aid the conservation of this charismatic and vulnerable species.

1.4.1. The objective of the study

Given the current information on the green sea turtles of West Africa, this thesis aims to study aspects related to FP disease among feeding aggregations from the region. This study was conducted in collaboration with the Instituto da Biodiversidade e Áreas Protegidas (IBAP) of Guinea-Bissau, the Parc National du Banc d'Arguin (PNBA) in Mauritania and the ISPA – Instituto Universitário, in partnership with the MAVA Foundation.

In order to support the conservation efforts made by these institutes and worldwide, this study on FP was conducted to better understand the *Chelonia mydas* population in West Africa, namely Guinea-Bissau and Mauritania (Figure 5). The objectives of this thesis are a) to detect and quantify the infection by Chelonid Herpesvirus 5 (ChHV5) in the skin of both healthy and afflicted green sea turtles, from Guinea-Bissau and Mauritania; b) to estimate the prevalence of FP in each geographic site; c) to establish a relationship between the macroscopic lesion pattern of FP and the viral charges of ChHV5; d) to assess which class-size is more affected, and e) to conduct a phylogenetic analysis of the viral strain variants with regards to the ChHV5 strains obtained at a global level.

Figure 5- Juvenile green sea turtle with fibropapillomas in the right shoulder (Photo: R. Patrício).

Figure 6- A work-flow diagram of the structure of Section 2- Materials and Methods.

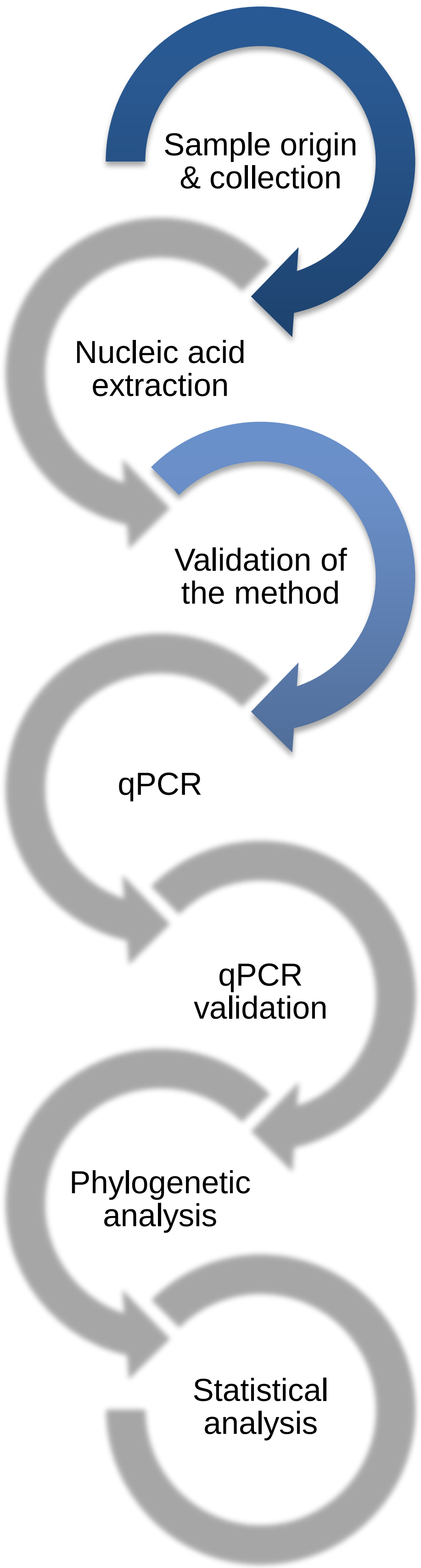
Sample origin & collection
Nucleic acid extraction
Validation of the method
qPCR
qPCR validation
Phylogenetic analysis
Statistical analysis

2. MATERIALS AND METHODS (Figure 6)

2.1. Sample origin

All samples included in this study were obtained from green sea turtles (*Chelonia mydas*) from the south of the National park of Banc D'Arguin in Mauritania (PNBA, N19.582373º, W16.423635º) shown in Figure 7, and the westernmost islands of the Bijagós Archipelago in Guinea-Bissau, Unhocomo and Unhocomozinho (N11.3129º, W16.40279º) shown in Figure 8.

Three separate missions were held on the islands of Unhocomo and Unhocomozinho in Guinea-Bissau. The first was held between the 18th of March and the 22nd of March 2018, and eleven turtles were captured (eight juveniles, two sub-adults and one adult). The second took place from the 21st of October 2018 until the 25th of October 2018 with fifteen individuals caught (eleven juveniles, two sub-adults and two adults). On the third fieldtrip, held from the 25th until the 28th of March 2019, ten individuals were caught (8 juveniles, 1 sub-adult and 1 adult). At the PNBA two fieldtrips were conducted on the 8th of May 2018 and between the 5th and 8th of March 2019, resulting in 73 captured turtles (1 adult, 16 sub-adults and 56 juveniles). In total 109 green turtles were captured.

Figure 7- Satellite map of Mauritania. Right figure- localization of the National Park Banc D'Arguin in Mauritania (source: https://www.google.com/maps/place/Parc+National+du+Banc+D'Arguin/).

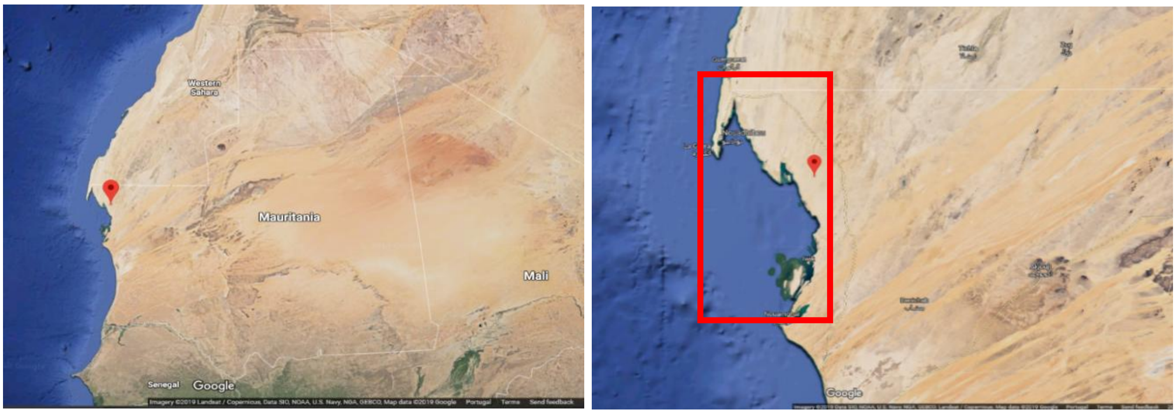

Figure 8- Satellite map of Guinea-Bissau. Right figure- localization of the Islands of Unhocomo and Unhocomozinho (source: https://www.google.com/maps/place/Unhacomo/).

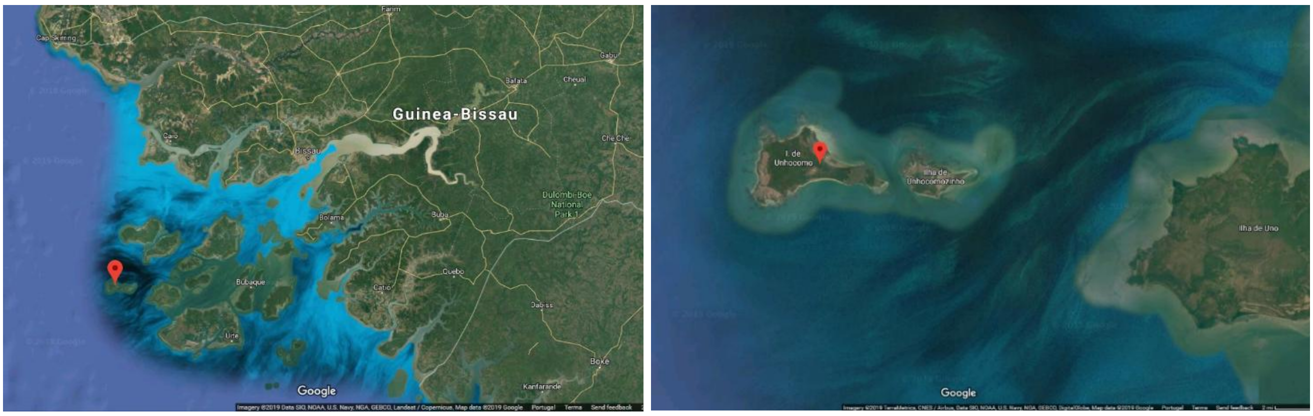

2.2. Collection of the samples

The animals were caught using a fish net and then brought onto the boat for processing. At the site of each capture, the time, the location with geographic positioning system (GPS) and the height of the tide were registered. For each animal, an identification photo was taken, and the curved carapace length (CCL), the curved carapace width (CCW), the tail length were measured with a flexible measuring tape to the nearest 0.1cm.

At the Guinea-Bissau site, for further identification of the turtles, both flipper tags and passive integrated transponder tags (PIT tags) were implanted and registered accordingly. This was not conducted at the PNBA, Mauritania, as a monitoring protocol is not yet established for that site.

After a visual assessment of the animals' general health, the collection of samples was carried out. Gloves were worn by the handlers and all the instruments used were sterilized with chlorhexidine. The area of the skin chosen for the biopsy was previously disinfected with a diluted povidone-iodine solution. Then, an approximately 0.5 square centimetre sample of skin was collected using a scalpel from the right shoulder and stored in a vial containing 90% alcohol. Normal skin tissue was collected from all individuals. Animals that presented macroscopic fibropapillomatosis-like tumours were biopsied and the collected tissue was preserved in vials with 90% alcohol due to inaccessibility to any freezing-methods.

All animals were handled according to "The Universal Declaration on Animal Welfare" (World Society for the Protection of Animals, 2007) and released at the end of the procedure.

In total, 76 normal skin biopsies were collected; 36 from turtles foraging around Unhocomo and Unhocomozinho, and 40 samples from turtles foraging in the Banc D'Arguin. A total of 28 tumour biopsies were also collected; 13 from Unhocomo/Unhocomozinho and 15 from the Banc D'Arguin.

2.3. Nucleic acid extraction

To extract and purify total DNA from the sea turtles' samples, the DNeasy Blood & Tissue kit (Qiagen, Hilden, Germany) was used following the protocol recommended for animal tissues (Spin-Column protocol).

At the laboratory, the hydrated samples were cut into fragments of 25mg and placed in microcentrifuge tubes. A volume of 180µL Buffer ATL and then 20µL of proteinase K was added to each tube. Buffer ATL contains SDS sodium hydroxide (NaOH) which provokes the lysis of the cells. SDS solubilizes the cell membrane, releasing the content within, while proteinase K digests the proteins including nucleases. The tubes were placed in the vortex for a thorough mixture and incubated at 56ºC until lysis was complete. Then 200µL of Buffer AL was added to the sample, which was vortexed, and had an additional 200µL of ethanol 100% added. Buffer AL contains chaotropic salts which allows the DNA to bind to silica

beads in the DNeasy Mini column (DNeasy Blood & Tissue Handbook, 2006).
The entire mixture was transferred into the DNeasy Mini column, previously placed in a 2mL collection tube. The tubes were centrifuged (Eppendorf 5415R) at 7000 rotations per minute (rpm) for one minute and the flow-through was discarded. The centrifugation allows for the binding of the DNA to the silica beads in the membrane due to the presence of the chaotropic salts (high ionic strength) and the removal of any contaminants. Afterwards, the columns were placed in another collection tube and 500µL of Buffer AW1 was added to each. The columns were centrifuged for one minute at 7000rpm, and the flow-through discarded. The last step was repeated with AW2 Buffer and then centrifuged for three minutes at 14000rpm to dry the DNeasy membrane. These two wash steps remove any remaining contaminants and enzyme inhibitors from the silica membrane. Finally, 200µL of Buffer AE was pipetted directly on the membrane, incubated at room temperature for one minute and centrifuged at 7000rpm for one minute to elute the DNA. The low ionic strength of the Buffer AE allows the DNA to elute through the column into the new tube (DNeasy Blood & Tissue Handbook, 2006).
A small set of samples were homogenised with phosphate buffered saline (PBS) and clarified at 3000g for 5min. Total DNA and RNA were extracted from 200µL of the clarified supernatants, using the MagAttract 96 cador Pathogen Kit in a BioSprint 96 nucleic acid extractor (Qiagen, Hilden, Germany), according to the manufacturer's protocol. DNA samples were kept at -20ºC until use.

2.4. Preparation of competent cells

A small sample of pGEM-T1(1) DNA plasmid recombinant was received for the present study to be used as a positive control in the conventional PCR assays and to validate a qPCR developed by Quackenbush et al. (2001). This recombinant DNA was obtained in a previous study on FP, and its nucleotide sequence is available in GenBank (https://www.ncbi.nlm.nih.gov/genbank/) under the accession number HM348895.1 (Duarte et al., 2012).
To produce enough quantity of recombinant DNA (pGEM-T1(1)) for the purposes of this work, *Escherichia coli* competent cells were prepared, transformed, cultured in solid media, picked and grown in a Luria-Bertani (LB) broth, from which plasmid DNA was purified using the boiling method and, later on, purified by the QIAGEN Plasmid Midi Kit (Qiagen, Hilden, Germany) and quantified.
The cells used for this procedure were DH5-α, an engineered strain of *E. coli* (Chromosomal Genotype *fhuA2 lac(del)U169 phoA glnV44 Φ80' lacZ(del)M15 gyrA96 recA1 relA1 endA1 thi-1 hsdR17).*
For the preparation of competent cells, firstly LB broth plates were prepared. LB is a nutrient-

rich media that permits the nutrition of the bacteria and with the incorporation of agar we create a solid medium on which the bacteria cannot digest the agar but are able to grow on top of it due to the LB (Liu & Usinger, 2019). This particular strain of *E. coli* bacteria does not contain any inherent resistant to antibiotics so for the culture no antibiotics were added to the plates. Using a sterile inoculating loop, a portion of the frozen pre-inoculum was scraped and streaked onto the LB plate. These plates were then placed upside down in an incubator at 37ºC overnight.

Next, a single colony was picked into 5mL of liquid LB medium and once again incubated overnight at 37ºC with shaking at 225rpm (Infors HT CH-4103 Incubator).

On the third day, 100µL of the culture was inoculated in each of the two flasks containing 10mL of LB and again incubated at 37ºC at 225 rpm for roughly two to three hours to ensure the exponential growth of the bacteria.

The optic density (OD) was measured each 30 min, using a spectrophotometer which lies on the principle of absorbance/transmission of light to verify the phase of the growth curve of the culture. As the light is pointed at the culture it is scattered and less light is received by the detector. This turbidity is directly proportional to the number of cells present in the culture. The bacteria reach the optimal growth stage (exponential stage) when the OD reaches 0.4 (Godbey, 2014).

When the optical density reached 0.4OD, the culture was taken out of the incubator and placed in an ice bath for ten minutes. Afterwards, it was centrifuged at 6000rpm (Eppendorf 5415R) for five minutes at 4ºC. When this operation was completed, calcium chloride ($CaCl_2$) was added to the cells for the transformation. Then, 1mL of the inoculate was suspended in 2mL of filtered TSS (0.03g of $MgCl_2$, 0.3g of PEG8000, 150µL of DMSO and 2.85mL of LB). After ten minutes of incubation on ice, the culture was divided into vials and stored at -80ºC.

2.5. Transformation of the E. coli DH5-α cells with pGEM-T1(1)

The transformation of the competent cells ensures the plasmid vector is transferred into the bacteria as an extrachromosomal DNA.

First, a LB with agar plate was prepared with 100µg/mL of ampicillin for the growth of the transformed cells. Only transformed *E.* coli cells will be able to grow in ampicillin supplemented medium due to the resistance conferred by the plasmid to this antibiotic. However, if present in the original plasmid DNA preparation, re-circularized DNA (without the insert) would also confer the ability of the transformed cell to grow. Therefore, in order to select bacteria containing the insert of interest, a selectable marker is use.

A vial containing 25µL of frozen *E. coli* DH5-α was thawed on ice. Then, 2µL of recombinant DNA was pipetted into this vial and incubated for 30 minutes on ice. A heat shock was given to the cells in order to alter the membrane permeability and allow the recombinant DNA to be up taken by the bacteria. Next, 250µL of S.O.C. medium was added to the vial and placed in an incubator at 37ºC and 225rpm for one hour (Infors HT CH-4103 Incubator). After the given time, the content of the vial was spread onto a LB-agar plate containing 40µL of X-Gal, 100µL/mL ampicillin and 40µL isopropyl β-D-1-thiogalactopyranosidae (IPTG) and incubated overnight at 37ºC.

2.6. Extraction and purification of recombinant DNA pGEM-T1(1)

Recombinant plasmid DNA was extract from six isolated colonies by the boiling method to be subsequently hydrolysed and sequenced. One was selected to be produced in larger scale using the QIAGEN Plasmid Midi Kit were used.

Each white colony grown in the LB agar plate was picked and placed in a flask containing 10mL of liquid LB. The flask was placed in an Infors HT CH-4103 Incubator overnight, at 37ºC and 225rpm.

Afterwards, 2mL of the culture was transferred into an Eppendorf tube and centrifuged at 11000rpm for 20 seconds. The supernatant was discarded and this step repeated twice more. The pellet formed was suspended with 750µL of STET buffer [8% sucrose, 50mM Tris-HCL (pH 8.0), 50mM EDTA (pH 8.0), 5% Triton X-100], 60µL of lysozyme and 30µL of Rnase. The plasmid DNA has a smaller size than the chromosomal DNA, which allows for the plasmid DNA to be removed without releasing the remaining chromosomal DNA. Lysozyme is an enzyme which enables the breakdown of the bacterial wall. The STET buffer contains sucrose, a substance which helps maintain the osmotic pressure within while preventing the collapse of the cell wall (“Key steps in plasmid purification protocols,” 2013).

The tube was then placed in boiling water (100ºC) for 4 minutes and immediately placed after in ice for 5 minutes. This allows the denaturing of the chromosomal DNA and proteins contained within the bacteria. The plasmid DNA is also affected, with the breakdown of the hydrogens bonds, however due to its supercoiled form it is able to remain intact (“Key steps in the plasmid purification protocols”, 2013).

Following this step, the tube was subjected to centrifugation at 11000rpm for 15 minutes (Kubota KR-2000C). After the centrifugation a bacterial pellet containing cell debris and protein is formed while the plasmid DNA remains in the supernatant. This supernatant was carefully verted into a new Eppendorf tube with equal volume of isopropanol added and placed at -20ºC for 30 minutes. The isopropanol allows for the precipitation of the DNA. The tube was centrifuged at 11000rpm (Kubota KR-2000C), and then put at 4ºC for 20 minutes to prevent overheating. A pellet was formed containing DNA which was washed with ethanol 70% then air-dried. The DNA was then dissolved with 50µL of RNase free water (“Key steps in the plasmid purification protocols”, 2013) and stored a -20ºC.

In order to produce a high yield of pure plasmid DNA (pGEM T1(1)) the QIAGEN Plasmid

Midi Kit was also used. In this case, 50µL of the original culture was transferred into an Erlenmeyer flask containing 25mL of LB medium and incubated overnight in the Infors HT CH-4103 Incubator at 37ºC and 225rpm. Next, the culture was centrifuged at 7000rpm (Eppendorf 5415R) for 15 minutes at 4ºC. A cell pellet was formed and the supernatant was discarded. To the pellet 4mL of Buffer P1 was added to harvest and re-suspend the pellet.
Then, 4mL of Buffer P2 was added and incubated to room temperature for 5 minutes. Buffer P2 contains SDS sodium hydroxide (NaOH) which provokes the lysis of the bacterial cells. SDS solubilizes the cell membrane, releasing the content within, while NaOH denatures the chromosomal and plasmid DNA as well as the proteins. In optimal conditions, this step allows for the plasmid DNA to be released from the cells without releasing the cell wall-bound chromosomal DNA, and also minimizes the time plasmid DNA is exposed to the denaturing conditions ("Key steps in the plasmid purification protocols", 2013).
Following this step, 4mL of Buffer P3 was added and the mixture was incubated on ice for 15 minutes. This buffer neutralizes the lysis using acidic potassium acetate, a high salt solution that after precipitation retains denatured proteins, chromosomal DNA and cell debris.
The sample was centrifuged at 12900rpm (Kubota KR-2000C) for 30 minutes at 4ºC. The consequent pellet formed contained the unwanted cellular debris and the supernatant contained all the plasmid DNA. The supernatant was centrifuged again to certify the elimination of any remaining proteins or chromosomal fragments.
The supernatant was then loaded onto a QIAGEN-tip and filtered by gravity flow. The resin within the QIAGEN-tip ensured that only the plasmid DNA binds, while the debris passed into the flow-through fraction. Buffer QC was then added to the QIAGEN-tip to remove any remaining contaminants.
To elute the plasmid DNA contained in the resin, Buffer QF was pipetted to the QIAGEN-tip and the solution was collected in a tube. This eluted DNA was then desalted and concentrated by isopropanol precipitation. After the centrifugation, the pellet was washed with 70% ethanol to remove any residual salt. The pellet was finally air-dried, re-dissolved using 50µL of water and stored at -20ºC.

2.7. Quantification and purity evaluation of pGEM-T1(1)

The quantification of the resulting DNA extraction was performed using the NanoDrop™ 2000 spectrophotometer. It permits determination of the quantity of nucleic acid in nanograms per microliter (ng/µL). Nucleic acid and proteins attain maximum light absorbance at 260nm (nanometres) and 280nm, respectively. The ratio of the maximum absorbance in relation to the 280nm absorbance is used as measure of the purity of the DNA extracted. In general, values close to 1.8 is accepted as "pure" for DNA samples. The absorbance at 230nm is considered as being the result of other contamination (e.g. by sugars), therefore the 260/230 is also calculated. The expected 260/230 value is between 2.00-2.2. (Matlock, 2015).

2.8. Analysis of recombinant DNA by restriction enzyme hydrolysis

In order to verify that the bacterial colony incorporated correctly the intended insert, the recombinant plasmid amplicon was extracted and subjected to enzymatic restriction. Plasmids are circular, double-stranded DNA molecules that replicate separately from a cell's chromosomal DNA. A restriction enzyme is an enzyme that recognizes specific sequences (usually 4 to 6 bp long and palindromes) in dsDNA molecule called restriction sites and cleaves both DNA strands at vicinity of these sites, generating cohesive or blunt ends. They occur naturally in bacteria and are used as a defence mechanism against invading organisms' DNA. The restriction enzyme used for the p-GEM T easy vector were *Sac* II and *Spe* I. The insert is cloned into the multiple cloning site (MCS) of the plasmid (Figure 9). These restriction sites are found on either side of the insert location. If the reaction is successful, the enzymes cleave the insert on either side producing a linear DNA strand that later can be visualized through agarose gel electrophoresis.

Figure 9- Visual representation of the pGEM-T Easy vector multi-cloning site. The sites SpeI and SacII are underlined (source: https://www.promega.com/-/media/files/resources/protocols/technical-manuals/0/pgem-t-and-pgem-t-easy-vector-systems-protocol.pdf).

To perform this restriction, 3µL of the recombinant DNA (0,5-1µg of DNA), 1µL of each enzyme (10.000U/L), 3µL of Buffer 10x and 23µL of water were mixed in a tube and incubated at 37ºC for two hours. The digestion products were visualised as described in section 3.3.3- Results.

2.9. Sequencing analysis (Sanger method)

The recombinant DNA pGEM-T1(1) was subjected to nucleotide sequencing to confirm the sequence of the insert was the desired ChHV5 selected gene sequence. Sequencing was performed with the ABI Prism BigDye Terminator v3.1 Cycle sequencing kit on a 3130 Genetic Analyser (*Applied Biosystems*, Foster City, CA, U.S.A) using two commercial primers (M13 forward and reverse) for the vector MCS flanking sequences.

The DNA template was prepared from the purified plasmid DNA. To perform the cycle sequencing the following components were added: 2µL of BigDye Terminator Ready Reaction Mix, 2µL of M13 forward primer, 1µL of M13 reverse primer, 3µL of DNase-free water and 3µL (0,25 µg) of the plasmid DNA. The tube was placed in the thermocycler with the following amplification protocol: 1 minute at 96ºC for denaturation and 25 cycles of 10 second denaturation (at 96ºC), 5 seconds for hybridization (at 50ºC) and 1 minute for elongation (at 60ºC).

The sequencing reaction was later purified using ethanol and sodium acetate precipitation. Accordingly, 2µL of 125mM EDTA, 2µL of 3M NaAc and 50µL of EtOH 95% were pipetted into the mixture and placed at -20ºC for 30 minutes. Then, it was centrifuged for 20 minutes at 15000rpm (4ºC). From the tubes, the supernatant is carefully aspirated and 170µL of EtOH 70% placed inside. Once again the mixture was centrifuged for 10 minutes. The supernatant was removed and the pellet dried. To dissolve the pellet, 20µL of formamide was added, prior reading.

2.10. Real-time polymerase chain reaction (qPCR) conditions

The PCR amplification was performed using the CFX96™ Optical Reaction Module (Bio-Rad). The reaction volume was 20µL containing 0.5µL of turtle *pol* probe (50pmol/µL), 0.5µL of Tartaruga RT Forward primer (50pmol/µL), 0.5µL of Tartaruga TR Reverse primer (50pmol/µL), 10µL of SensiFAST Probe Hi-RoxMix 2x (Bioline Reagents Ltd., United Kingdom), 3.5µL of Rnase-free water and 5µL of the DNA template. These PCR mixtures were subjected to the following amplification cycles: 10 minutes at 95ºC to activate the *Taq* polymerase, then 45 cycles of denaturation 15 seconds at 90º and elongation 1 minute at 60ºC.

At the end of each PCR elongation step the amount of fluorescence emitted and the threshold cycle (Ct) value were registered. Ct values above or equal to 38 were considered negative.

2.11. qPCR validation

2.11.1. Standard Curve Construction

To produce quantitative results of the target gene in the field samples a standard curve was created using external standards. The external standards were prepared with 10-fold serial dilutions of the recombinant DNA pGEM-T(1), with known concentrations. The Ct values were used to construct the standard curve with regards to the number of copies in each dilution, calculated from the initial concentration of plasmid DNA. Afterwards, it is possible to determine the number of viral particles in each sample extrapolating from the standard curve.

The recombinant DNA pGEM-T1(1) was diluted in 10-fold series; 5µL of the recombinant was pipetted into 45µL of RNase-free water, the mixture was vortexed and then 5µL was pipetted into a new tube with 45µL of RNase-free water. This procedure was repeated until 11 tubes were obtained with dilutions from 10^{-1} to 10^{-11}. The dilution series (10^{-1} to 10^{-11}) of the pGEM-T1(1) were subjected to qPCR amplification to construct a standard curve. Each dilution was repeated in a series of 4 and the outlier was excluded from the analysis.
These dilutions were subjected to qPCR with the same conditions referred previously in section 2.10- Materials and Methods. At the end the Ct value were registered.

2.11.2. Specificity of the qPCR method

In order to guarantee that the method only detects the targeted sequence (an 86bp fragment within the *Polymerase gene* of ChHV5), the specificity of the oligonucleotides (primers and probe) were checked by *in silico* analysis by performing searches against DNA sequences publicly available in databases (16th May 2019). This was quite relevant taking into consideration that the method was developed 17 years ago.
Due to the lack of a set of ChHV5 negative turtle reference materials, the determination of the false positive rate (number of misclassified known negative samples divided by the total of known negative samples times 100) was not carried out. Instead, we used a set of 14 herpesviruses positive samples from other taxa (Table 1) to demonstrate that the qPCR system was specific. The samples were subjected to qPCR with the same conditions referred previously. At the end the Ct value were registered.

Table 1- Identification of the samples used to test the specificity of the qPCR. The subfamily and specie are referent to the virus.

Sample identification	Subfamily	Specie	Disease caused
4505/09 Avian	Alphaherpesvirinae	Gallid alphaherpesvirus 1	Infectious larynhotracheitis
4505/09 Avian	Alphaherpesvirinae	Gallid alphaherpesvirus 2	Marek's disease
4788/88 Avian	Alphaherpesvirinae	Psittacid herpesvirus 1	Pacheco's disease
2572-1 Equine	Alphaherpesvirinae	Equid alphaherpesvirus 1	Equine herpesvirus myeloencephalopathy
44790 + 4814	Alphaherpesvirinae	Felid alphaherpesvirus 1	Feline viral rhinotracheitis
10520-17	Alphaherpesvirinae	Canid alphaherpesvirus 1	Canine herpesvirus
34878	Gammaherpesvirinae	Alcelaphine gammaherpesvirus 1	Bovine malignant catarrhal fever
Porcine vaccines: Porcine gE, Suivax, PRV-WT, ADV- WT	Alphaherpesvirinae	Suid alphaherpesvirus 1	Aujeszky's disease

2.11.3. Sensitivity the qPCR method (Limit of detection)

The sensitivity of the qPCR method was expressed as the limit of detection (LOD) by using the serial dilutions of the pGEM-T1(1) recombinant DNA (10^{-1} to 10^{-11}). The last dilution where all four replicates gave a positive and specific amplification was considered as the LOD. Again, the lack of a set of ChHV5 positive turtle reference material, hampered the determination of the false negative rate (number of misclassified known positive samples divided by the total of known positive samples times 100). These dilutions were subjected to qPCR with the same conditions referred previously. At the end the Ct value were registered.

2.11.4. Reproducibility of the qPCR method

The reproducibility of the method was tested by repeating the qPCR of the dilution series in three other independent runs. The qPCR amplification conditions and the reaction quantities were maintained, the variable was the CFX96™ Optical Reaction Modules (Bio-Rad). This measurement is to assess inter-assay variability.

2.11.5. Repeatability of the qPCR method

The repeatability of the method was tested by repeating the dilution series from 10^{-2} until 10^{-6} and subjecting this series to three independent runs qPCR amplifications using the same conditions with the CFX96™ Optical Reaction Module (Bio-Rad). This measurement is to assess intra-assay variability.

2.12. Phylogenetic analysis of ChHV5 positive samples

A subset of samples were subjected to conventional PCR with primers from the ChHV5 *pol* genes to be amplified and sequenced. For this purpose, the samples were selected based on the Ct value and the location where the animal was captured. The Ct value is inversely proportional to the herpesvirus DNA load therefore samples with the lowest Ct value were selected for the study.

The genes chosen for analysis were: UL18, UL34, DNA *polymerase* and glycoprotein B.

The primers selected amplify a partial sequence of UL18 for 1212bp. It encodes a major capsid protein gene of the virus. It shows similarities to the VP-23 gene “capsid triplex subunit 2” of the human herpesvirus 2. The UL34 gene is an 861bp long sequence that encodes a membrane-associated phosphoprotein. Two primers were used (UL34A and UL34B) that amplify two overlapping amplicons from the UL34 region. The primers used amplify a final 483bp partial sequence within the DNA *polymerase* family B. It encodes a putative DNA *polymerase* catalytic subunit. Six pairs of primers were used for the glycoprotein B amplification that produce overlapping amplicons totalizing 2486bp. This membrane protein is predicted to be a signal peptide and to codify 3 transmembrane helices. These primers had previously been published and used for phylogenetic analysis and synthesized by STABVIDA (Caparica, Portugal) and its sequences are listed in Table 2 (Patrício et al., 2012; Ene et al., 2005; Greenblatt et al., 2005; Quackenbush et al., 2001). A total of 5042bp were predicted to be obtained from each sample.

Table 2- Primers used for the amplification for the ChHV5 genes.

Gene	Reaction	Primer sequence (5'-3')	Product length	PCR amplification conditions	Reference of the method
DNA *pol* (GTHV)	Forward (GTHV1)	TGTCTGGAGGTGGCGGCCACG	483bp	94°C for 5 min, 35 cycles of 94°C for 30s, 62°C for 30s, 72°C for 30s, One cycle at 72°C for 10 min	(Quackenbush et al., 2001)
	Reverse (GTHV2)	GACACGCAGGCCAAAAAGCGA			
UL18	Forward	AGGCCTGTATCTCCTGCTCA	1212bp	94ºC for 5 min, 35 cycles of 94ºC for 30s, 58ºC for 45s, 68ºC for 1 min, One cycle at 68ºC for 5 min	(Ene et al., 2005)
	Reverse	TATCGCGAGCTCGTACAATG			
UL34	UL34-A Forward	CCTGAGCAAATTTCTGGACCTG	861bp	94ºC for 5 min, 35 cycles of 94ºC for 30s, 55ºC for 45s, 68ºC for 30s, One cycle at 68ºC for 5 min	(R. J. Greenblatt et al., 2005)
	UL34-A Reverse	AATTTTCGCGGCTTCTCG			
	UL34-B Forward	GGGCGGTTTTTGGGGGTCAG			
	UL34-B Reverse	ACTCAAGATCGCGGTCAGCAGA			
Glyco--protein B (gB)	gB-A Forward	CCGTCCGGCAATGATGAAAAA	2486bp	94ºC for 5 min, 35 cycles of 94ºC for 30s, 57ºC for 45s, 68ºC for 30s, One cycle at 68ºC for 5 min	(R. J. Greenblatt et al., 2005)
	gB-A Reverse	GTTGCAACTGCCGCCACTCCTG			
	gB-B Forward	TTCCGCTACCGCCATCAAACACAACT			
	gB-B Reverse	ATTAACCCCCGACGGCACCACAAGAG			
	gB-C Forward	TGCGCGTTATCCACTCTTCTTCCTAT			
	gB-C Reverse	TTTTTGGCCGCGACCCGTTTTC			
	gB-D Forward	GTCAACAACACGCGAGCCAGAGC			
	gB-D Reverse	AAACCCCGCCGAACATAAAATACTTG			
	gB-E Forward	CCTACTTGGGGTTGACGGAGAG			
	gB-E Reverse	GCCAGCGCCCCACCTACTAC			
	gB-F Forward	GCTGGCCGGCGTGCTCAAT			

gB-F Reverse	CTAGATACATACTGGCCGTGCTCGTC

2.12.1. Conventional PCR conditions

The stock solutions of the primers were diluted to a final concentration of 200pmol/µL, and the working solutions, at 50 pmol/µL, were prepared by dilution in dH_2O. The PCR mixtures consisted of 6.5µL RNase free water, 12.5µL AccuStart II PCR SuperMix 2x, 0.5µL of each primer and 5µL of total DNA, totalling in 25µL of mixture.
The amplified fragments resulting from each conventional PCR were analysed in an agarose gel electrophoresis. It enables the separation of the DNA fragments according to molecular size.
The gel was prepared using TE Buffer (Tris-EDTA) and 1.5% agarose. To the mixture GreenSafe was added, a nucleic acid staining agent. When bound to DNA/RNA it emits a green fluorescence that be visualized when exposed to UV light. In the agarose gel, the marker QuickLoad (100bp) was run in parallel to the samples, allowing for the identification of the molecular size of each fragment. The products were run for approximately 40-60 minutes at 120V. The results were visualized in a Chromato-Vue Transilluminator and the amplified DNA fragments size were compared with the bands from the 100bp marker. All the results were photo documented.

2.12.2. Fragment purification from agarose gel

DNA fragments were excised from the agarose gel using a razor blade and transferred into a microcentrifuge tube. Then, 3 volumes of Agarose Dissolving Buffer (ADB) solution was added to each tube and they were placed in a heated bath (55ºC) for 10 minutes until the agarose was completely melted. The solution was then transferred to a Zymo-Spin Column in a collection tube and centrifuged for 60 seconds. The flow-through was discarded. DNA wash buffer (200µL) was added to each tube and centrifuged for 30 seconds, with the flow-through discarded at the end. This step was repeated to ensure the solution was properly washed. Finally, 15µL of DNA Elution Buffer was placed directly on the column matrix and placed in a 1.5mL tube. It was centrifuged for 60 seconds to elute the DNA. The resulting solution contained the purified DNA fragment of each PCR product. These samples were sent to STABVIDA (Caparica, Portugal) for Sanger sequencing.

2.12.3. Phylogenetic analysis

The nucleotide sequences from the UL18, UL34 and glycoprotein B from the 6 strains were subjected to a BLAST (Basic local alignment search tool) search (http://blast.ncbi.nlm.nih.gov/Blast.cgi) in the National Center for Biotechnology Information

(NCBI) data base (3rd June 2019). This search enabled to find other ChHV5 nucleotide sequences to which similarity was higher. From this search, accession numbers that showed a percentage of similarity over 80% were registered and the nucleotide sequences retrieved. The accession number of the sequences used as references for phylogenetic reconstruction are listed in Appendix 7.2.

Nucleotide sequences of each gene were noted in FASTA format and aligned using the Clustal Omega algorithm (Sievers et al., 2011), implemented in MEGA version X (Kumar, Stecher, Li, Knyaz, & Tamura, 2018) with the following parameters for multiple alignments: gap opening penalty=3, gap extension penalty=1.8. The other parameters were kept as default and the files were exported in NEXUS format for further analysis. For each gene, the aligned sequences were corrected manually for optimal genetic similarity.

For phylogenetic analysis MCMC inference methods were employed using BEAST v1.10.4 (Suchard et al., 2018). The MCMC analyses were made using HKY (Hasegawa, Kishino, & Yano, 1985) and GTR (Tavaré, 1986) nucleotide substitution models. Each model ran under the assumptions of constant population size and exponential growth (Ho, Phillips, Cooper, & Drummond, 2005). The prior combinations were run for 100 million generations, subsampling every 10000 generations. The summary trees were created using TreeAnnotator v1.10.4 (Suchard et al., 2018) and edited in FigTree v1.4.4 (Suchard et al., 2018). Phylogenies were constructed for each gene and for a concatenated gene matrix.

2.13. Statistical analysis

The association of size of the captured individuals (CCLn-n) and the Ct values of the skin samples within each location (Guinea-Bissau and Mauritania) was assessed using a Mann-Whitney U test. The test was evaluated with a statistical significance of 5% ($\alpha=0.05$).

The ANOVA F-test was used to assess the statistical association between the turtle size, stage and the Ct value of the normal skin sample, the tumour score and Ct value and to test the similarities of the Ct values between locations. The test was evaluated with a statistical significance of 5% ($\alpha=0.05$). Statistical association was established when $p<0.05$.

The association between the presence of tumours and the size of turtles was evaluated using generalized additive modelling (GAM) available in package mcgv (Wood & Wood, 2015). GAMs are semi-parametric models used to smooth functions to fit the data. It allows to create nonlinear relationships between the FP tumours and explanatory variables (in this case the size of turtles). Adult turtles were excluded from this analysis as they have a low risk of having tumours, and sample size was very reduced (n=5).

Figure 10- A work-flow diagram of the structure of Section 3- Results.

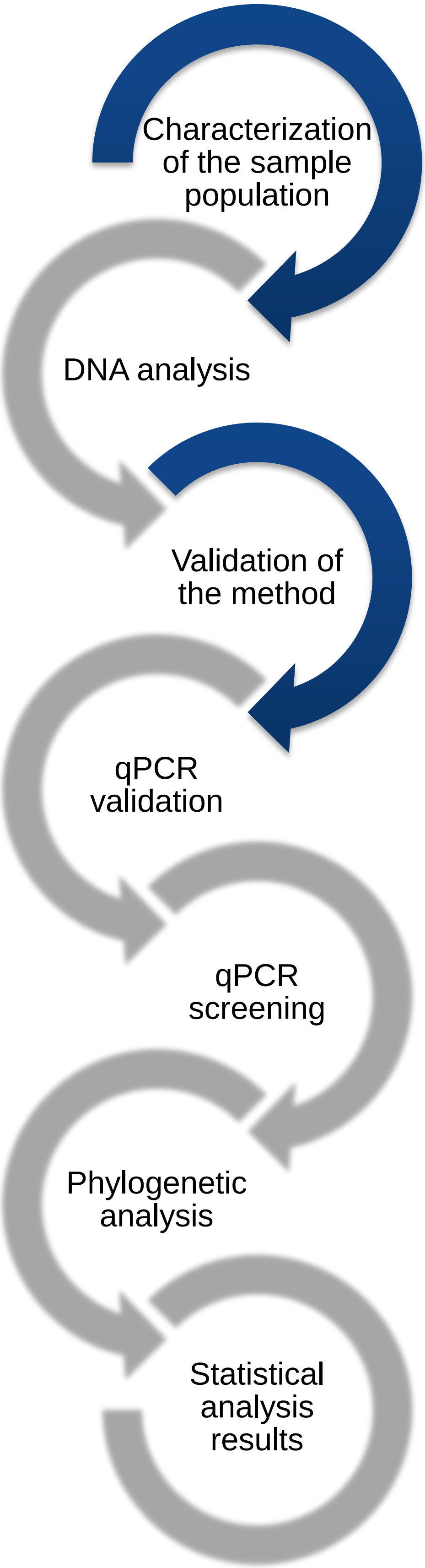

3. RESULTS (Figure 10)

3.1. Characterization of the sample population

The normal skin samples (i.e. FP-free samples) from Mauritania were coded in order of their capture, from M1 to M73. For animals with FP lesions, the code was FP and the number of the turtle from capture order, as above. Samples from Unhocomozinho were also coded from U1 to U36 and the FP biopsies respected the same rule as before.

The captured green sea turtles were classified into three different life-stages based on their Curved Carapace Length (CCL): juvenile, sub-adult and adult. This classification follows previous studies with green sea turtles from the Atlantic region (Patrício et al. 2014), as there is no available report about the somatic growth of these aggregations. The CCL classes are: under 65cm they were classified as juveniles (Patrício et al., 2016), between 65cm and 83cm as sub-adults and over 83cm they were classified as adults, as this is the minimum size for nesting females from this population. Among the 109 captured individuals, morphometric information was taken of 108. Of these individuals 82 were juveniles (76%), 21 sub-adults (19.4%) and 5 adults (4.6%) and their distribution is shown in Figure 11.

Figure 11- Distribution of the captured individuals in the CCL size classes with the respective number of individuals with macroscopic FP lesions. On the left a representation of the total sample population, on the right the distribution for Guinea-Bissau (GB) and Mauritania (MAU). Created using Excel.

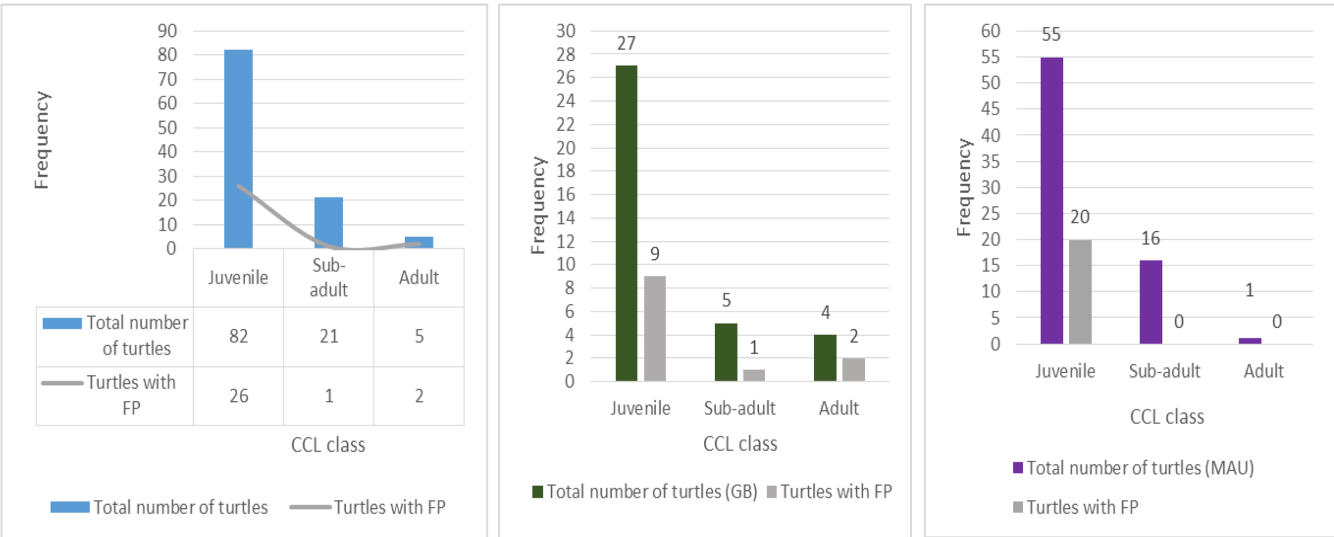

The CCL of the captured green turtles ranged from 37.5 cm to 97cm (mean ± SD= 59.09±11.67cm). The average CCL for individuals from Guinea-Bissau was 58.24cm (SD=15.3) and from Mauritania was 59.52cm (SD=9.44).

The size of individuals affected with macroscopic FP lesions ranged between 39.7cm and 92.5cm (mean ± SD= 56 ± 11.6125cm) while individuals without evidences of FP varied between 37.5cm and 97cm (mean ± SD= 60.22 ± 11.56cm).

The gender of the individuals was not determined given the evident absence of morphologic dimorphism before the adult life stage and the difficulty in examine the genitalia. The body mass was not registered for most the individuals due to lack of human resources and imbalanced working area (measures conducted onboard a small research vessel).

3.1.1. Tumour scoring

Each individual tumour was classified depending on the approximate diameter: Class A- less than 1cm; Class B- 1 to 4cm; Class C- greater than 4 to 10 cm; Class D- greater than 10cm. The turtles were then assigned an overall score, from 0 to 3, based on the number of lesions they had in each class (Table 3, Work & Balazs, 1999).

Table 3- The tumour scoring criteria for placement of the individual in each category (Work & Balazs, 1999).

Tumour class (tumour size in cm)	**Number of tumours present**			
A (<1 cm)	0	1-5	>5	>5
B (1- 4 cm)	0	1-5	>5	>5
C (>4-10 cm)	0	0	1-3	>4
D (>10 cm)	0	0	0	>1
Tumour Score	0	1	2	3

This scoring system reflects the spectrum of severity of FP lesions in green turtles. A score of 0 is attributed to non-afflicted turtles (Figure 12), 1 means lightly affected (Figure 13), 2 moderately, and 3 are heavily afflicted individuals (Figure 14) (Balazs, 1991).
The count of turtles in each tumour score category is presented in Table 4. The CCL of green turtles with tumour score 0 ranged from 37.5 to 97cm (mean ± SD = 60.22 ± 11.56cm), with score 1 from 42 to 92.5cm (mean ± SD = 55.12 ± 9.66cm) and with score 3 from 49.5 to 87.5cm (mean ± SD = 65.5 ± 16.03cm). Only one turtle had a tumour score of 2 (CCL= 39.7cm).

Table 4- Count of turtles with each tumour score partitioned by life-stage.

	Tumour score			
Life-stage	0 (n=76)	1 (n=27)	2 (n=1)	3 (n=4)
Juvenile	53	26	1	2
Sub-adult	20	0	0	1
Adult	3	1	0	1

Figure 12- Image of a green sea turtle with FP tumour scoring 0 (original).

Figure 13- Image of a green sea turtle with FP tumour scoring 1 (original).

Figure 14- Image of a green sea turtle with FP tumour scoring 3 (original)

3.2. Analysis of the yield of total DNA extracted from tissue samples

The DNA yield was determined for all the DNA preparations obtained from both normal and tumour skin samples. Skin samples were taken from 76 individuals, 76 normal skin samples and 28 tumour samples from FP afflicted individuals. In total 108 samples were obtained. For total DNA extraction, a 10% (10ng/100mL) homogenate (w/v) was prepared in PBS with each skin sample. DNA was extracted from 200µL of this suspension (0.2 mL- 0.02ng=20 mg), which corresponds to the amount present in 20 mg of tissue and eluted in 100µL of PBS. Therefore, 1µL of the DNA preparation corresponds to the amount of nucleic acid extracted from approximately 0.2 mg of tissue.

The DNA concentration varied between 6.9 and 51.7 ng/µL. For 21 turtles, normal and affected tissues were obtained. In these samples, the amount of DNA obtained from tumours was, in general, higher than from normal skin (mean ± SD= 38.11 ± 5.85 ng/mL and 18.34 ± 19.48ng/mL, respectively).

For the 108 samples, the mean value for normal skin was 17.44ng/mL, while for the tumour skin was 38.11ng/mL.

3.3. Implementation and validation of the quantitative PCR method developed by Quackenbush et al., 2001

ChHV5 has been implicated as the viral agent to cause the FP lesion observed in marine turtles through distinct laboratorial methods such as PCR assays (Devanter et al., 1996; Lackovich et al., 1999; Quackenbush et al., 1998), electron microscopy and transmission of filtered, cell-free homogenates to green sea turtles (Herbst et al., 1995; Herbst, Moretti, Brown, & Klein, 1995; Jacobson et al., 1991). Even though standard PCR methods show a strong correlation between the presence of the herpesvirus *DNA polymerase* gene and the FP tumours, it does not provide quantitative data of the herpesvirus DNA load present in the lesion and other tissue samples (Quackenbush et al., 2001). The method designed by Quackenbush et al. (2001) further implicates ChHV5 as the infectious agent by providing a way to quantify the viral DNA loads. The qPCR (Quackenbush et al., 2001) was implemented and validated through the construction in the laboratory before being used to infer the viral loads in the samples.

3.3.1. Producing recombinant plasmid DNA pGEM-T1(1)

To identify and characterize herpesviruses associated with the green turtle fibropapillomatosis, a consensus primer PCR which amplifies a region of herpesviral DNA *polymerase* gene was designed by VanDevanter *et al.* (1996), using degenerated primers in a nested format. The first amplification uses the degenerated primers DFA (forward), ILK (forward), and KG1(reverse) allowing the amplification of an 800bp-long sequence within the coding region of DNA polymerase gene (Figure 15), containing highly conserved amino acids motifs of the DNA polymerase gene of the Alpha, Beta and *Gammaherpesvirinae* subfamilies. The subsequent semi-nested PCR uses the degenerate primer (DFA) and a green turtle specific herpesvirus 2 primer (GTHV2) designed after the turtle herpesvirus DNA polymerase gene was entirely sequenced and made public. Primers DFA and GTHV2 amplify a sequence of 483bp of herpesvirus DNA polymerase (Figure 15). This fragment contains discriminatory power for phylogenetic analysis which shall be discussed further ahead.

Figure 15- Relative location of the primers used in Herpesvirus nested PCR (Devanter et al., 1996; Quackenbush et al., 2001).

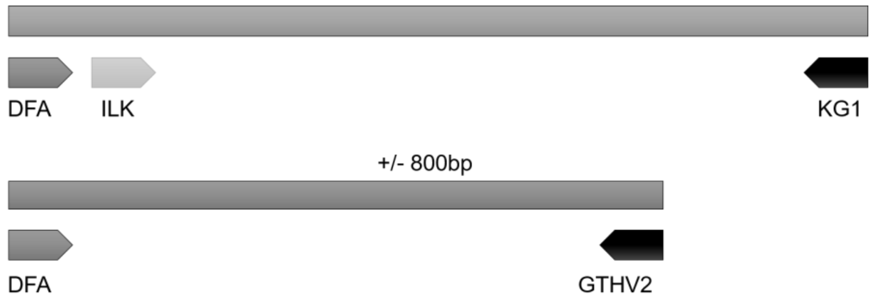

Using the system described above, a 483bp fragment was obtained from a green sea turtle, and cloned into the pGEM T Vector generating the recombinant plasmid pGEM-T1(1). A sample of this recombinant was provided at the beginning of this work for this thesis.
In order to obtain pGEM-T1(T1) DNA in enough amount for the validation of the method, E.*coli* DH5-α cells were transformed and DNA was extracted as described in Section 2.4.-2.6.- Materials and Methods.

3.3.2. Quantification and purity evaluation of pGEM-T1(1)

Plasmid DNA yield was assessed by absorbance at 260 nm and the purity regarding sugar and protein contaminants was determined by investigating the optical density at 230 and 280 nm. The results are presented in the following table (Table 5).

Table 5- Nucleic acid quantification of the plasmid DNA colony T1(1).

Colony identification	Nucleic acid quantification (ng/µL)	260/280 ratio	260/230 ratio
T1(1)	338.3	1.90	2.06

3.3.3. Analysis of recombinant DNA by restriction enzyme hydrolysis

The restriction enzymes cleave the specific sites in the circular plasmid, creating two linear DNA fragments that can be visualized in agarose gel after electrophoresis. Fragments are visualized under UV light (Chromato-Vue Transilluminator) by staining the gel with molecules that intercalate dsDNA.

In this case, the hydrolysis products comprise the pGEM vector (3015bp) and the inserted, around 483bp-long (Figure 16). The predicted bands were confirmed in a 1.5% agarose gel in TBE buffer, stained with Red-Safe™ DNA stain (Applied Biological Material Inc.).

Figure 16- Photograph of the agarose gel with the resulting restriction fragments of the pGEM-T1(1) with *Sac I* and *Spe* II enzymes. Line M- DNA markers, lines 1 to 6 correspond to different clones that resulted from the transformation.

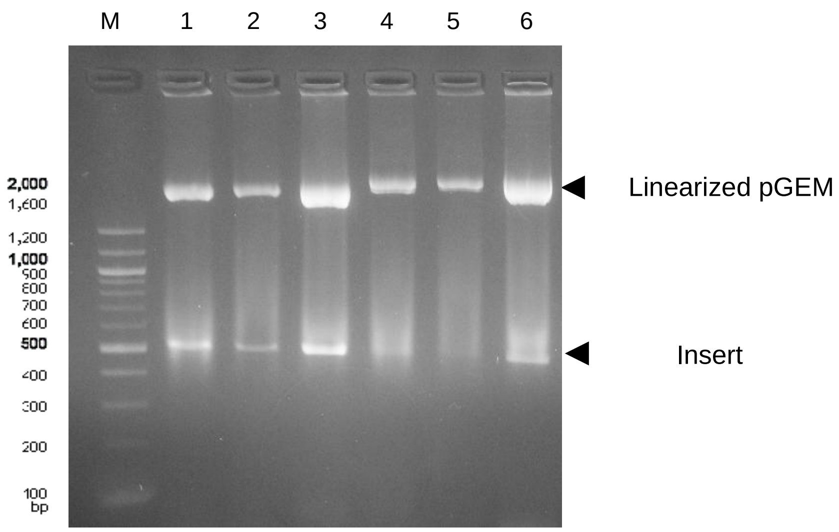

The insert fragment from clone 1, was then cut from the agarose gel and subjected to purification using a commercial kit as described before. The product was Sanger sequenced to confirm the presence of the desired insert. Sequencing of polymerase gene fragment was carried out during this work as described in Section 2.9. The sequence was subjected to a BLAST (Basic local alignment search tool) search (http://blast.ncbi.nlm.nih.gov/Blast.cgi) in the National Center for Biotechnology Information (NCBI) data base (28th May 2019) to confirm its identity (Figure 17).

Figure 17- Results from BLAST search (28th May 2019) of the pGEM-T1(1) sequence. The sequences are aligned with the pGEM sequence on top and the sequence AF035003.3 on bottom. (https://blast.ncbi.nlm.nih.gov/Blast.cgi).

```
Range 1: 15711 to 16214 GenBank  Graphics                 ▼ Next Match  ▲ Previous Match

 Score            Expect   Identities        Gaps          Strand
 893 bits(483)    0.0      497/504(99%)      0/504(0%)     Plus/Minus

Query  1      GACACGCAGGCCAAAAAGCGATTCGGGTCGTCGAAACGCGGCCAGTTCTGGCGCGTCGAC  60
              |||||||||||||||||||||||||||||||||||||||||||||||| |||||||||||
Sbjct  16214  GACACGCAGGCCAAAAAGCGATTCGGGTCGTCGAAACGCGGCCAGTTCCGGCGCGTCGAC  16155

Query  61     CAACAAGGCTTCGAAATCCGTTCCCCAGCGGGTGTGAATAAAATCCCGCGTGGCCAGAAG  120
              ||||||||||||||||||||||||||||||||||||||||||||||||||||||||||||
Sbjct  16154  CAACAAGGCTTCGAAATCCGTTCCCCAGCGGGTGTGAATAAAATCCCGCGTGGCCAGAAG  16095

Query  121    CATGTCGCGCCCTACGGTGGTGACCGTGGCCGCCACCTCCAGACAAGGTAGGAATCCGGT  180
              ||||||||||||||||||||||||||||||||||||||||||||||||||||||||||||
Sbjct  16094  CATGTCGCGCCCTACGGTGGTGACCGTGGCCGCCACCTCCAGACAAGGTAGGAATCCGGT  16035

Query  181    GGCCACGCCGGTAAAACCGTAAACGGAATTGCACGTCAGCTTGATGGCCAGCTGCTGCTT  240
              ||||||||||||||| ||||||||||||||||||||||||||||||||||||||||||||
Sbjct  16034  GGCCACGCCGGTAAACCCGTAAACGGAATTGCACGTCAGCTTGATGGCCAGCTGCTGCTT  15975

Query  241    GTCCAAAAGCAAGCGTTGGTCGCTCGGTGCGGTTTTCATCGATGCGCGGttttttttCCT  300
              ||||||||||||||||||||||||||||||||||||||||||||||||| ||||||||||
Sbjct  15974  GTCCAAAAGCAAGCGTTGGTCGCTCGGTGCGGTTTTCATCGATGCGCGGATTTTTTTCCT  15915

Query  301    GAGTGCCAGCCAGTCGGTCAGCAGCTCGCCCAAAAGGCTGCGGCGCACGTGAGGCTTGAC  360
              ||||||||||||||||||||||||||||||||||||||||||||||||||||||||||||
Sbjct  15914  GAGTGCCAGCCAGTCGGTCAGCAGCTCGCCCAAAAGGCTGCGGCGCACGTGAGGCTTGAC  15855

Query  361    GTAGAAAAGGGACATGCCCTGAACCTTGAACTCCTCGTAATCTTCACCGGCTTTTAGCTC  420
              ||||||||||||||||||||||||||||||||||||||||||||||||||||||||||||
Sbjct  15854  GTAGAAAAGGGACATGCCCTGAACCTTGAACTCCTCGTAATCTTCACCGGCTTTTAGCTC  15795

Query  421    CTTGAGCGTTTCGGCTCGCCGGGTCAAAGTGGTGAAGCACAGATTGTGGGCCTGGATGAT  480
              ||||||||||||||||||||||||||||||||||||||||||||||||||||||||||||
Sbjct  15794  CTTGAGCGTTTCGGCTCGCCGGGTCAAAGTGGTGAAGCACAGATTGTGGGCCTGGATGAT  15735

Query  481    GCTAGGGTACAGGCTTGCAAAGTC  504
              |||||| ||||| || ||||| ||
Sbjct  15734  GCTAGGATACAGACTGGCAAAATC  15711
```

3.3.4. pGEM-T1(1) sequence analysis

The sequence showed a similarity of 99% with a sequence AF035003.3 (sequence from a green turtle with 504bp). The sequence identity matches in 497 of the 503 nucleotides with 0 gaps. The variable sites are at position 49 Y, 196 M, 290 W, 487 R, 493 R, 496 K, and 502 R of the AF035003.3 sequence. The differences in the sequences are highlighted in the Figure 18.

Figure 18- The aligned sequences pGEM-T1(1) (top sequence) and AF035003.3 (bottom sequence) using Jalview Version 2 (Waterhouse, Procter, Martin, Clamp, & Barton, 2009).

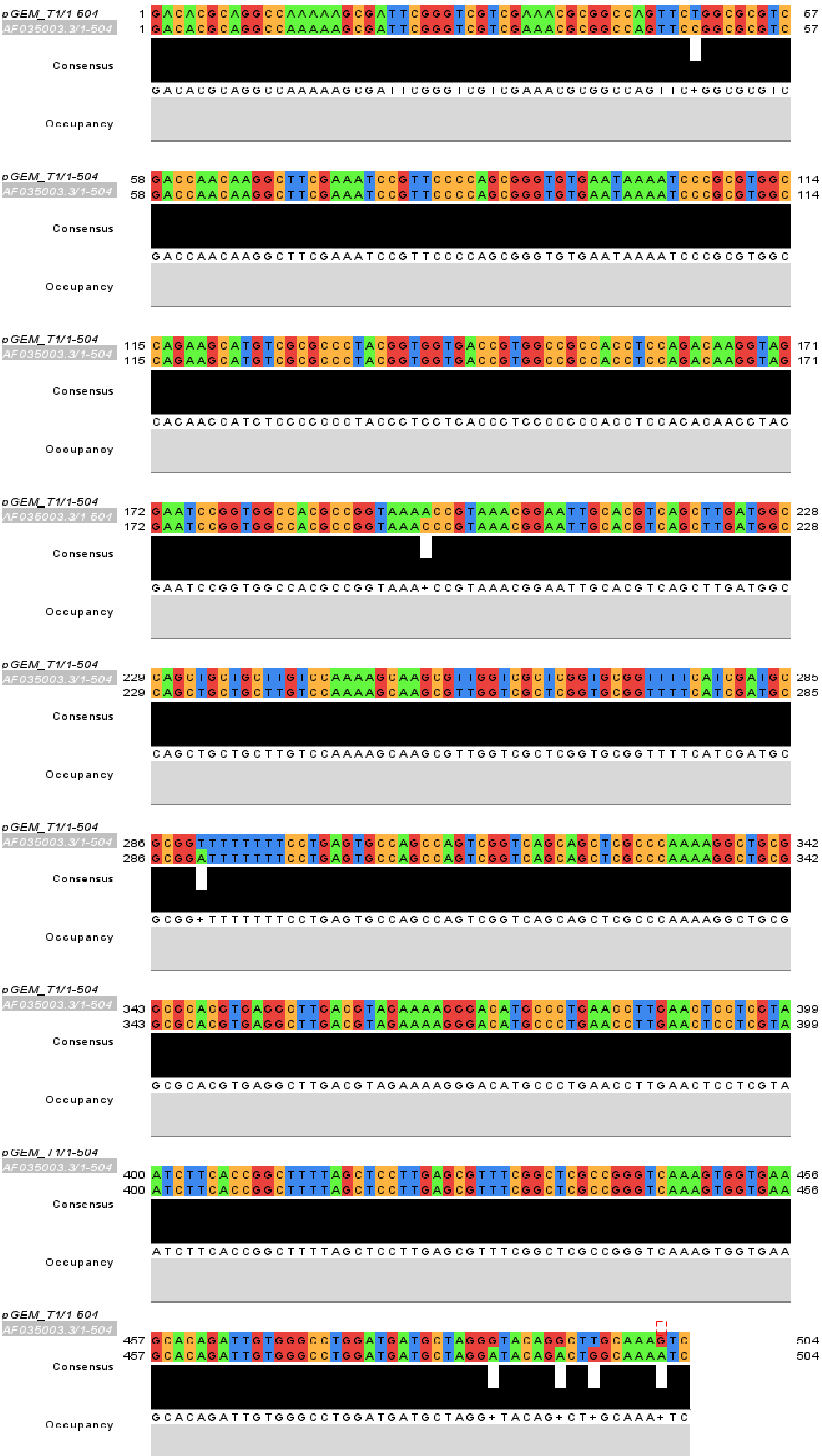
pGEM_T1/1-504 1 GACACGCAGGCCAAAAAGCGATTCGGGTCGTCGAAACGCGGCCAGTTCTGGCGCGTC 57
AF035003.3/1-504 1 GACACGCAGGCCAAAAAGCGATTCGGGTCGTCGAAACGCGGCCAGTTCCGGCGCGTC 57
Consensus
GACACGCAGGCCAAAAAGCGATTCGGGTCGTCGAAACGCGGCCAGTTC+GGCGCGTC
Occupancy
pGEM_T1/1-504 58 GACCAACAAGGCTTCGAAATCCGTTCCCCAGCGGGTGTGAATAAAATCCCGCGTGGC 114
AF035003.3/1-504 58 GACCAACAAGGCTTCGAAATCCGTTCCCCAGCGGGTGTGAATAAAATCCCGCGTGGC 114
Consensus
GACCAACAAGGCTTCGAAATCCGTTCCCCAGCGGGTGTGAATAAAATCCCGCGTGGC
Occupancy
pGEM_T1/1-504 115 CAGAAGCATGTCGCGCCCTACGGTGGTGACCGTGGCCGCCACCTCCAGACAAGGTAG 171
AF035003.3/1-504 115 CAGAAGCATGTCGCGCCCTACGGTGGTGACCGTGGCCGCCACCTCCAGACAAGGTAG 171
Consensus
CAGAAGCATGTCGCGCCCTACGGTGGTGACCGTGGCCGCCACCTCCAGACAAGGTAG
Occupancy
pGEM_T1/1-504 172 GAATCCGGTGGCCACGCCGGTAAAACCGTAAACGGAATTGCACGTCAGCTTGATGGC 228
AF035003.3/1-504 172 GAATCCGGTGGCCACGCCGGTAAACCCGTAAACGGAATTGCACGTCAGCTTGATGGC 228
Consensus
GAATCCGGTGGCCACGCCGGTAAA+CCGTAAACGGAATTGCACGTCAGCTTGATGGC
Occupancy
pGEM_T1/1-504 229 CAGCTGCTGCTTGTCCAAAAGCAAGCGTTGGTCGCTCGGTGCGGTTTTCATCGATGC 285
AF035003.3/1-504 229 CAGCTGCTGCTTGTCCAAAAGCAAGCGTTGGTCGCTCGGTGCGGTTTTCATCGATGC 285
Consensus
CAGCTGCTGCTTGTCCAAAAGCAAGCGTTGGTCGCTCGGTGCGGTTTTCATCGATGC
Occupancy
pGEM_T1/1-504 286 GCGGTTTTTTTTCCTGAGTGCCAGCCAGTCGGTCAGCAGCTCGCCCAAAAGGCTGCG 342
AF035003.3/1-504 286 GCGGATTTTTTTCCTGAGTGCCAGCCAGTCGGTCAGCAGCTCGCCCAAAAGGCTGCG 342
Consensus
GCGG+TTTTTTTCCTGAGTGCCAGCCAGTCGGTCAGCAGCTCGCCCAAAAGGCTGCG
Occupancy
pGEM_T1/1-504 343 GCGCACGTGAGGCTTGACGTAGAAAAGGGACATGCCCTGAACCTTGAACTCCTCGTA 399
AF035003.3/1-504 343 GCGCACGTGAGGCTTGACGTAGAAAAGGGACATGCCCTGAACCTTGAACTCCTCGTA 399
Consensus
GCGCACGTGAGGCTTGACGTAGAAAAGGGACATGCCCTGAACCTTGAACTCCTCGTA
Occupancy
pGEM_T1/1-504 400 ATCTTCACCGGCTTTTAGCTCCTTGAGCGTTTCGGCTCGCCGGGTCAAAGTGGTGAA 456
AF035003.3/1-504 400 ATCTTCACCGGCTTTTAGCTCCTTGAGCGTTTCGGCTCGCCGGGTCAAAGTGGTGAA 456
Consensus
ATCTTCACCGGCTTTTAGCTCCTTGAGCGTTTCGGCTCGCCGGGTCAAAGTGGTGAA
Occupancy
pGEM_T1/1-504 457 GCACAGATTGTGGGCCTGGATGATGCTAGGGTACAGGCTTGCAAAGTC 504
AF035003.3/1-504 457 GCACAGATTGTGGGCCTGGATGATGCTAGGATACAGACTGGCAAAATC 504
Consensus
GCACAGATTGTGGGCCTGGATGATGCTAGG+TACAG+CT+GCAAA+TC
Occupancy

3.3.5. Standard curve construction

The standard curve was generated by the CFX Manager™ Software using the dilutions up to 10^{-8} shown in Figure 19 (Bio-Rad, USA).

The concentration of pGEM-T(1) DNA sample was 338.3ng/mL. From this value the number of copies in each dilution was calculated the following formula:

DNA copy number in 5µL PCR mixture= amount of DNA in the reaction (g)/[molecular weight of DNA/ 6.022×10^{23}]

The result was 4.69×10^{11} copies of herpesvirus in each 5µL of DNA, the amount used in each PCR. The number of copies in each dilution was extrapolated from the original sample.

The optimal slope for a standard curve is -3.32 with a correlation coefficient (R^2) close to 1. Removing obvious outlier helps create an optimal standard curve (Singh & Roy-Chowdhuri, 2016). The resulting standard curve is shown in figure 20. The slope revealed 100% amplification efficiency (slope= 3.322) and a high correlation coefficient (R^2=0.995). The equation for the linear regression line (y=mx+b) is y= -3.322x + 44.11 and shown in Figure 21.

Figure 19- The relative fluorescence units (RFU) on the y-axis and threshold cycle (Ct) on the x-axis of the dilution series from 10^{-1} to 10^{-8} (Image from Bio-Rad CFX Manager™).

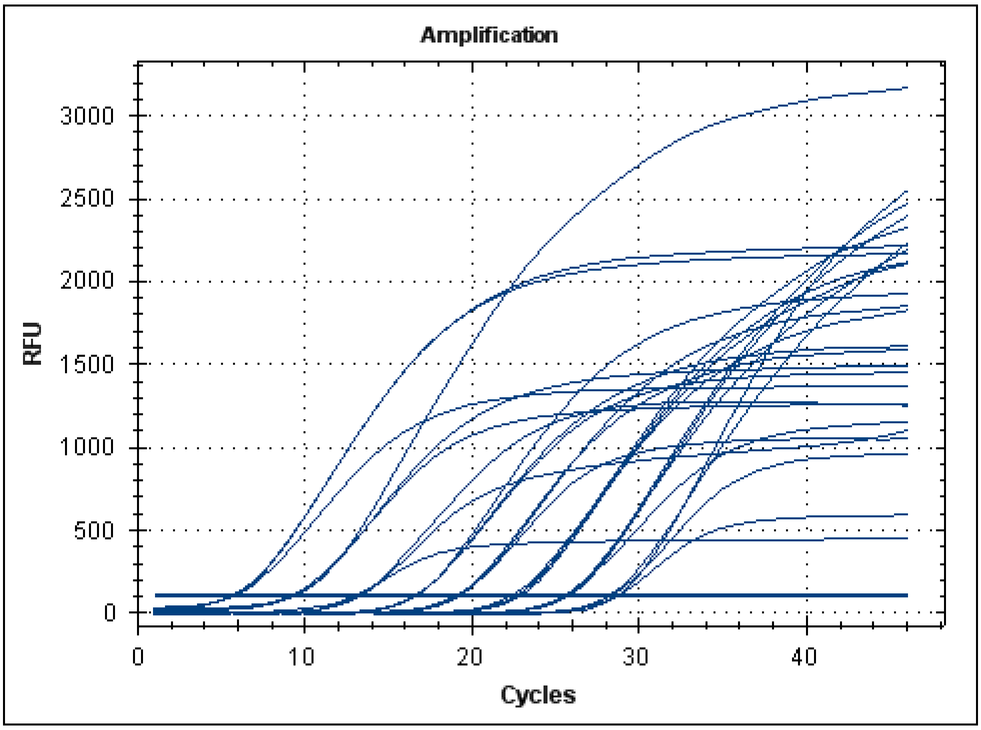

Figure 20- Standard curve constructed by Bio-Rad CFX Manager™ showing the Cq value on the y-axis (Cq- threshold cycle (Ct)) plotted against the log of the pGEM-T1(1) dilutions on the x-axis. (Image from Bio-Rad CFX Manager™).

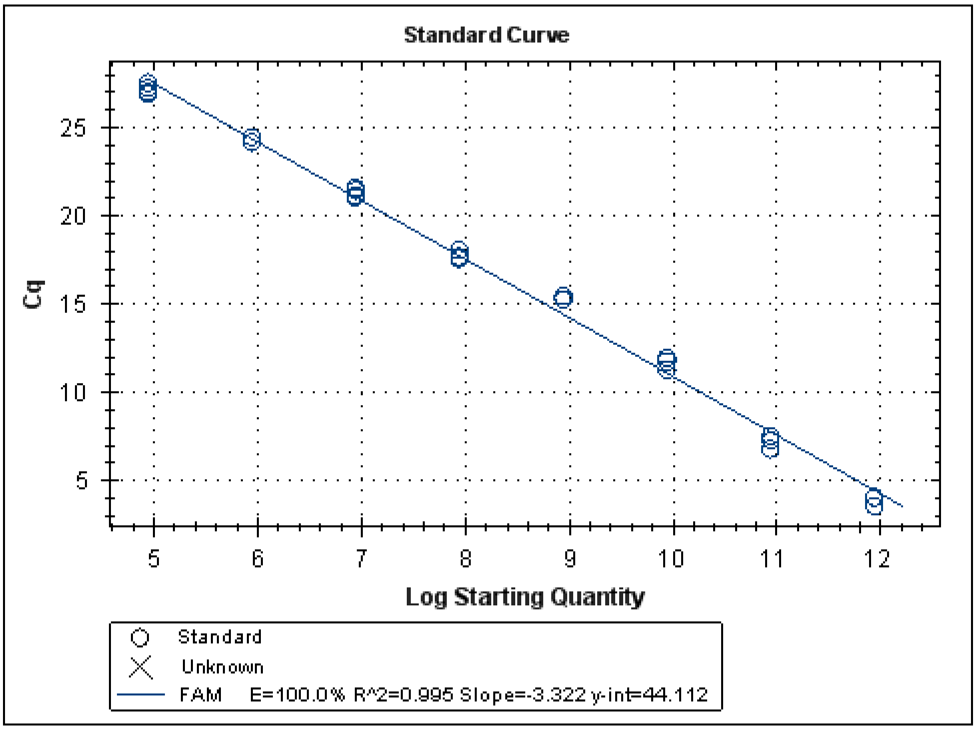

Figure 21- Standard curve obtained by linear regression analysis of the dilution samples with Ct values on the y axis and the number of copies on the x axis using Excel.

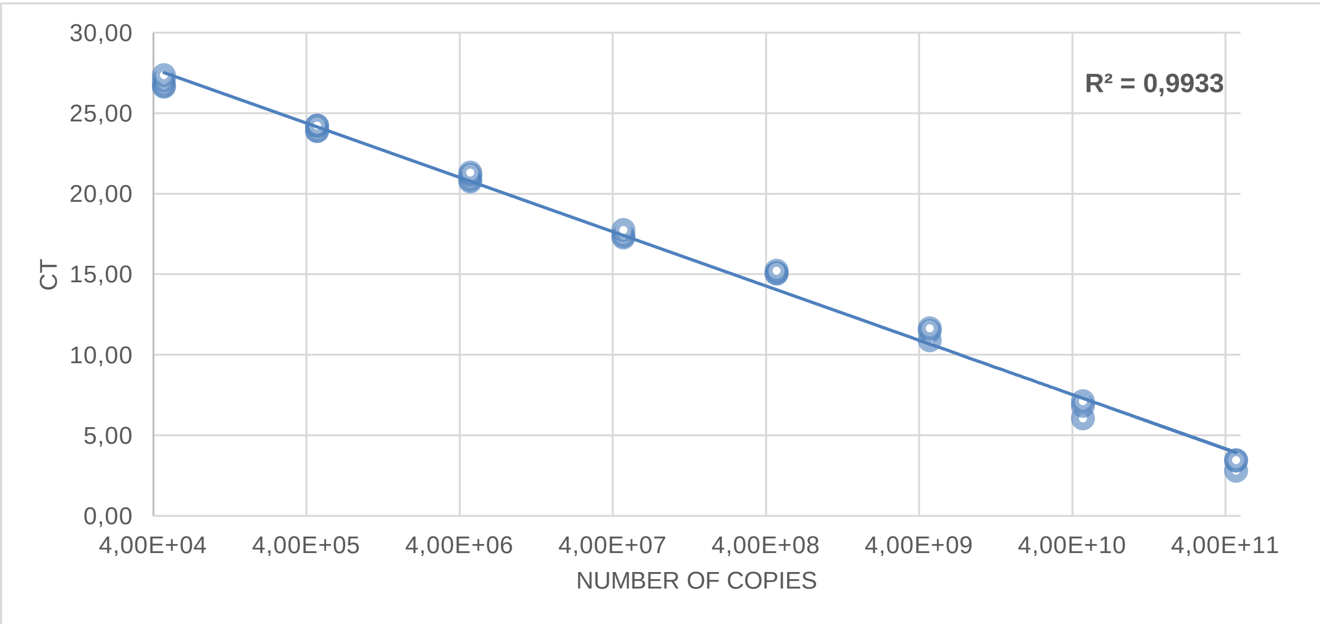

3.3.6. Specificity of the qPCR

The results of the PCR amplification of herpesvirus positive samples from individuals of other taxa are shown in Figure 22. None of the samples used to test the specificity of qPCR crossed the threshold line, demonstrating that the method does not amplify other herpesvirus positive samples besides ChHV5. The positive control (dilution 10^{-3} of pGEM-T1(1)) registered a Ct value of 13.13.

Figure 22- The relative fluorescence units (RFU) and threshold cycle (Ct) of the herpesvirus positive samples. **+** is the positive control (Image from Bio-Rad CFX Manager™).

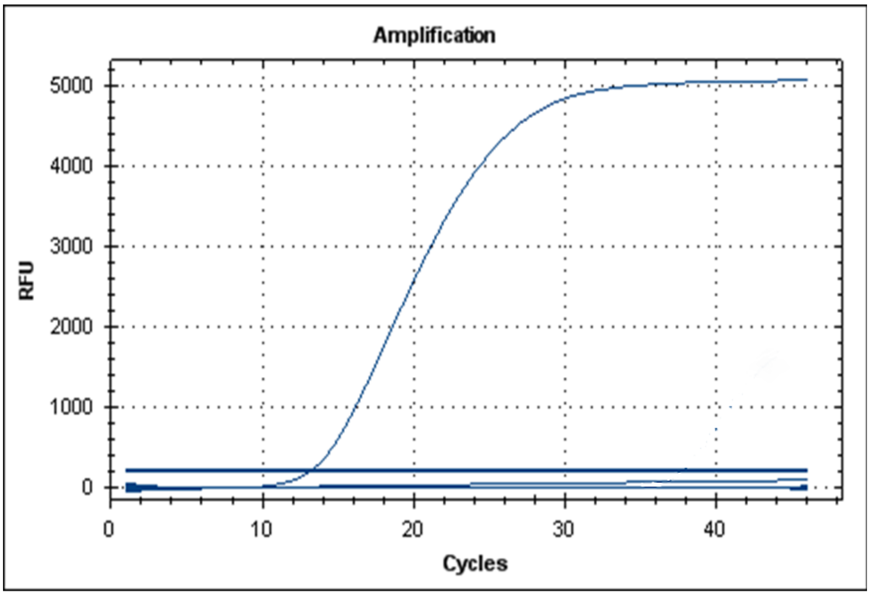

3.3.7. Sensitivity of the qPCR method (Limit of detection)

The limit of detection (LOD) is the lowest amount of DNA in a sample that can be detected with stated probability even though it may not be quantified as an exact value. LOD is the concentration that produces at least 95% positive replicates.

The resulting Ct of the dilution series revealed to be positive until the dilution 10^{-11}.. From this we can estipulate that the LOD of qPCR method is 5 copies of viral DNA ($1.8x10^{-17}$g) deducted from the standard curve.

3.3.8. Repeatability of the qPCR method

The results of the PCR amplification of the dilution series using other CFX96™ Optical Reaction Module (Bio-Rad) machine number 360 are shown in Table 6. The standard deviation (SD) and coefficient of variation (CV %) were calculated for within each amplification replicate.

Table 6- Intra-assay variability of the qPCR method with the respective SD and CV % values.

Dilution	Mean Ct	SD	CV (%)
10^{-1}	3.24	0.368	11
10^{-2}	6.97	0.742	10.6
10^{-3}	11.31	0.328	2.89
10^{-4}	15.13	0.082	0.54
10^{-5}	17.37	0.3	1.72
10^{-6}	21.03	0.258	1.23
10^{-7}	24.07	0.188	0.77
10^{-8}	26.94	0.331	1.22
10^{-9}	30.18	0.38	1.26
10^{-10}	35.35	0.59	1.67
10^{-11}	37.87	0.89	2.35

3.3.9. Reproducibility of the qPCR method

The results of the PCR amplification of a new dilution series (10^{-2} to 10^{-6}) using different CFX96™ Optical Reaction Module (Bio-Rad) machines are shown in Table 7. The standard deviation and the coefficient of variation were calculated for within and between the dilution series.

Table 7- Intra-assay and inter-assay variability of the qPCR method with the respective SD and CV % values.

Dilution	Machine	Mean		SD		CV (%)	
	173	8.78		0.169		1.9	
10^{-2}	174	7.16	8.01	0.109	0.692	1.5	8.6
	360	8.15		0.189		2.4	
10^{-3}	173	13.03	12.17	0.075		0.58	
	174	12.09		0.175	0.731	1.44	6.0
	360	11.38		0.315		2.77	
	173	15.84		0.089		0.56	
10^{-4}	174	15.49	15.51	0.203	0.304	1.31	1.96
	360	15.21		0.15		0.99	
10^{-5}	173	18.73	18.85	0.190		1.0	
	174	18.62		0.439	0.43	2.36	2.28
	360	19.20		0.442		2.3	
	173	22.05		0.133		0.6	
10^{-6}	174	21.30	21.59	0.304	0.394	1.42	1.82
	360	21.42		0.182		0.8	

3.4. Screening of green turtle skin samples by qPCR

DNA extracted from skin samples was screened by qPCR, allowing to identify which turtles were positive to ChHV5 and also providing quantitative information regarding the viral loads present in the affected tissues. Recombinant DNA pGEM-T1(1) was used as a positive control in all amplification reactions. In Table 8 are the primers used for the qPCR reactions.

Table 8- Primers and probe used in the qPCR reaction. Note- Tartaruga RT reverse is a reverse complement sequence.

Identification	Sequence (5'-3')	Product length	Position in genome Accession number: AF299107.1
Tartaruga RT Forward	ACTGGCTGGCACTCAGGAAA		169- 189
Tartaruga RT Reverse	CAGCTGCTGCTTGTCCAAAA	86bp	236-255
Tartaruga probe	[6FAM] -CGATGAAAAC-CGCACCGAGCGA- [TAMRA]		203-224

The cut-off for the Ct was 38. For the 28 tumor samples, 24 were positive in the qPCR, confirming the strong correlation between FP and ChHV5 presence. The Ct values determined in the tissue samples ranged from 21.10 to 35.38 in tumor biopsies with a mean of 27.22 (Figure 23). Appendix 7.1. contains the Ct value of each sample. The blank spaces represent negative reactions/lack of amplification or non-amplified samples.

The results of the qPCR of the samples showed that 26 (68.4%) of the normal skin samples from Mauritania were positive for ChHV5-DNA, while for Guinea-Bissau the value was smaller, namely 5 (approximately 14%) (Figure 24). The mean Ct of normal skin sample was 35.24, however most 'healthy' skin samples did not yield a Ct value (negative for ChHV5 DNA).

The viral DNA copy number for each sample was calculated using the following equation:

Quantity=$10(\frac{\text{Ct-b}}{\text{m}})$, where b is the y-int=44.11 and m is the slope=-3.322. The results are shown in Appendix 7.1.

The tumour samples presented lower Ct values than the normal skin samples as shown in Figures 23 and 24.

Figure 23- The relative fluorescence units (RFU) on the y-axis and threshold cycle (Ct) on the x-axis of each tumour sample (red lines) and the positive controls 10^{-2} and 10^{-3} (blue lines) (Image from Bio-Rad CFX Manager™).

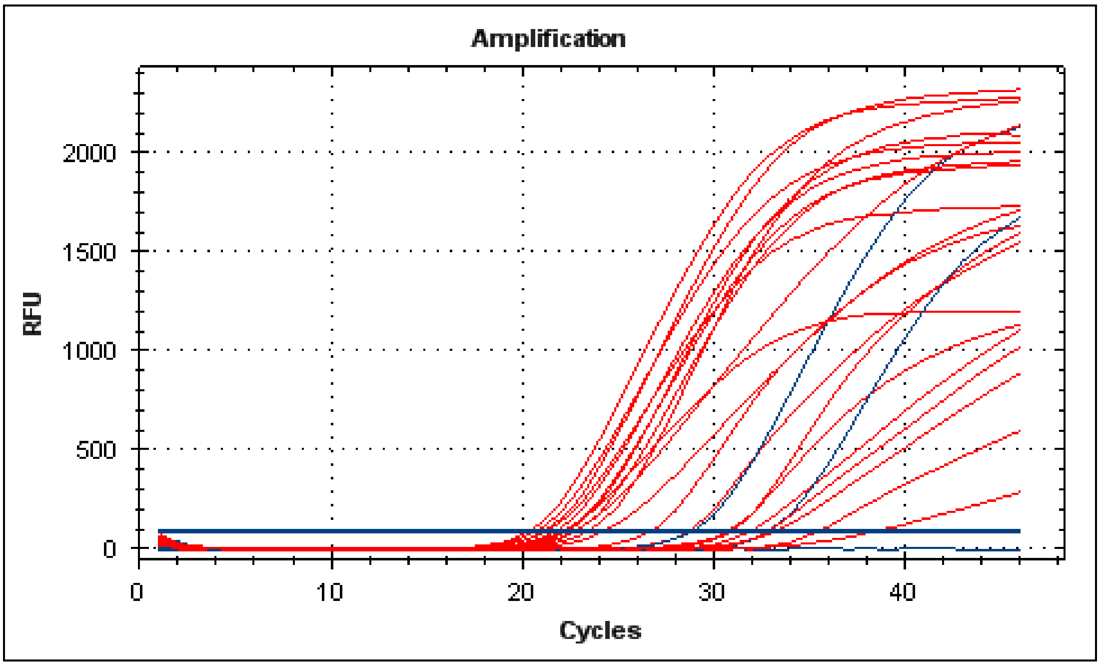

Figure 24- The relative fluorescence units (RFU) on the y-axis and threshold cycle (Ct) on the x-axis of each normal skin sample (green lines) and the positive controls 10^{-2} and 10^{-3} (blue lines) (Image from Bio-Rad CFX Manager™).

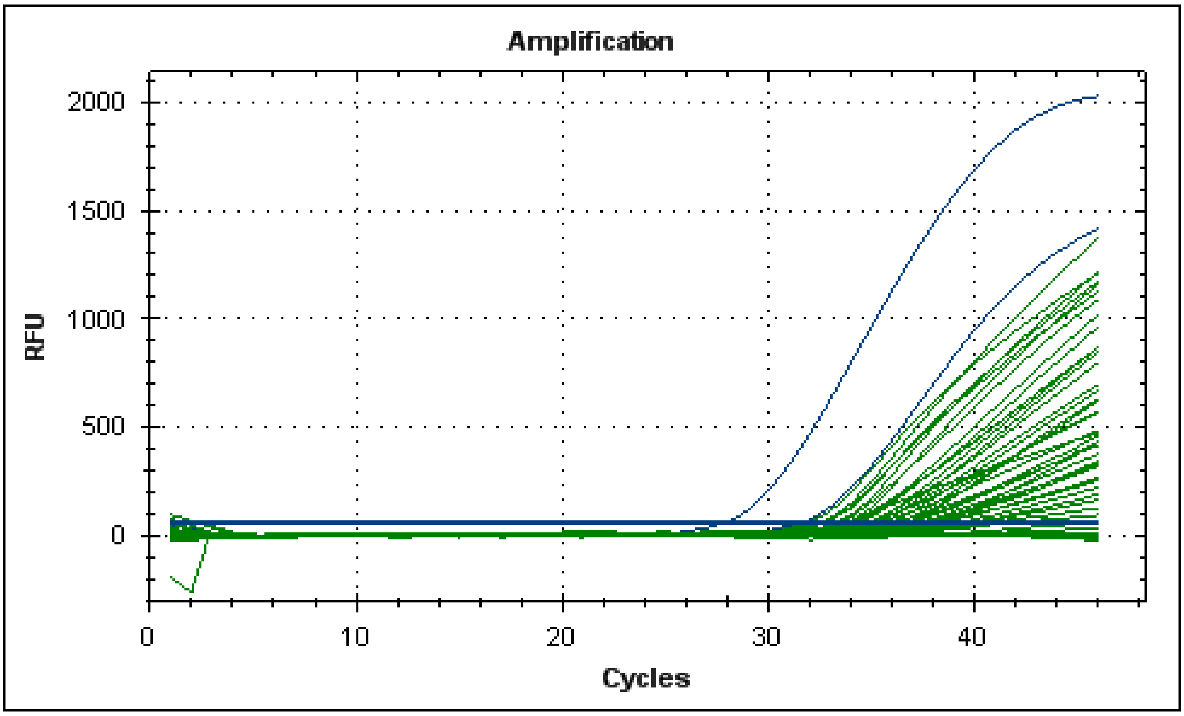

3.5. Phylogenetic analysis of the ChHV5 positive samples

3.5.1. Amplification of ChHV5 *pol* genes from ChHV5 positive samples

The samples selected for the phylogenetical analysis were U11FP2, U18FP, U24FP, M1FP, M4FP and M18FP. The characteristics of the samples regarding the specimens, are described in Table 9.

Table 9- Identification of the sample subgroup for PCR amplification of the ChHV5 *pol* genes

Turtle_ID	Sample Number	Date of capture	Place of capture	CCL (cm)	CCW (cm)	Tail length (cm)	Weight (kg)	Ct value
11_GB	**U11FP2**	22/03/2018	Etimbato, Unhocomo	87,5	87,0	Not measured	Not Measured	**21.20**
18_GB	**U18FP**	21/10/2018	Ancante, Unhocomozinho	50	44	2.5	12.0	**26.63**
24_GB	**U24FP**	25/10/2018	Etimbato, Unhocomo	50	45.0	2.5	12,0	**28.58**
1_TID_18	**M1FP**	08/05/2018	Tidra	61	Not Measured	Not Measured	Not Measured	**22.68**
4_TID_18	**M4FP**	08/05/2018	Tidra	42	Not Measured	Not Measured	Not Measured	**20.26**
18_TID_18	**M18FP**	08/05/2018	Tidra	49.4	Not measured	Not Measured	Not Measured	**21.63**

The PCR method described by Quackenbush (2001) and the PCR conditions for each gene were detailed in the Materials and Methods Section 2.12.1. In Table 2, the primers used and the amplification conditions are described for each gene. In total, 5042bp were expected to be obtained from each sample.

The amplification of the complete glycoprotein B gene was attempted by six overlapping fragments (A to F). However only fragment F was successfully sequenced in the 6 strains. The UL34 region was amplified with two overlapping fragments. For the remaining regions (DNA polymerase and UL18), only one fragment was amplified. A total of 55 fragments were successfully amplified from the sub-group, meaning that 5 fragments were not obtained due to insufficient or absent amplification. The fragments were given codes according to the sample number and the gene amplified (example U3-UL18, U11-UL18, etc.). Figures 25-27 represent some of the DNA fragments obtained from the various PCR amplifications. The amplicons were purified as described in Materials and Methods section 2.12.2. and were sent to STABVIDA (Caparica, Portugal) for Sanger sequencing.

Figure 25- Visualization of the agarose gel using Chromato-Vue Transilluminator. Line M- DNA markers, the following pair of lines correspond to amplified glycoprotein fragments from A to F of the sample M4. The arrow head points to a ~500bp DNA fragment.

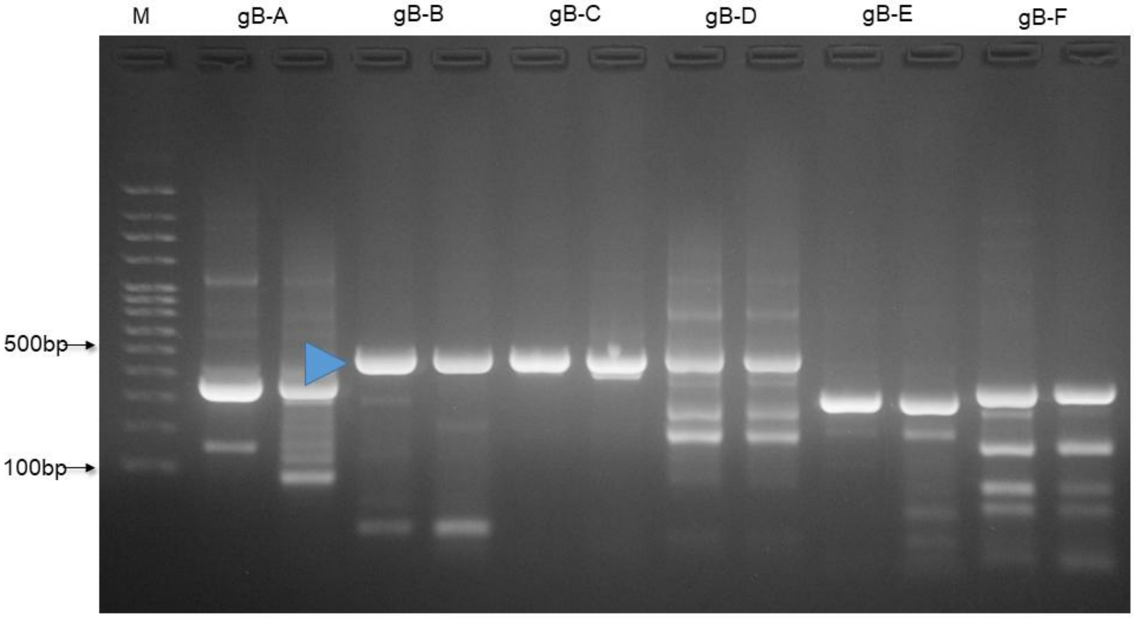

Figure 26- Visualization of the agarose gel using Chromato-Vue Transilluminator. Line M- DNA markers. The top arrow head points to a ~1200bp fragment and the bottom arrow head to a ~500 DNA fragment.

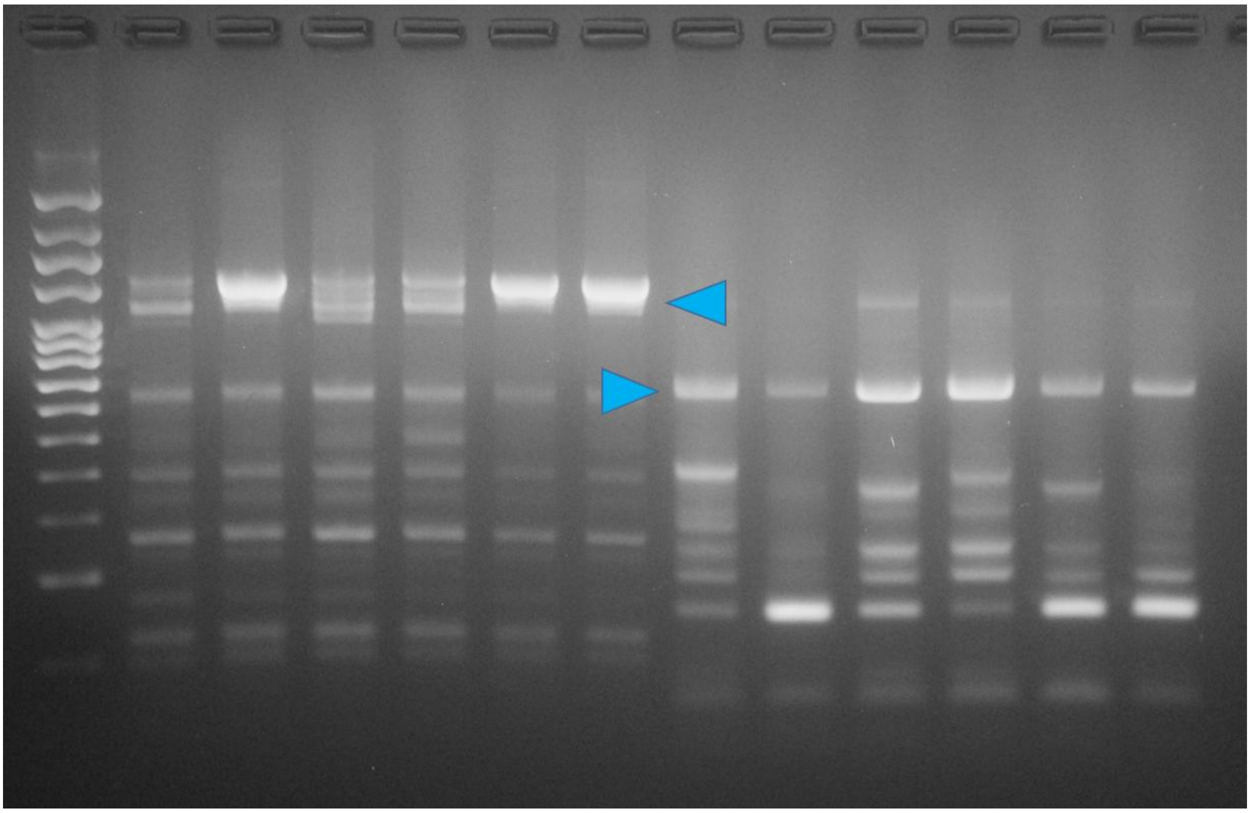

Figure 27- Visualization of the agarose gel using Chromato-Vue Transilluminator. Line M- DNA markers. The arrow head points to a ~500bp DNA fragment.

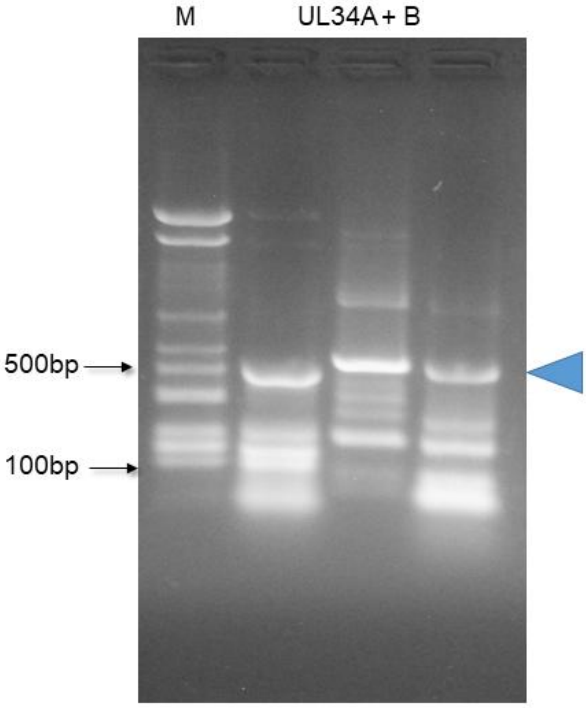

3.5.2. Sequencing analysis (Sanger method) and nucleotide comparison

Of the 55 samples sent to STABVIDA, only 32 were successfully sequenced. Given the lack of quality reads, the DNA *pol* partial gene was not considered for the phylogenetic analysis. An additional ORF (HP20) was identified within the fragment amplified for the UL18 gene.
Nucleotide sequences were used rather than protein sequences to evaluate populations geographically separated within the same species to explore variability.

3.5.3. Phylogenetic reconstruction

As not all partial genes sequences were obtained from the ChHV5 positive samples the number of sequences used for each gene tree varied. The sequences available in GenBank for each sample are also not available for all partial genes thus the number of geographic sites also varied.

For the glycoprotein B gene, three sequences were used from Guinea-Bissau, three from Mauritania and 20 reference sequences from California, Costa Rica, Florida, Barbados, Australia, Puerto Rico, Sao Tome e Principe and Hawaii. The statistical model used was the HKY model (Hasegawa et al., 1985).

For the UL18 and HP20 gene, two sequences were used from Guinea-Bissau, three from Mauritania and 11 reference sequences from Florida, Puerto Rico and Hawaii. The statistical model used was the GTR model (Tavaré, 1986).

Regarding the UL34 gene, one sequence was used from Guinea-Bissau, two from Mauritania and 16 reference sequences from California, Costa Rica, Florida, Barbados, Australia, Puerto Rico, Sao Tome e Principe and Hawaii. The statistical model used was the GTR model (Tavaré, 1986).

For the concatemers, two sequences were used from Guinea-Bissau, three from Mauritania and 22 reference sequences from Puerto Rico, São Tomé e Principe, Hawaii, Australia, Florida, Barbados, Costa Rica and California. The statistical model used was the HKY model (Hasegawa et al., 1985).

The codon positions 1st, 2nd, 3rd and non-coding were all included. All the trees were drawn to scale with branch lengths in the same units as those of the evolutionary distances used to infer the phylogenetic tree. The bootstrap method was employed with 1000 replicates.

However, only the UL34 gene-based tree is presented for discussion for the other trees did not compute correctly according to what is known in the literature.

3.5.4. Phylogeographical analysis of the ChHV5

The gene and concatemered trees are unrooted meaning the likelihood of the leave (operational taxonomical units) are calculated without a known ancestor.

The UL34 gene-based tree formed four distinct clusters, supported by a bootstrap value of >98%, each two sharing a common ancestor (Figure 28). The scale represents the time distance of the samples.

Figure 28 shows the 4 geographical groups that formed in the UL34 gene tree and figure 29 shows a time-tree for the samples used.

Figure 29 shows a time-tree with a scale of the time in which the samples were taken.

In figure 30 represents the HP20 gene tree and figure 31 the concatemered tree. All the trees were constructed using the methodology described in 2.12.3- Materials and Methods and in 3.5.3.-Results.

Figure 28- Phylogenetic tree based on *gene* UL34 inferred using BEAST V1.10.4, edited using FigTree V1.4.4., with visual colour-coded representation of each sequence on a global map and the corresponding geographically groups. The corresponding bootstrap value next to each nodes (original).

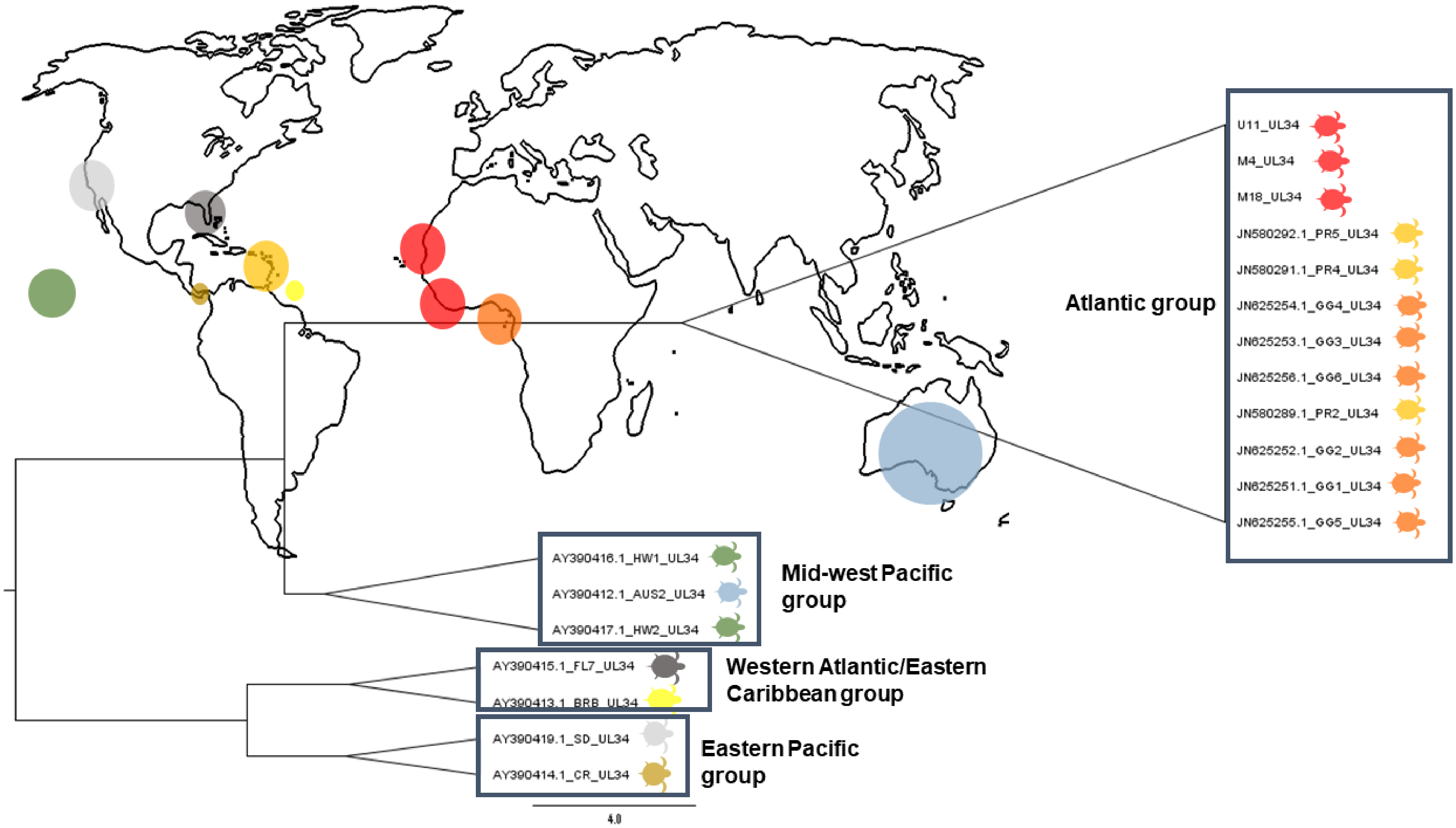

Figure 29- Phylogenetic tree based on gene UL34 inferred using BEAST V1.10.4, edited using FigTree V1.4.4., with visual colour-coded representation of each sequence on a global map and a colour-coded time bar of each samples (original).

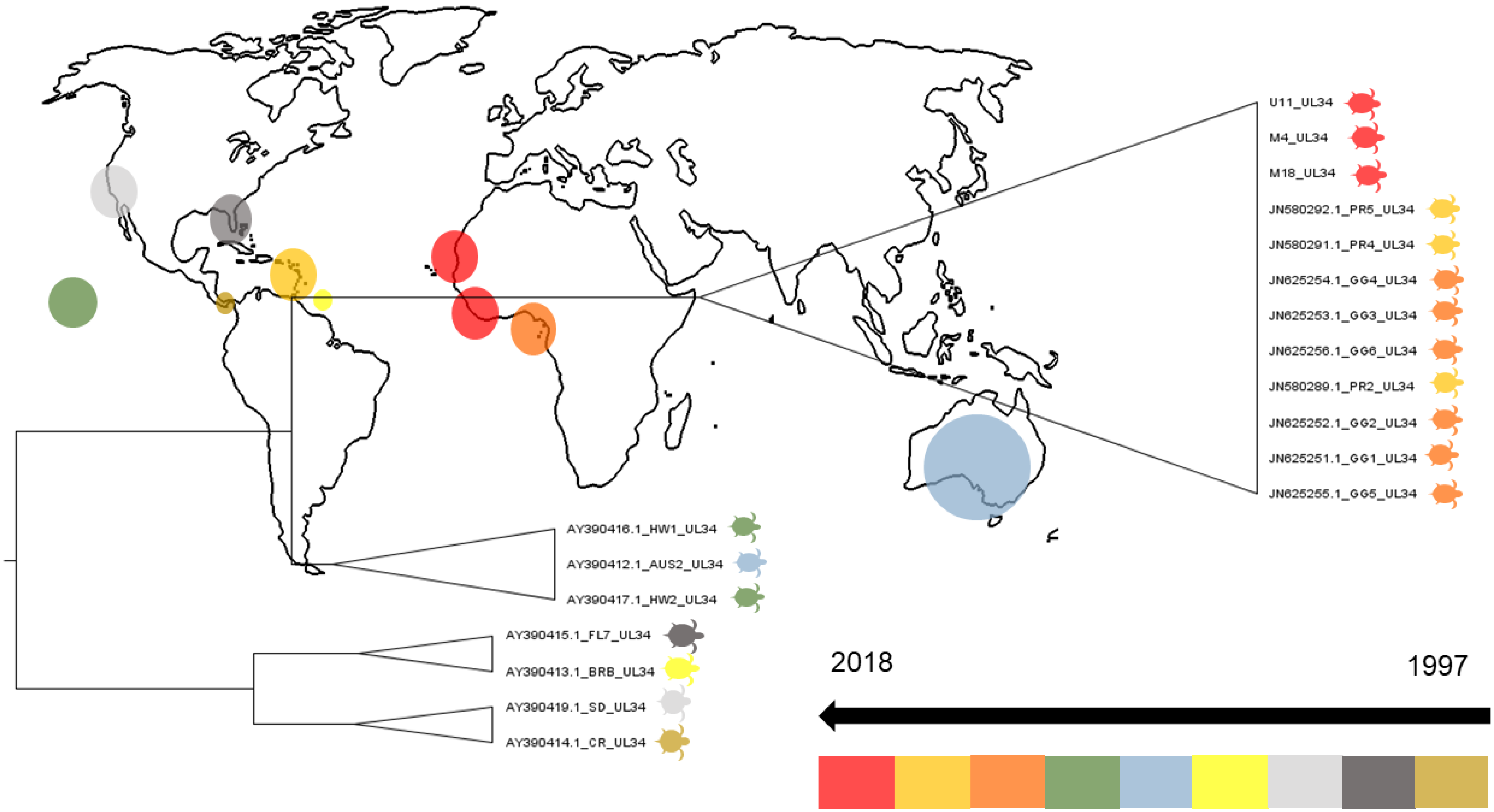

Figure 30- Phylogenetic tree based on gene HP20 inferred using BEAST V1.10.4, edited using FigTree V1.4.4., with visual colour-coded representation of each sequence on a global map and the corresponding geographically groups (original).

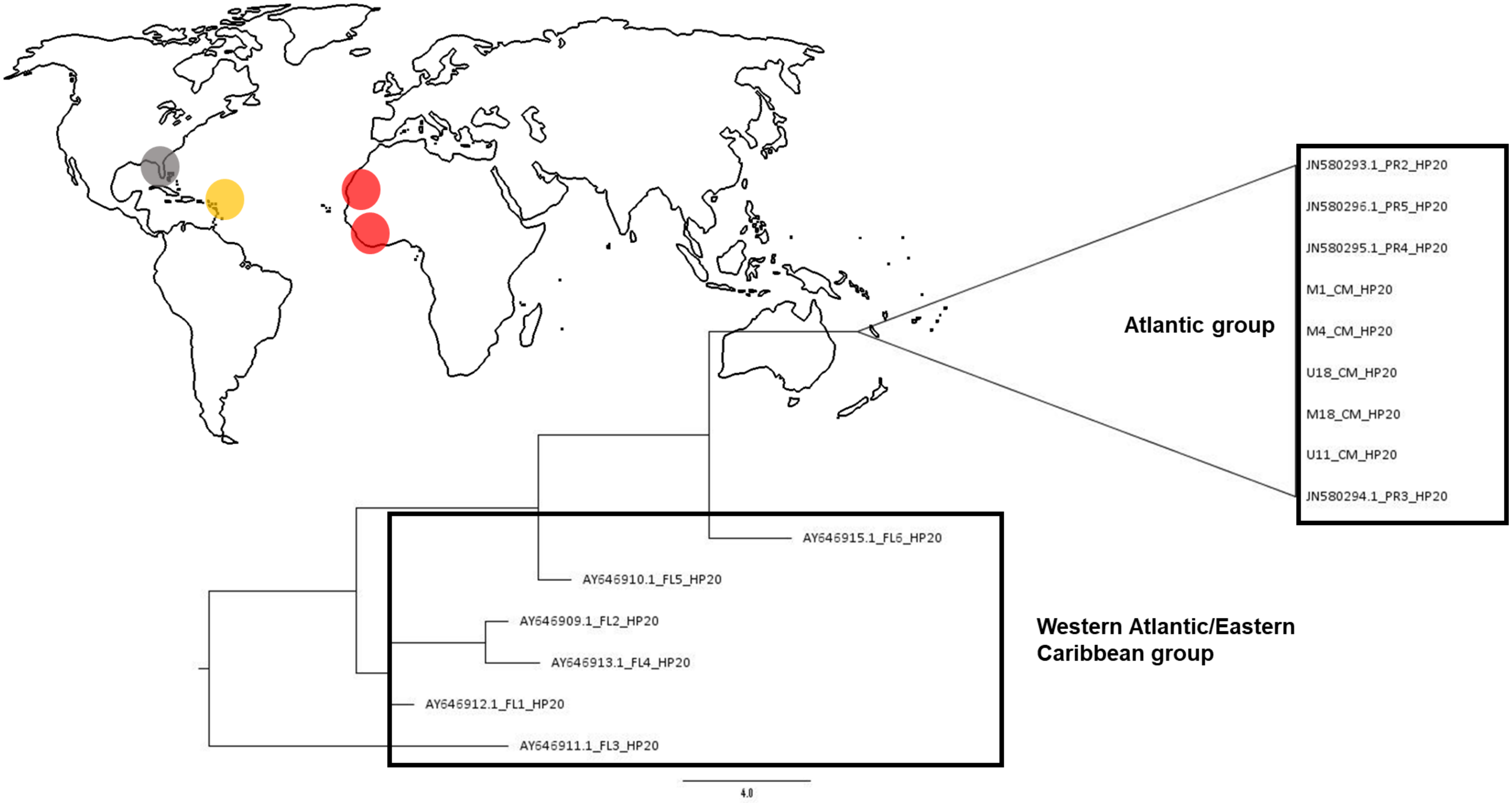

Figure 31- Phylogenetic tree of the concatermered genes inferred using BEAST V1.10.4, edited using FigTree V1.4.4., with visual colour-coded representation of each sequence on a global map and the corresponding geographically groups (original).

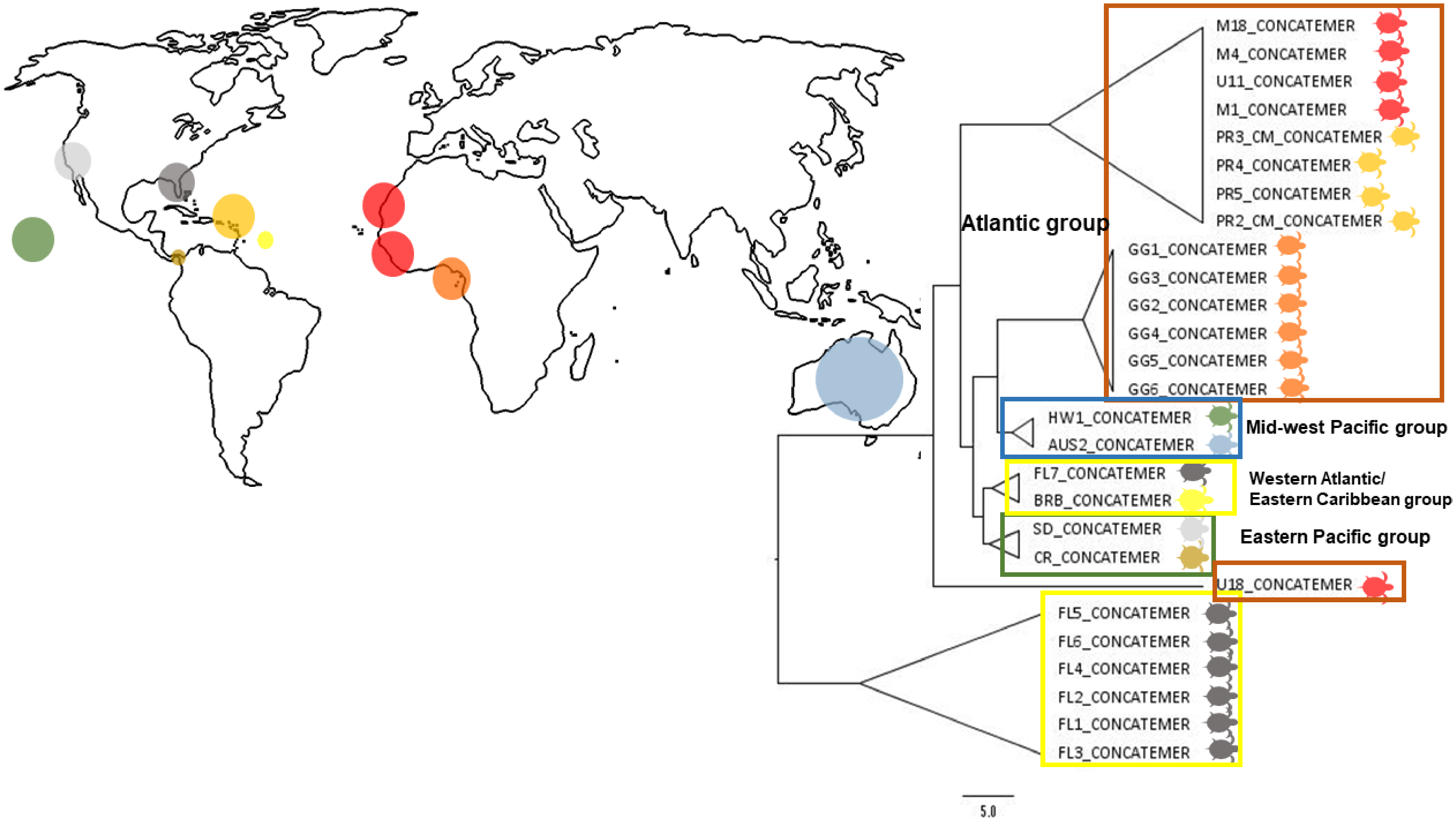

3.6. Statistical analysis results

All the information gathered regarding the captured turtles in available in appendix 7.1.

The size of the turtles (CCL) and the resulting Ct values were tested for normality using the Shapiro-Wilk test. The CCL was not normally distributed (W = 0.938, p-value = 7.86×10^{-05}) and the Ct values were marginally normally distributed (W = 0.940. p-value = 0.03). Thus, for consistency, non-parametric tests were employed for statistical analysis.

No significant difference was found on the CCL of turtles between the two study sites (W = 1101, p-value = 0.2049). There was also no significant difference on Ct values of the normal skin samples or the turtle life-stage (p-value=0.68322) between sites. Marginal significance was found between the presence of tumours and the size of the turtle (p-value = 0.0576). The average size of the turtles with FP lesions was less than that of animals without FP as shown in Figure 32.

No statistical association was found between the Ct obtained for the tumour samples and the geographic locations ($p>0.05$), however the normal skin samples were significantly different (p-value = $0.00231<0.005$) between locations. The Ct values were higher in turtles from Guinea-Bissau (GB), as shown in figure 32, meaning the samples from Mauritania (MAU) had higher viral loads (as Ct is inversely correlated with viral load).

The minimal adequate GAM showed that the CCL is significantly correlated with FP risk (GAM edf= 2.846, ref.df= 3.572, χ^2= 9.499, $p<0.05$). The function was non-monotonic (figure 32), as the FP lesions increase with the CCL, plateauing around 50-55cm and then decreasing (Figure 33).

Figure 32- Boxplot showing CCL range (cm) of individual with (YES) and without (NO) FP lesions on the left and on the right showing the mean Ct value of normal skin (Ct_N) from Guinea-Bissau (GB) and Mauritania (MAU). Made using RStudio (RStudioTeam, 2018).

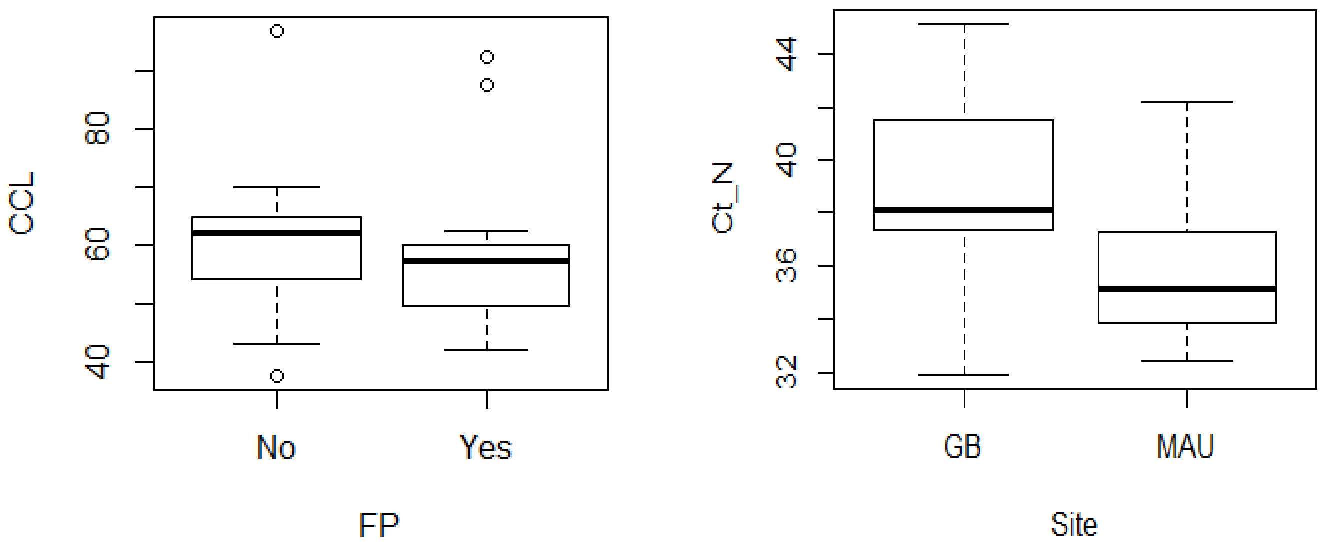

Figure 33- Graphical summary of GAM fitted to the CCL and FP lesions data. Made using RStudio (RStudioTeam, 2018).

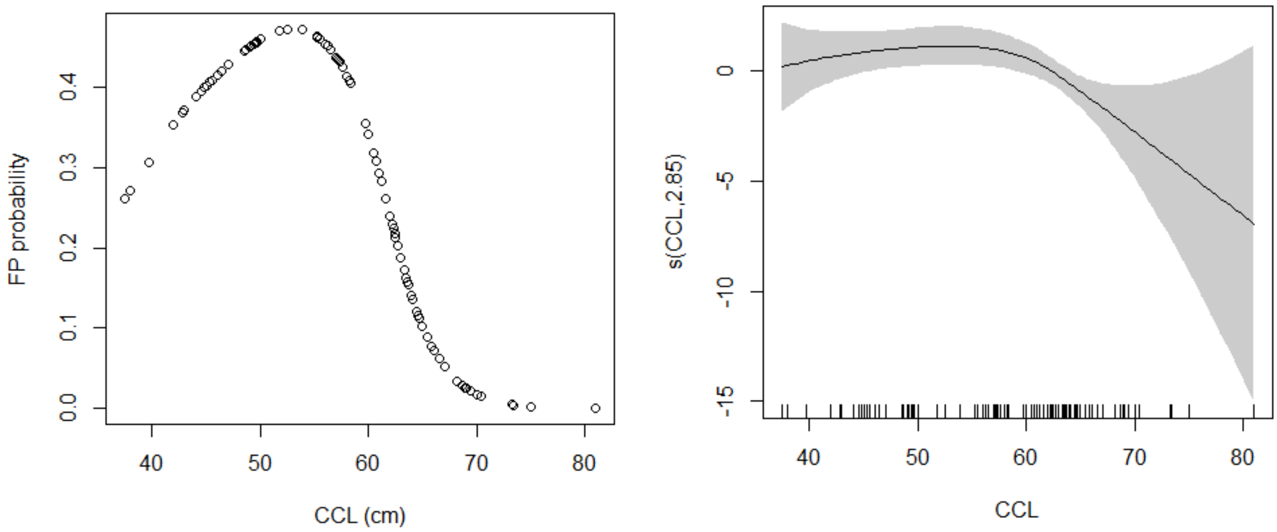

4. DISCUSSION

Prevalence of Fibropapillomatosis and expression

Fibropapillomatosis, a panzootic neoplastic disease, was first documented in the 1940s' (Smith and Coates, 1938). However, little information is available about this disease in sea turtles of West Africa (Duarte et al., 2012; Formia et al., 2007). This study is the first virological report of ChHV5, the leading aetiological agent candidate for FP, in green sea turtles from Guinea-Bissau (GB) and Mauritania (MAU).

The total prevalence of individuals with FP tumours was 32 of the 108 analysed (27%), with 12 (33%) in GB and 20 (28%) in MAU. Given this is the first report of FP in the region, the prevalence cannot be compared to data from previous studies on the same geographic sites. However, compared to other regions worldwide with reports of FP, this prevalence is lower than average, i.e. Hawaiian Islands up to 92% (Balazs, 1991); Florida up to 72.5% (Lackovich et al., 1999); Gulf of Mexico: 51.9% (Foley, Schroeder, Redlow, Fick-Child, & Teas, 2005); Indian River Lagoon, Florida: 61.6% (Hirama & Ehrhart, 2007); Australia up to 70% (Aguirre et al., 1999); Puerto Manglar: up to 75% (Patrício et al., 2016).

High prevalence of FP have been linked to anthropogenic activity and degradation of habitat (Keller et al., 2014; Van Houtan et al., 2010; Williams et al., 1994), and as the detection of ChHV5 variants have been shown to pre-date major outbreaks of the disease (Herbst et al., 2004; Patrício et al., 2012), this further implicates the role the environment has in influencing the expression of the disease. The sites where the turtles were captured for this study have very little human activity, limited to artisanal fisheries and some few local inhabitants. This may explain the lower prevalence registered in these areas. Another important factor is the high fidelity to foraging sites that green turtles typically demonstrate (Hirama & Ehrhart, 2007; Patricio et al., 2011). This behaviour may be important in limiting the spread of the infection from other regions with high FP prevalence (Patrício et al., 2016; Work et al., 2015).

Captured turtles with FP lesions were marginally smaller (mean=56.00cm) than those without (mean=60.22cm). Even though these results are inconsistent with previous studies (Aguirre, Balazs, Zimmerman, & Spraker, 1994; Baptistotte, 2007; Foley et al., 2005) the average size of the afflicted turtles is in accordance to most studies (Balazs, 1991; Dos Santos et al., 2010; Foley et al., 2005; Patrício et al., 2016). Our study showed that turtles with FP ranged from 39.7 to 97cm. The lower risk of lesions in smaller size classes (≤38cm) along with the high prevalence in intermediate juvenile size classes, as shown in Figure 33, supports the hypothesis that the FP associated agent is acquired after the recruitment of juveniles to the neritic zone, meaning local infection (Ene et al., 2005; Herbst, 1994; Rodenbusch et al., 2014). The average recruitment size is 30cm. Patrício et al. (2016), demonstrated that it takes up to 3 years for FP expression after recruitment, and up to 4 years for full recovery after the disease expression. Assuming a somatic growth of 5cm per year (Patrício, Diez, & van Dam, 2014), this supports the peak of FP risk around 45-55cm, as observed here.

In our study, the predominant FP tumour score was 1. The average size of the turtles increased in higher tumour scores. This phenomenon has been observed in other turtle populations (Work, Balazs, Rameyer, & Morris, 2004; Work, Balazs, Wolcott, & Morris, 2003) and is consistent with the development of tumours over time.

Although in most studies larger size classes are rarely afflicted (>80cm), which could potentially be explained due to increasing resistance to disease with age (Foley et al., 2005; Hirama & Ehrhart, 2007; Patrício et al., 2016; Work et al., 2004), in our study of the five adults captured, two had FP. One of the individuals had a tumour score of 1 and the other was heavily afflicted (tumour score=3). Despite tumour regression having been documented (Patrício et al., 2016; Tagliolatto, Guimarães, Lobo-Hajdu, & Monteiro-Neto, 2016), the pathway is still unclear. The adult (ID 19_GB) with tumour score 1 may potentially be going through tumour regression, which could explain the non-detection of virus in the tumour sampled. The continuation of the in-water capture-mark-recapture monitoring of the green turtles in GB may confirm this hypothesis, if this individual is recaptured in the future. The development of FP has also been linked to other co-infections and/or the immunological status of the individuals, which may explain why some animals develop more severe infections than others (Herbst & Klein, 1995). The heavily afflicted individual may have been exposed to other factors that led to development of the disease. A limiting factor to the assessment of the individuals in this study may have been the inability to collect information regarding their overall health condition through haematological parameters, which may be linked to the development of the disease.

It is to acknowledge that the sample size, particularly for GB, was small and may not represent the full scale of ChHV5 infectivity prevalence. The projects in GB and MAU are ongoing so further research shall give more insight into the prevalence of ChHV5 in these sea populations.

ChHV5 prevalence

A total of 55 of the 108 samples (51%) screened by qPCR were positive, 31 of the 76 normal skin samples (40%) and 24 of the 28 tumour samples (86%). Overall, 42 of the 76 (55%) individuals tested were positive to the detection of ChHV5.

The detection of ChHV5 in most (86%) of the tumour samples is consistent with the role of this virus as aetiological agent of FP (Yuanan Lu et al., 2000; Quackenbush et al., 1998). The high positive percentage also demonstrates that tumour samples are the best matrix for viral detection. However, this study also revealed a proportion of asymptomatic individuals (21 turtles) that tested positive for ChHV5.

This phenomenon was higher in turtles captured from MAU (32% of clinical healthy individuals) than those from GB (16%). The Ct values of the normal skin samples were also significantly lower in the turtles from MAU, indicating higher viral loads in the tissues. Given that FP is likely a multi-factorial disease, this difference could indicate a difference in resistance in the populations or environment factors that, in combination with herd immunity, may influence the prevalence/ development of FP in each region (Alfaro-Núñez et al., 2014; Patrício et al., 2016; Work et al., 2001). Given that the populations from these areas are small, the influence of a spreader may be particularly important in these locations (Patrício et al., 2016). Even though the FP prevalence was low, the high viral loads in the MAU population and the high prevalence of ChHV5 DNA may mean that there could be a start of an epidemic linked to an individual with very high viral shedding. Vigilance of the evolution of this group is important as the results suggest a high FP risk.

Our qPCR results suggest that these turtles may be carriers of the virus (asymptomatic reservoirs), or alternatively, may undergo early infection or latent infection, meaning that they may develop clinical disease in the future (Alfaro-Núñez et al., 2014; Quackenbush et al., 2001). Even though this result does not correlate to the prevalence of FP, it is important evidence to help understand the pathogenesis of the disease and supports its panzootic status (Herbst & Klein, 1995; Herbst, 1994).

Only 36% of the samples from non-tumoured areas of FP exhibiting turtles were positive to ChHV5. This result is in concordance with the detection of ChHV5 found by some studies (Chaves et al., 2017; Quackenbush et al., 2001), however is lower than the value obtained in others reports from other regions (Chaves et al., 2017; Yuanan Lu et al., 2000; Page-Karjian et al., 2012). Latency, a known ability within herpesviruses, is an important point to research with ChHV5. This virus is not a “new” virus, as research has shown that it has co-evolved with its’ host for at least 8.9 millions of years (Herbst et al., 2004; Patrício et al., 2012). They have the ability, after establishing latency, to have minimal viral expression to avoid detection by the immune system. This may lead to an unequal tissue distribution within the same individual, were only the affected tissue has high viral loads. During the active viraemic phase, viral DNA may be detected throughout the body, while in chronic infections viral activity may be limited to tumours (Alfaro-Núñez et al., 2014), which may explain this difference in detection between sample type and between studies.

There was no statistical significance between the tumour score and the Ct value in tumour samples. This reveals that the viral load is unrelated to the severity of the tumours.

Lastly, the ChHV5 DNA copies were substantially higher in tumour samples (range= 4.23E+02 to 1.15E+07 copies) compared to samples of normal skin tissue (range=6.95E+01 to 4.67E+03 copies), further implicating the ChHV5 in the formation of FP tumours.

Validation of the method for ChHV5 detection by Quackenbush et al. (2001)

The standard curve showed a 100% efficiency (equation= [10(-1/slope-1)]) demonstrating the robustness of the qPCR method. This result, along with the results of the specificity of this method, demonstrate that the primers designed by Quackenbush (2001) are efficient and precise in the amplification of the target region, even though they were only tested for cross-reactivity by in silico analysis. This method also revealed a low LOD reflecting its high sensitivity.

In regard to the reproducibility and repeatability of the qPCR assay, results showed some variability. In the intra-assay test the dilutions 10^{-1} and 10^{-2} showed higher variation percentages (10.6%-11%) however the other dilutions revealed low variations (0.54%-2.89%). In the inter-assay tests the dilutions 10^{-2} and 10^{-3} showed higher inter-assay variation (6%-8.6%), despite the other dilutions revealed low variations (1.82%-2.28%). These results indicate that the qPCR assay has more reliable results with lower DNA copies than with high, as expected. However, this method still reveals high repeatability and reproducibility as all CV values were <20% (Page-Karjian et al., 2015).

qPCR has the advantage of being a fast and quantitative method for detection of this virus. However, other methods have been described for the detection of ChHV5 in both tumour and non-tumour samples, namely PCR assay. Alfaro-Núñez et al. (2014) described a sensitive singleplex assay that revealed to have better amplification levels that the standard nested assay described by Quackenbush et al. (2001) used in this study. This competitive alternative could be considered for future research. The limitation of the singleplex assay method is that does not give quantitative information of the viral load.

This quantitative feature of qPCR allows to furthermore implicate the virus as causative agent of FP, for not only does it reveal whether a sample is positive or not, but it also allows to estimate the viral load present.

ChHV5 phylogenetic analysis

Previous phylogenetic analysis of ChHV5 variants showed that there is a strong spatial heterogeneity in the distributions of variants (Greenblatt et al., 2005; Herbst et al., 2004; Patrício et al., 2012). Patrício et al. (2012) identified four major geographical groups that included: the eastern Pacific group (samples from San Diego and Costa Rica); the western Atlantic/eastern Caribbean group (samples from Florida and Barbados); the Atlantic group (samples from São Tomé e Principe and Puerto Rico); the mid-west Pacific group (samples from Australia and Hawaii).

From phylogenetic analysis based on the UL34 sequences obtained from GB and MAU and 16 available sequences from the NCBI database, the West African sequences clustered with the Atlantic group (Figure 26), along with the samples from Puerto Rico and São Tomé e Principe. This result is as expected, given the geographical location of the new sequences. In our tree, the other samples also clustered as previous studies have shown (Patrício et al., 2012). The HP20 gene formed two clusters (Atlantic group and Western Atlantic/Eastern

Caribbean group) however the Western Atlantic group did not form a single clade as in previous literature (Patrício et al., 2012). This may due to the different species used in the analysis (*Caretta caretta*, *Lepidochelys olivacea* and *Lepidochelys kempii*) and the small sample group. The concatemered tree also showed some inconsistencies as the Western Atlantic group also did not cluster together and the sample U18 from GB formed its own node.

Sea turtles have a complex life history, passing through an oceanic stage (the "lost years"), then as juveniles recruiting to a foraging area where they remain for several years (Patrício et al., 2012). These foraging areas are often cohabited by juveniles from different nesting areas. Evidence shows that infection normally occurs during this phase highlighting the importance of studying this life-stage of the turtles (Ene et al., 2005). Given that the individuals are most likely infected in the neritic areas, then the similarities between ChHV5 variants within each geographical group are consistent with horizontal transmission. The clear geographical isolations and divergence of the virus also supports this (Patrício et al., 2012). It also demonstrates that the viral particles are probably transmitted and distributed through skin shedding (Patrício et al., 2012; Work et al., 2017).

The closeness of the Puerto Rican and African variants is unexpected, however Patrício et al. (2012) suggested that the equatorial current that exists between the Gulf of Guinea and Brazil (with a northern arm continuing to the Eastern Greater Antilles) may be responsible of the dispersal of hatchlings from Puerto Rico to eastern Atlantic waters. Moreover, mixed-stock analysis of the mitochondrial DNA demonstrated that shared haplotypes between the Puerto Rican foraging areas and West African rookeries (Patrício et al., 2012), indicated a possible viral gene flow between the areas.

Phylogenetic analysis is also important in understanding the co-evolution between the host and virus. The identification of viral variants may explain differences in pathogenesis (Alfaro-Núñez et al., 2014), one of the lacunas that needs investigation in this disease. Host specific response to infectious diseases is likely heritable and may explain the differences observed in the individuals, however there is a possibility that the genetic variant may also be responsible for disease susceptibility and pathogenicity (Alfaro-Núñez et al., 2014). ChHV5 has co-evolved with its turtles' hosts for at least 8.9 millions of years (Patrício et al., 2012). Recently, it has been proposed that disrupted co-evolution between the host and virus may explain the variations in disease outcomes, however it has not been proven adequate in explaining the heterogeneity of FP pathology (Alfaro-Núñez et al., 2014). This leads back to other factors being more likely cause of FP expression, such as environmental factors and herd immunity.

The other trees (based on genes UL18, glycoprotein B and HP20) and the concatemered tree revealed contradicting information in comparison of what is presently accepted, therefore were not presented in this study. This may be due to the quality of the sequencing, as many sequences were only partial amplifications, which may not have enough discriminatory power, or due to mutations in the genes, and needed further investigation.

5. FINAL CONSIDERATIONS

The marine turtles, once abundant in tropical and temperate waters up to the 19th century, are now globally facing various threats. West Africa is home to some of the biggest Atlantic green sea turtle populations, therefore an important site for conservation. This study is not only the first scientific report of FP in Guinea-Bissau and Mauritania, but also the first time that the ChHV5 has been detected in these sites.

Green sea turtles are under numerous environmental pressures, such as loss of habitat, degradation of the water quality, by-catch, illegal harvesting, among others. The recent epidemic outbreaks of FP are of pressing concern as they may pose an additional threat to the future survival of this vulnerable specie. Little is known about the pathology of this disease, but its presence in such an important population could bring negative consequences. The life-cycle of free-ranging sea turtles still has some lacunas, however it is know that they travel thousands of kilometres, establishing connections between distant areas. This connectivity between different geographical areas has been proven by the similarity of the viral variants. The spread of ChHV5 across the Atlantic may be due to the movement of the individuals, carrying the disease to previous naïve populations, expanding a local issue to a global issue (Patrício et al., 2016). This possibility should be investigated and may encourage the collaboration of the various marine turtle projects across the Atlantic.

The ongoing climate change is also a global issue that is driving the adaption of marine turtle populations as well as bringing new threats. Emerging infectious diseases in marine ecosystems have increased in recent decades, reactivating previously latent diseases and introducing new, potentially fatal, diseases to the populations (Patrício et al., 2017). The future implications of the changes in climate on FP are uncertain, nonetheless, it should be closely studied as research has already shown its effect on other species (Patrício et al., 2017).

To better understand the dynamics of the green sea turtle population from West Africa (GB and MAU), further research is needed. This study has contributed by establishing a baseline of information on FP and ChHV5 prevalence. Recapture of the individuals is important to be able to study the evolution of FP afflicted turtles as well as to study the prevalence of the disease throughout the years. Patrício et al. (2016) showed that the prevalence of FP may fluctuate through the years, therefore long-term monitoring is beneficial.

Future research should focus on more information regarding the health conditions of the turtles, which can be assessed through haematological data and water quality studies. Further molecular research should also be considered as it brings new insights to this old yet new disease. Success in the conservation of this marine species depends on measures that minimize the anthropogenic effects on their migratory path, foraging and nesting areas. Even though GB and MAU have successfully implemented these measures, sea turtles are global animals, meaning these measures have to be considered worldwide.

FP is a threat on an individual scale, nevertheless, understanding its impact on the population is fundamental for creating long-lasting conservation plans for the marine turtle population worldwide.

6. REFERENCES

Ackermann, M., Koriabine, M., Hartmann-Fritsch, F., de Jong, P. J., Lewis, T. D., Schetle, N., … Leong, J. A. C. (2012). The genome of Chelonid Herpesvirus 5 harbors atypical genes. *PLoS ONE*, *7*(10).

Adams, M. J., & Carstens, E. B. (2012). Ratification vote on taxonomic proposals to the International Committee on Taxonomy of Viruses (2012). *Archives of Virology*, *157*(7), 1411–1422.

Aguirre, A. A., Balazs, G. H., Zimmerman, B., & Spraker, T. R. (1994). Evaluation of Hawaiian green turtles (Chelonia mydas) for potential pathogens associated with fibropapillomas. *Journal of Wildlife Diseases*, *30*(1), 8–15.

Aguirre, A. A., Limpus, C., Spraker, T., & Balazs, G. (1999). Survey of fibropapillomatosis and other potential diseases in marine turtles from Moreton Bay, Queensland, Australia. *The 19th Annual Symposium on Sea Turtle Biology and Conservation*.

Aguirre, A. A., Ostfeld, R. S., Tabor, G. M., House, C., & Pearl, M. C. (2002). Monitoring of Fibropapillomatosis in sea turtles. In Oxford University Press, Inc. (Ed.), *Conservation Medicine: Ecological Health in Practice*. (pp. 82-83).

Airaud, B. F., Regalla, A., Barbosa, C., & Betunde, D. (2016). SWOT Report- The State of the World’s Sea Turtles, Vol. XI. *Special Feature- South America*, *XI*, 40–41.

Alfaro-Núñez, A., Bertelsen, M. F., Bojesen, A. M., Rasmussen, I., Zepeda-Mendoza, L., Olsen, M. T., & Gilbert, M. T. P. (2014). Global distribution of Chelonid fibropapilloma-associated herpesvirus among clinically healthy sea turtles. *BMC Evolutionary Biology*, *14*(1), 1–11.

Alfaro-Núñez, A., Bojesen, A. M., Bertelsen, M. F., Wales, N., Balazs, G. H., & Gilbert, M. T. P. (2016). Further evidence of Chelonid herpesvirus 5 (ChHV5) latency: high levels of ChHV5 DNA detected in clinically healthy marine turtles. *PeerJ*, *4*, e2274.

Alfaro-Nuñez, A., & Thomas, M. G. P. (2014). Validation of a sensitive PCR assay for the detection of Chelonid fibropapilloma-associated herpesvirus in latent turtle infections. *Journal of Virological Methods*, *206*, 38–41.

Alfaro, A., Koie, M., & Buchmann, K. (2006). Synopsis of infections in sea turtles caused by virus, bacteria and parasites: an ecological review. *NOAA Technical Memorandum NMFS SEFSC*, 30.

Balazs, G. H. (1991). Current status of fibropapillomas in the Hawaiian green turtle, Chelonia mydas. *Research Plan for Marine Turtle Fibropapilloma*, (U.S. Dep. Commer., NOAA Tech. Memo. NMFS-SWFSC-156), 47–57.

Baptistotte, C. (2007). *Caracterização espacial e temporal da fibropapilomatose em tartarugas marinhas da costa brasileira*. Tese de doutoramento em Ecologia aplicada. São Paulo: Universidade de São Paulo- Escola Superior de Agricultura "Luiz de Queiroz".

Bjorndal, K. A., & Jackson, J. B. C. (2003). Roles of Sea Turtles in Marine Ecosystems: Reconstructing the Past. In CRC Press (Ed.), *The Biology of Sea Turtles* (3rd ed.). (pp. 259–273). Boca Raton, Florida.

Bouchard, S. S., & Bjorndal, K. A. (2008). Sea Turtles as Biological Transporters of Nutrients and Energy from Marine to Terrestrial Ecosystems. *Ecological Society of America*, *81*(8), 2305–2313.

Brunner, C. H. M., Dutra, G., Silva, C. B., Silveira, L. M. G., & Monteiro Martins, M. de F. (2014). Electrochemotherapy for the treatment of fibropapillomas in *Chelonia* mydas. *Journal of Zoo and Wildlife Medicine*, *45*(2), 213–218.

Cárdenas, D. M., Cucalón, R. V., Medina-Magües, L. G., Jones, K., Alemán, R. A., Alfaro-Núñez, A., & Cárdenas, W. B. (2019). Fibropapillomatosis in a Green Sea Turtle (*Chelonia mydas*) from the Southeastern Pacific. *Journal of Wildlife Diseases*, *55*(1), 169–173.

Casey, R. N., Quackenbush, S. L., Work, T., Balazs, G., Bowser, P. R., & Casey, J. W. (1997). Evidence for retrovirus infections in green turtles Chelonia mydas from the Hawaiian Islands. *Diseases of Aquatic Organisms* (Vol. 31).

Catry, P., Barbosa, C., Indjai, B., Almeida, A., Godley, B. J., & Vié, J. C. (2002). First census of the green turtle at Poilão, Bijagós Archipelago, Guinea-Bissau: The most important nesting colony on the Atlantic coast of Africa. *Oryx*, *36*(4), 400–403.

Catry, P., Barbosa, C., Paris, B., Indjai, B., Almeida, A., Limoges, B., … Pereira, H. (2009). Status, Ecology, and Conservation of Sea Turtles in Guinea-Bissau. *Chelonian Conservation and Biology*, *8*(2), 150–160.

Cavicchioli, R., Ripple, W. J., Timmis, K. N., Azam, F., Bakken, L. R., Baylis, M., … Webster, N. S. (2019). Scientists' warning to humanity: microorganisms and climate change. *Nature Reviews Microbiology*.

Chaves, A., Aguirre, A. A., Blanco-Pena, K., Moreira-Soto, A., Monge, O., Torres, A. M., … Lierz, M. (2017). Examining the Role of Transmission of Chelonid Alphaherpesvirus 5. *EcoHealth*, *14*(3), 530–541.

D'Amatto, A. F., & Moraes-Neto, M. (2000). First documentation of fibropapillomas verified by histopathology in Eretmochelys imbricata. *Marine Turtle Newsletter*, *89*, 12–13.

Deem, S. L. (2015). Conservation Medicine to One Health: The Role of Zoologic Veterinarians. In *Fowler's Zoo and Wild Animal Medicine (*Volume 8). (pp. 698–703).

Devanter, D. R. V. A. N., Warrener, P., Bennett, L., Schultz, E. R., Coulter, S., Garber, R. L., … Black, J. (1996). Detection and Analysis of Diverse Herpesviral Species by Consensus Primer PCR, *34*(7), 1666–1671.

DNeasy Blood & Tissue Handbook. (2006). Protocol : Purification of Total DNA from Animal Tissues (Spin-Column Protocol). *DNeasy Blood & Tissue Handbook*, *7*, 28–30.

Dos Santos, R. G., Martins, A. S., Torezani, E., Baptistotte, C., Da Nóbrega Farias, J., Horta, P. A., … Balazs, G. H. (2010). Relationship between fibropapillomatosis and environmental quality: A case study with chelonia mydas off Brazil. *Diseases of Aquatic Organisms*, *89*(1), 87–95.

Duarte, A., Faísca, P., Loureiro, N. S., Rosado, R., Gil, S., Pereira, N., & Tavares, L. (2012). First histological and virological report of fibropapilloma associated with herpesvirus in Chelonia mydas at Príncipe Island, West Africa. *Archives of Virology*, *157*(6), 1155–1159.

Ene, A., Su, M., Lemaire, S., Rose, C., Schaff, S., Moretti, R., … Herbst, L. H. (2005). Distribution of Chelonid Fibropapillomatosis-Associated Herpesvirus Variants in Florida:

Molecular Genetic Evidence for Infection of Turtles Following Recruitment To Neritic Developmental Habitats. *Journal of Wildlife Diseases*, *41*(3), 489–497.

Flint, M., Patterson-Kane, J., Limpus, C., & Mills, P. (2010). Health Surveillance of Stranded Green Turtles in Southern Queensland, Australia (2006-2009): An Epidemiological Analysis of Causes of Disease and Mortality. *EcoHealth* (Vol. 7).

Foley, A. M., Schroeder, B. A., Redlow, A. E., Fick-Child, K. J., & Teas, W. G. (2005). Fibropapillomatosis in Stranded Green Turtles (Chelonia Mydas) From the Eastern United States (1980–98): Trends and Associations With Environmental Factors. *Journal of Wildlife Diseases*, *41*(1), 29–41.

Formia, A., Deem, S., Billes, A., Ngouessono, S., Parnell, R., Collins, T., … Spraker, T. (2007). Fibropapillomatosis confirmed in Chelonia mydas in the Gulf of Guinea, West Africa. *Marine Turtle Newsletter* (Vol. 116).

Frazier, J. (2005). Marine turtles: the role of flapship species in interactions between people and the sea. *Maritime Studies*, 5–38.

Godbey, W. T. (2014). Cell Growth. In Elsevier Ltd. (Ed.), *An Introduction to Biotechnology* (1st ed., Vol. 1). (pp. 107–142).

Godley, B. J., Barbosa, C., Bruford, M., Broderick, A. C., Catry, P., Coyne, M. S., … Matthew, J. (2010). Unravelling migratory connectivity in marine turtles using multiple methods. *Journal of Applied Ecology*, *47*(4), 769–778.

Greenblatt, R. J., Quackenbush, S. L., Casey, R. N., Rovnak, J., Balazs, G. H., Work, T. M., … Sutton, C. A. (2005). Genomic Variation of the Fibropapilloma-Associated Marine Turtle Herpesvirus across Seven Geographic Areas and Three Host Species. *Journal of Virology*, *79*(2), 1125–1132.

Greenblatt, Rebecca J., Work, T. M., Balazs, G. H., Sutton, C. A., Casey, R. N., & Casey, J. W. (2004). The Ozobranchus leech is a candidate mechanical vector for the fibropapilloma-associated turtle herpesvirus found latently infecting skin tumors on Hawaiian green turtles (Chelonia mydas). *Virology*, *321*(1), 101–110.

Greenblatt, Rebecca J., Work, T. M., Dutton, P., Sutton, C. A., Spraker, T. R., Casey, R. N., … Casey, J. W. (2005). Geographic Variation in Marine Turtle Fibropapillomatosis. *Journal of Zoo and Wildlife Medicine*, *36*(3), 527–530.

Hama, F. L., Dyc, C., Samba, A., Bilal, O., Wagne, M. M., Mullie, W., … Fretey, J. (2018). Chelonia mydas and Caretta Caretta nesting activity along the Mauritanian coast. *Salamandra*, *54*, 45–55.

Harshbarger, J. C. (1991). Sea turtle fibropapilloma cases in the registry of tumors in lower animals. In *Workshop research plan for marine turtle fibropapilloma* (pp. 63–70).

Harvell, C. D., Mitchell, C. E., Ward, J. R., Altizer, S., Dobson, A. P., Ostfeld, R. S., & Samuel, M. D. (2002). Climate warming and disease risks for terrestrial and marine biota. *Science*, *296*(5576), 2158–2162.

Hasegawa, M., Kishino, H., & Yano, T. (1985). Dating of the human-ape splitting by a molecular clock of mitochondrial DNA. *Journal of Molecular Evolution*, *22*(2), 160–174.

Herbst, L. H., Jacobson, E. R., Moretti, R., Brown, T., Sundberg, J. P., & Klein, P. A. (1995). Experimental transmission of green turtle fibropapillomatosis using cell-free tumor extracts. *Diseases of Aquatic Organisms*, *22*(1), 1–12.

Herbst, L. H., & Klein, P. A. (1995). Green turtle fibropapillomatosis: Challenges to assessing the role of environmental cofactors. *Environmental Health Perspectives*, *103*(4), 27–30.
Herbst, Larry, Ene, A., Su, M., Desalle, R., & Lenz, J. (2004). Tumor outbreaks in marine turtles are not due to recent herpesvirus mutations. *Current Biology*, *14*(17), 697–699.

Herbst, Lawrence H. (1994). Fibropapillomatosis of Marine Turtles. *Anual Review of Fish Diseases*, *4*, 389–425.

Herbst, LH, Moretti, R., Brown, T., & Klein, P. (1995). Sensitivity of the transmissible green turtle fibropapillomatosis agent to chloroform and ultracentrifugation conditions. *Diseases of Aquatic Organisms*, *25*, 225–228.

Hirama, S., & Ehrhart, L. M. (2007). Description, prevalence and severity of green turtle fibropapillomatosis in three developmental habitats on the east coast of Florida. *Florida Scientist*, (70), 435–448.

Ho, S. Y. W., Phillips, M. J., Cooper, A., & Drummond, A. J. (2005). Time dependency of molecular rate estimates and systematic overestimation of recent divergence times. *Molecular Biology and Evolution*, *22*(7), 1561–1568.

Huerta, P., Pineda, H., Aguirre, A. A., Spraker, T., Sarti, L., & Barragán, A. (2002). First confirmed case of fibropapilloma in a leatherback turtle (Dermochelys coriacea). *Proc 20th Ann Symp Sea Turtle Biol Cons*.

Jacobson, E., Buergelt, C., Williams, B., & Harris, R. (1991). Herpesvirus in cutaneous fibropapillomas of the green turtle Chelonia mydas. *Diseases of Aquatic Organisms*, *12*(1), 1–6.

Jacobson, E. R. (2007). *Infectious Diseases and Pathology of Reptiles: Color Atlas and Text*.
Jones, K., Ariel, E., Burgess, G., & Read, M. (2016). A review of fibropapillomatosis in Green turtles (Chelonia mydas). *Veterinary Journal*, *212*, 48–57.

Keller, J. M., Balazs, G. H., Nilsen, F., Rice, M., Work, T. M., & Jensen, B. (2014). Investigating the potential role of persistent organic pollutants in Hawaiian green sea turtle fibropapillomatosis National Institute of Standards and Technology , Chemical Sciences Division , Hollings Marine National Marine Fisheries Service , Pacific Is.

Key steps in plasmid purification protocols. (2013). Retrieved April 15, 2019, from https://www.qiagen.com/us/service-and-support/learning-hub/technologies-and-research-topics/plasmid-resource-center/key-steps-in-the-plasmid-purification-protocols/

Knöbl, T., Reiche, R., & Menão, M. C. (2011). Fibropapilomatose em tartarugas marinhas. *Neotropical Biology and Conservation*, *6*(1), 64–69.

Kumar, S., Stecher, G., Li, M., Knyaz, C., & Tamura, K. (2018). MEGA X: Molecular evolutionary genetics analysis across computing platforms. *Molecular Biology and Evolution*, *35*, 1547–1549.

Lackovich, J. K., Daniel, R., Homer, L., Garber, R. L., Douglas, R., Moretti, R. H., … Klein, P. A. (1999). Association of herpesvirus with fibropapillomatosis of the Green turtle Chelonia mydas and the loggerhead turtle Carreta Carreta in Florida. *Diseases of Aquatic Organisms*, (37), 89–97.

Lipkin, W. I. (2009). Microbe hunting in the 21st century. *Proceedings of the National Academy of Sciences of the United States of America*, (106), 6–7.

Lloyd-Smith, J. O., Cross, P. C., Briggs, C. J., Daugherty, M., Getz, W. M., Latto, J., … Swei,

A. (2005). Should we expect population thresholds for wildlife disease? *Trends in Ecology & Evolution*, *20*(9), 511–519.

Lu, Y, Aguirre, A. A., Work, T. M., Balazs, G. H., Nerurkar, V. R., & Yanagihara, R. (2000). Identification of a small, naked virus in tumor-like aggregates in cell lines derived from a green turtle, Chelonia mydas, with fibropapillomas. *Journal of Virological Methods*, *86*(1), 25–33.

Lu, Yuanan, Yu, Q., Zamzow, J., & Al., E. (2000). Detection of green turtle herpesviral sequence in saddleback wrasse Thalassoma duperrey: a possible mode of tranmission of green turtle fibropapilloma. *Journal of Aquatic Animal Health*, (12), 58–63.

Matlock, B. (2015). Assessment of Nucleic Acid Purity. *Thermo Fisher Scientific*.

McGeoch, D. J., & Gatherer, D. (2005). *Integrating reptilian herpesviruses into the Family Herpesviridae*.

Mint Hama, L., Fretey, J., & Aksissou, M. (2013). Nouvelles données sur le statut des Tortues marines en Mauritanie. *Bull. Soc. Herp. Fr*, (December), 127–142.

Monezi, T. A., Mehnert, D. U., de Moura, E. M. M., Müller, N. M. G., Garrafa, P., Matushima, E. R., … Borella, M. I. (2016). Chelonid herpesvirus 5 in secretions and tumor tissues from green turtles (Chelonia mydas) from Southeastern Brazil: A ten-year study. *Veterinary Microbiology*, *186*, 150–156.

Monzón-Argüello, C., López-Jurado, L. F., Rico, C., Marco, A., López, P., Hays, G. C., & Lee, P. L. M. (2010). Evidence from genetic and Lagrangian drifter data for transatlantic transport of small juvenile green turtles. *Journal of Biogeography*, *37*(9), 1752–1766.

Page-Karjian, A. (2019). Fibropapillomatosis in Marine Turtles. In Elsevier Inc. (Ed.), *Fowler's Zoo and Wild Animal Medicine Current Therapy (Volume 9)*. (pp 398-403).

Page-Karjian, A., Gottdenker, N. L., Whitfield, J., Herbst, L., Norton, T. M., & Ritchie, B. (2017). Potential Noncutaneous Sites of Chelonid Herpesvirus 5 Persistence and Shedding in Green Sea Turtles Chelonia mydas. *Journal of Aquatic Animal Health*, *29*(3), 136–142.

Page-Karjian, A., Norton, T., Ritchie, B., Brown, C., Mancia, C., Jackwood, M., & Gottdenker, N. (2015). Quantifying chelonid herpesvirus 5 in symptomatic and asymptomatic rehabilitating green sea turtles. *Endangered Species Research* (Vol. 28).

Page-Karjian, A., Torres, F., Zhang, J., Rivera, S., Diez, C., Moore, P. A., … Brown, C. (2012). Presence of chelonid fibropapilloma-associated herpesvirus in tumored and non-tumored green turtles, as detected by polymerase chain reaction, in endemic and non-endemic aggregations, Puerto Rico. *SpringerPlus*, *1*(1), 1–8.

Paladino, F. V., & Morreale, S. J. (2001). Sea Turtles. In *Encyclopedia of Ocean Sciences* (pp. 212–219).

Patrício, A. R., Herbst, L. H., Duarte, A., Vélez-Zuazo, X., Loureiro, N. S., Pereira, N., … Toranzos, G. A. (2012). Global phylogeography and evolution of chelonid fibropapilloma-associated herpesvirus. *Journal of General Virology*, *93*(5), 1035–1045.

Patrício, A. R., Varela, M. R., Broderick, A. C., Catry, P., Hawkes, L. A., Regalla, A., & Godley, B. J. (2017). Climate change resilience of a globally important green turtle population. *Ecology of the Green Sea Turtle (Chelonia Mydas L) in a Changing World*, 113.

Patricio, A., Velez-Zuazo, X., E. Diez, C., Van Dam, R., & Sabat, A. (2011). *Survival Probability of Immature Green Turtles in Two Foraging Grounds at Culebra, Puerto Rico*. *Marine Ecology Progress Series* (Vol. 440).

Patrício, Ana R., Diez, C. E., Van Dam, R. P., & Godley, B. J. (2016). Novel insights into the dynamics of green turtle fibropapillomatosis. *Marine Ecology Progress Series*, *547*(April), 247–255.

Patrício, R., Diez, C. E., & van Dam, R. P. (2014). Spatial and temporal variability of immature green turtle abundance and somatic growth in Puerto Rico. *Endangered Species Research*, *23*(1), 51–62.

Pauly, D., & Christensen, V. (1995). Primary production required to sustain global fisheries. *Nature*, *374*, 255–257.

Poloczanska, E. S., Limpus, C. J., & Hays, G. C. (2009). Vulnerability of Marine Turtles to Climate Change. In Elsevier Ltd. (Ed.), *Advances in Marine Biology* (1st ed.). (pp. 151–212).

Postel, S. L., Daily, G. C., & Ehrlich, P. R. (1996). Human Appropriation of Renewable Fresh Water Author, *271*(5250), 785–788.

Putman, N. (2018). Marine migrations. *Current Biology*, *28*(17), 972–976.

Quackenbush, S. L., Casey, R. N., Murcek, R. J., Paul, T. A., Work, T. M., Limpus, C. J., … Casey, J. W. (2001). Quantitative analysis of herpesvirus sequences from normal tissue and fibropapillomas of marine turtles with real-time PCR. *Virology*, *287*(1), 105–111.

Quackenbush, S. L., Work, T. M., Balazs, G. H., Casey, R. N., Rovnak, J., Chaves, A., … Casey, J. W. (1998). Three closely related herpesviruses are associated with fibropapillomatosis in marine turtles. *Virology*, *246*(2), 392–399.

Rands, M. R. W., Adams, W. M., Bennun, L., Butchart, S. H. M., Clements, A., Coomes, D., … Vira, B. (2010). Biodiversity Conservation: Challenges Beyond 2010. *Science*, *329*(5997), 1298–1303.

Reading, R. P., Kenny, D. E., & Fitzgerald, K. T. (2013). The crucial contribution of veterinarians to conservation biology. *Topics in Companion Animal Medicine*, *28*(4), 131–134.

Reis, E. C., & Goldberg, D. W. (2017). Biologia, ecologia e conservação de tartarugas marinhas. In Elsevier Ltd. (Ed.), *Mamíferos, Quelônios e Aves.* (1st ed.). (pp 63-89).

Rodenbusch, C. R., Baptistotte, C., Werneck, M. R., Pires, T. T., Melo, M. T. D., De Ataíde, M. W., … Canal, C. W. (2014). Fibropapillomatosis in green turtles Chelonia mydas in Brazil: Characteristics of tumors and virus. *Diseases of Aquatic Organisms*, *111*(3), 207–217.

Rodríguez, C. E., Duque, A. M. H., Steinberg, J., & Woodburn, D. B. (2018). Chelonia. *Pathology of Wildlife and Zoo Animals*, 825–854.

Rojstaczer, S., Sterling, S. M., & Moore, N. J. (2001). Human Appropriation of Photosynthesis Products. *Science*, *294*(5551), 2549–2552.

Romero Zarco, C. M., Carapeto, A., Pinto Cruz, C., García Murillo, P. G., Ríos Ruiz, S., & Fraga i Arquimbau, P. (2018). The IUCN Red List of Threatened Species 2018. Retrieved January 18, 2019, from https://www.iucnredlist.org/

RStudioTeam. (2018). RStudio: Integrated Development for R. RStudio. Boston, MA: RStudio, Inc. Retrieved from http://www.rstudio.com/

Sievers, F., Wilm, A., Dineen, D., Gibson, T. J., Karplus, K., Li, W., … Higgins, D. G. (2011). Fast, scalable generation of high-quality protein multiple sequence alignments using Clustal Omega. *Molecular Systems Biology*, *7*(539).

Singh, C., & Roy-Chowdhuri, S. (2016). Quantitative real-time PCR: Recent Advances. In *Clinical Applications of PCR. Methods in Molecular Biology* (Vol. 1392, pp. 161–176). Humana Press, New York, NY.

Smith, G. M., & Coates, C. W. (1938). Fibro-epithelial growths of the skin in large marine turtles, Chelonia mydas (Linnaeus). *Zoologica : Scientific Contributions of the New York Zoological Society.*, *23*, 93–98. Retrieved from https://www.biodiversitylibrary.org/part/203654

Stringell, T. B., Clerveaux, W. V., Godley, B. J., Phillips, Q., Ranger, S., Richardson, P. B., … Broderick, A. C. (2015). Fisher choice may increase prevalence of green turtle fibropapillomatosis disease. *Frontiers in Marine Science*, *2*(August), 1–8.

Suchard, M. A., Lemey, P., Baele, G., Ayres, D. L., Drummond, A. J., & Rambaut, A. (2018). Bayesian phylogenetic and phylodynamic data integration using BEAST 1.10. *Virus Evolution*, *4*(1).

Tagliolatto, A. B., Guimarães, S. M., Lobo-Hajdu, G., & Monteiro-Neto, C. (2016). Characterization of fibropapillomatosis in green turtles Chelonia mydas (Cheloniidae) captured in a foraging area in southeastern Brazil. *Diseases of Aquatic Organisms*, *121*(3), 233–240.

Tavaré, S. (1986). Some probabilistic and statistical problems in the analysis of DNA sequences. *Lecture Math Life Science*, *17*, 57–86.

The State of the World's Sea Turtles. (2019). Retrieved from https://www.seaturtlestatus.org/threats-to-turtles

Van Houtan, K. S., Hargrove, S. K., & Balazs, G. H. (2010). Land use, macroalgae, and a tumor-forming disease in marine turtles. *PLoS ONE*, *5*(9).

Van Houtan, K. S., Smith, C. M., Dailer, M. L., & Kawachi, M. (2014). Eutrophication and the dietary promotion of sea turtle tumors. *PeerJ*, *2*, e602.

Vitousek, P. M., Ehrlich, P. R., Ehrlich, A. H., & Matson, P. A. (1986). Human Appropriation of the Products of Photosynthesis. *Bioscience*, (36(6)), 368–373.

Waterhouse, A. M., Procter, J. B., Martin, D. M. A., Clamp, M., & Barton, G. J. (2009). Jalview Version 2- a multiple sequence alignment editor and analysis workbench. Bioinformatics25.

Williams, E. H., Bunkley-Williams, L., Peters, E. C., Pinto-Rodriguez, B., Matos-Morales, R., Mignucci-Giannoni, A. A., … Boulon, R. H. (1994). An epizootic of cutaneous fibropapillomas in green turtles chelonia mydas of the caribbean: Part of a panzootic? *Journal of Aquatic Animal Health*, *6*(1), 70–78.

Work, T. M., Dagenais, J., Balazs, G. H., Schettle, N., & Ackermann, M. (2015). Dynamics of Virus Shedding and In Situ Confirmation of Chelonid Herpesvirus 5 in Hawaiian Green Turtles With Fibropapillomatosis. *Veterinary Pathology*, *52*(6), 1195–1201.

Work, Thierry M., & Balazs, G. H. (1999). Relating Tumor Score to Hematology in Green Turtles with Fibropapillomatosis in Hawaii. *Journal of Wildlife Diseases*, *35*(4), 804–807.

Work, Thierry M., Balazs, G. H., Rameyer, R. A., & Morris, R. A. (2004). Retrospective pathology survey of green turtles Chelonia mydas with fibropapillomatosis in the Hawaiian Islands, 1993-2003. *Diseases of Aquatic Organisms*, *62*(1–2), 163–176.

Work, Thierry M., Balazs, G. H., Wolcott, M., & Morris, R. (2003). Bacteraemia in free-ranging Hawaiian green turtles Chelonia mydas with fibropapillomatosis. *Diseases of Aquatic Organisms*, *53*(1), 41–46.

Work, Thierry M., Dagenais, J., Balazs, G. H., Schumacher, J., Lewis, T. D., Leong, J. A. C., … Casey, J. W. (2009). In vitro biology of fibropapilloma-associated turtle herpesvirus and host cells in Hawaiian green turtles (Chelonia mydas). *Journal of General Virology*, *90*(8), 1943–1950.

Work, Thierry M., Dagenais, J., Weatherby, T. M., Balazs, G. H., & Ackermann, M. (2017). *In-vitro* replication of Chelonid herpesvirus 5 in organotypic skin cultures from Hawaiian green turtles (*Chelonia mydas*). *Journal of Virology*, *91*(17).

Work, Thierry M., Rameyer, R. A., Balazs, G. H., Cray, C., & Chang, S. P. (2001). Immune Status of Free-Ranging Green Turtles With Fibropapillomatosis From Hawaii. *Journal of Wildlife Diseases*, *37*(3), 574–581.

World Society for the Protection of Animals. The Universal Declaration on Animal Welfare (2007).

7. APPENDIX

7.1. Supplementary material 1- Captured individuals' morphometric information, sample quantification, Ct values and DNA viral copies.

Turtle_ID	Year	Site	Stage	CCL (cm)	FP lesions	Tumour score	DNA quantification	Ct (normal skin)	Ct (tumour)	Viral copies (normal skin)	Viral copies (tumour)
1_MAU	2018	MAU	Juvenile	61	yes	1	13,8	35.97	22,68	2,82E+02	2,82E+06
2_MAU	2018	MAU	Juvenile	57	no	0	34,7	42.21			
3_MAU	2018	MAU	Juvenile	45,3	yes	1	25,7	35.14	24.18	5,01E+02	9,99E+05
4_MAU	2018	MAU	Juvenile	42	yes	1	19,3		20.26		1,51E+07
5_MAU	2018	MAU	Juvenile	57	no	0	17,9	40.01			
6_MAU	2018	MAU	Juvenile	49,5	no	0	14,9	37.33		1,10E+02	
7_MAU	2018	MAU	Sub-adult	66,5	no	0	12,7	36.81		1,58E+02	
8_MAU	2018	MAU	Juvenile	64,5	no	0	34,9	32.81		2,52E+03	
9_MAU	2018	MAU	Juvenile	55,3	no	0	19,4	35.22		4,74E+02	
10_MAU	2018	MAU	Juvenile	48,6	no	0	12,3				
11_MAU	2018	MAU	Juvenile	49,7	yes	1	13	34.10	38.35	1,03E+03	
12_MAU	2018	MAU	Juvenile	57,3	no	0	14,8				
13_MAU	2018	MAU	Juvenile	62,7	no	0	21,8	35.43		4,10E+02	
14_MAU	2018	MAU	Juvenile	63,5	no	0	14,7	34.36		8,61E+02	
15_MAU	2018	MAU	Juvenile	57,6	no	0	18,9	35.08		5,23E+02	
16_MAU	2018	MAU	Juvenile	63,7	no	0	21,3	39.10			
17_MAU	2018	MAU	Juvenile	62,3	no	0	20,2				
18_MAU	2018	MAU	Juvenile	49,4	yes	1	13,4	37.30	21.63	1,12E+02	5,85E+06
19_MAU	2018	MAU	Juvenile	64,7	no	0	17,9	34.89		5,96E+02	
20_MAU	2018	MAU	Juvenile	57,3	yes	1	16,6	33.88	32.77	1,20E+03	2,59E+03
21_MAU	2018	MAU	Juvenile	56,2	no	0	15,8	36.64		1,77E+02	
22_MAU	2018	MAU	Juvenile	44,8	yes	1	24		20.61		1,19E+07
23_MAU	2018	MAU	Juvenile	59,7	yes	1	19,5	32.41	22.61	3,33E+03	2,96E+06
24_MAU	2018	MAU	Juvenile	57,1	no	0	12,8	33.21		1,91E+03	
25_MAU	2018	MAU	Sub-adult	69,4	no	0	15,9	35.80		3,17E+02	
26_MAU	2018	MAU	Sub-adult	68,9	no	0	18,4	37.78		80,44122	
27_MAU	2018	MAU	Sub-adult	68,2	no	0	14,1				
28_MAU	2018	MAU	Juvenile	63,5	no	0	7,1	39.51			
29_MAU	2018	MAU	Juvenile	64,6	no	0	29,3	34.79		6,39E+02	

Supplementary material 1- continuation

Turtle_ID	Year	Site	Stage	CCL (cm)	FP lesions	Tumour score	DNA quantification	Ct (normal skin)	Ct (tumour)	Viral copies (normal skin)	Viral copies (tumour)
30_MAU	2018	MAU	Juvenile	52,5	no	0	21.6	34.30		8,98E+02	
31_MAU	2018	MAU	Juvenile	49,6	yes	1	12.5	32.66	31.88	2,80E+03	4,80E+03
32_MAU	2018	MAU	Juvenile	57,2	yes	1	22	33.71	30.63	1,35E+03	1,14E+04
33_MAU	2018	MAU	Juvenile	63,6	no	0	19.3	37.87		7,56E+01	
34_MAU	2018	MAU	Juvenile	42,8	yes	1	30.3		22.26		3,78E+06
35_MAU	2018	MAU	Juvenile	64,1	no	0	13.4	36.87		1,51E+02	
36_MAU	2018	MAU	Juvenile	46,4	yes	1	20.6		23.32		1,81E+06
37_MAU	2018	MAU	Sub-adult	65	no	0	19.2	33.34		1,75E+03	
38_MAU	2018	MAU	Juvenile	58,3	yes	1	21.7		22.06		4,34E+06
39_MAU	2018	MAU	Juvenile	57,3	yes	1			21.10		8,44E+06
40_MAU	2018	MAU	Juvenile	58,2	yes	1		33.79	35.38	1,28E+03	4,25E+02
42_MAU	2019	MAU	Sub-adult	75,0	no	0					
43_MAU	2019	MAU	Juvenile	57,0	no	0					
44_MAU	2019	MAU	Juvenile	64,0	no	0					
45_MAU	2019	MAU	Juvenile	63,3	no	0					
46_MAU	2019	MAU	Sub-adult	65,4	no	0					
47_MAU	2019	MAU	Juvenile	61,0	no	0					
48_MAU	2019	MAU	Juvenile	56,0	yes	1					
49_MAU	2019	MAU	Adult	96,0	no	0					
50_MAU	2019	MAU	Sub-adult	66,0	no	0					
51_MAU	2019	MAU	Juvenile	39,7	yes	2					
52_MAU	2019	MAU	Juvenile	49,1	no	0					
53_MAU	2019	MAU	Sub-adult	68,7	no	0					
54_MAU	2019	MAU	Juvenile	55,2	no	0					
55_MAU	2019	MAU	Juvenile	49,4	no	0					
56_MAU	2019	MAU	Juvenile	53,9	yes	1					
57_MAU	2019	MAU	Juvenile	49,5	no	0					
58_MAU	2019	MAU	Juvenile	60,7	no	0					
59_MAU	2019	MAU	Juvenile	50,0	no	0					
60_MAU	2019	MAU	Sub-adult	73,3	no	0					
61_MAU	2019	MAU	Juvenile	58,0	no	0					

Supplementary material 1- continuation

Turtle_ID	Year	Site	Stage	CCL (cm)	FP lesions	Tumour score	DNA quantification	Ct (normal skin)	Ct (tumour)	Viral copies (normal skin)	Viral copies (tumour)
62_MAU	2019	MAU	Sub-adult	70,4	no	0					
63_MAU	2019	MAU	Sub-adult	70,0	no	0					
64_MAU	2019	MAU	Juvenile	51,8	no	0					
65_MAU	2019	MAU	Juvenile	62,4	no	0					
66_MAU	2019	MAU	Sub-adult	65,8	no	0					
67_MAU	2019	MAU	Juvenile	60,0	no	0					
68_MAU	2019	MAU	Sub-adult	73,4	no	0					
69_MAU	2019	MAU	Juvenile	60,0	yes	3					
70_MAU	2019	MAU	Juvenile	48,5	no	0					
71_MAU	2019	MAU	Sub-adult	81,0	no	0					
72_MAU	2019	MAU	Sub-adult	67,0	no	0					
73_MAU	2019	MAU	Juvenile	61,6	yes	1					
1_GB	2018	GB	Juvenile	44,5	no	0	8				
2_GB	2018	GB	Juvenile	60,5	yes	1	14				
3_GB	2018	GB	Juvenile	49,5	yes	3	14		32,055		4,25E+03
4_GB	2018	GB	Sub-adult	67	no	0	17.2	31.92		4,67E+03	
5_GB	2018	GB	Juvenile	62,5	no	0	16.9				
6_GB	2018	GB	Sub-adult	70	no	0	11.4				
7_GB	2018	GB	Juvenile	62	no	0	12.4				
8_GB	2018	GB	Juvenile	46	no	0	12.1	40.76			
9_GB	2018	GB	Juvenile	61,2	no	0	20.4	38.15			
10_GB	2018	GB	Juvenile	62,2	yes	1	13.1				
11_GB	2018	GB	Adult	87,5	yes	3	9.4		21,695		5,59E+06
12_GB	2018	GB	Juvenile	45	no	0	6.9	38.08			
13_GB	2018	GB	Juvenile	43	no	0	15.1				
14_GB	2018	GB	Juvenile	47	no	0	18.5				
15_GB	2018	GB	Juvenile	44,5	no	0	16	45.14			
16_GB	2018	GB	Juvenile	60	yes	1	25.3				
17_GB	2018	GB	Juvenile	56,5	no	0	29.5				
18_GB	2018	GB	Juvenile	50	yes	1	11.8		26,63		1,83E+05
19_GB	2018	GB	Adult	92,5	yes	1	7.9	37.99		6,95E+01	

Supplementary material 1- continuation

Turtle_ID	Year	Site	Stage	CCL (cm)	FP lesions	Tumour score	DNA quantification	Ct (normal skin)	Ct (tumour)	Viral copies (normal skin)	Viral copies (tumour)
20_GB	2018	GB	Adult	97	no	0	22.4	36.85		1,53E+02	

21_GB	2018	GB	Juvenile	60	no	0	10.5	36.33		2,20E+02	
22_GB	2018	GB	Juvenile	45,5	no	0	17				
23_GB	2018	GB	Juvenile	37,5	no	0	12.4				
24_GB	2018	GB	Juvenile	50	yes	1	24.2		28,58		4,12E+04
25_GB	2018	GB	Sub-adult	67	no	0	18				
26_GB	2018	GB	Sub-adult	69	no	0	15.8				
27_GB	2019	GB	Juvenile	57	no	0					
28_GB	2019	GB	Adult	92	no	0					
29_GB	2019	GB	Juvenile	38	no	0					
30_GB	2019	GB	Juvenile	38	no	0		37,87		7,56E+01	
31_GB	2019	GB	Juvenile	44	no	0					
32_GB	2019	GB	Juvenile	49	yes	1		42,21			
33_GB	2019	GB	Juvenile	63	no	0					
34_GB	2019	GB	Sub-adult	65	yes	3			31,73		5,33E+03
35_GB	2019	GB	Juvenile	58	yes	1			44,98		
36_GB	2019	GB	Juvenile	55,5	yes	1		44,23007			

7.2. Supplementary material 2- GenBank accession numbers and sample information for phylogenetic analysis

Sample ID	Sampling Site	Host species	Sample year	GenBank accession number		Reference
				UL34	HP20	
U11	Guinea-Bissau	*Chelonia mydas*	2018	-	-	Present study
U18	Guinea-Bissau	*Chelonia mydas*	2018	-	-	
M1	Mauritania	*Chelonia mydas*	2018	-	-	
M4	Mauritania	*Chelonia mydas*	2018	-	-	
M18	Mauritania	*Chelonia mydas*	2018	-	-	
PR2	Puerto Rico	*Chelonia mydas*	2009	JN580289	JN580293	(Patrício et al., 2012)
PR4	Puerto Rico	*Chelonia mydas*	2010	JN580291	JN580295	
PR5	Puerto Rico	*Chelonia mydas*	2010	JN580292	JN580296	
GG1	São Tomé e Principe	*Chelonia mydas*	2009	JN625251	-	(Duarte et al., 2012)
GG2	São Tomé e Principe	*Chelonia mydas*	2009	JN625252	-	
GG3	São Tomé e Principe	*Chelonia mydas*	2009	JN625253	-	
GG4	São Tomé e Principe	*Chelonia mydas*	2009	JN625254	-	
GG5	São Tomé e Principe	*Chelonia mydas*	2009	JN625255	-	
GG6	São Tomé e Principe	*Chelonia mydas*	2009	JN625256	-	
FL1	Florida	*Chelonia mydas*	1990	AY646891	AY646912	(Ene et al., 2005)
FL2	Florida	*Caretta Caretta*	1993	AY646888	AY646909	
FL3	Florida	*Caretta Caretta*	1993	AY646890	AY646911	
FL4	Florida	*Chelonia mydas*	1994	AY646892	AY646913	
FL5	Florida	*Caretta Caretta*	1995	AY646889	AY646910	
FL6	Florida	*Lepidochelys kempii*	2002	AY646894	AY646915	
FL7	Florida	*Chelonia mydas*	1997	AF035004	-	(Greenblatt et al., 2005; Quackenbush et al., 1998)
HW1	Hawaii	*Chelonia mydas*	2001	AY390416	-	(Greenblatt et al., 2005)
HW2	Hawaii	*Chelonia mydas*	1995-1997	AY390417	-	(Greenblatt et al., 2005; Quackenbush et al., 1998)
AUS2	Australia	*Caretta Caretta*	1999-2000	AY390412	-	(Greenblatt et al., 2005; Quackenbush et al., 2001)
BRB	Barbados	*Chelonia mydas*	1999-2000	AY390413	-	(Greenblatt et al., 2005; Quackenbush et al., 2001)
SD	San Diego	*Chelonia mydas*	1999-2000	AY390419	-	(Greenblatt et al., 2005)
CR	Costa Rica	*Lepidochelys olivacea*	1997	AY390414	-	(Greenblatt et al., 2005; Quackenbush et al., 1998)